Basic Well Logging and Formation Evaluation

Prof. Dr. Jürgen Schön

bookboon
The eBook company

Prof. Dr. Jürgen Schön

Basic Well Logging and Formation Evaluation

Download free eBooks at bookboon.com

Basic Well Logging and Formation Evaluation
1st edition
© 2015 Prof. Dr. Jürgen Schön & bookboon.com
ISBN 978-87-403-0979-9

Download free eBooks at bookboon.com

Contents

1	**Introduction**	**8**
1.1	History, present and future of a science and technology	8
1.2	Fundamental problems and the way we go	10
2	**Reservoir Rocks, Reservoir Properties**	**14**
2.1	Reservoir rock types	14
2.2	Porosity	19
2.3	Fluids in the pore space: Saturation and bulk volume fluid	19
2.4	Permeability	21
2.5	Core analysis	24
2.6	Summary	26
3	**Well Logging – Overview**	**28**
3.1	Introduction	28
3.2	Principle of log measurement	28
3.3	Logging methods – Classification	33
3.4	The tool (probe) and the environment of measurement	36

Click on the ad to read more

Download free eBooks at bookboon.com

4	**Well Logging – The Methods**	**41**
4.1	Borehole geometry	41
4.2	Electrical and electromagnetic logs	44
4.3	Nuclear logs	66
4.4	Acousticlog, Sonic log	90
4.5	NMR measurements	97
4.6	Imaging Techniques	105
5	**Log Interpretation – Introduction**	**109**
5.1	Overview	109
5.2	Quick-Look methods	112
5.3	Quantitative Interpretation: Shale Content	113
5.4	Quantitative Interpretation: Porosity from a single log	114
5.5	Porosity and Mineral Composition – Multiple Porosity Methods	116
5.6	Water Saturation from logs	125
6	**Some Applications in Water Exploration**	**133**
6.1	Water well in an unconsolidated formation	134
6.2	Mineral water well in a fractured carbonate formation	137

Click on the ad to read more

Download free eBooks at bookboon.com

7	**Examples and Exercises**	**139**
7.1	Oil-bearing Sandstone	139
7.2	Shaly sand profile	149
7.3	Mixed lithology Carbonate rock	157
8	**Appendix**	**165**
8.1	Physical properties of rock-forming minerals	165
8.2	Some conversions	167
9	**Recommended books and sources**	**169**
10	**References**	**170**
11	**Index**	**176**
12	**Endnotes**	**179**

Discover the truth at www.deloitte.ca/careers

Deloitte.

© Deloitte & Touche LLP and affiliated entities.

Click on the ad to read more

Download free eBooks at bookboon.com

Preface and mission of this textbook:

The textbook is addressed to students of applied geosciences and petroleum engineering. It is based on the experience I gained over a long time at different universities – Bergakademie Freiberg/Germany, Colorado School of Mines/USA, Montanuniversität Leoben/Austria and Technical University Graz/Austria – and during various courses I prepared and teached for the industry.

Subject of the textbook are the fundamental techniques of well logging/borehole geophysics and the interpretation of the measured data. Practical examples help to understand different methods and algorithms. Exercises are designed to practice the methods and rules learned.

The user will get to know:

- The physical reservoir properties (porosity, saturation, fluids, permeability, capillary pressure).
- The physical background of well logging methods and the response with respect to reservoir characterization (physical principle and primary information from logging methods).
- Rules for optimal log combinations, basic equations and models, and fundamental techniques of log interpretation.

I thank Dr. Edith Müller-Huber for careful reading and correcting the text and Dr. Nina Gegenhuber for preparing Interactive Petrophysics Logplots, and I thank all my students for response, interest and patience during our classes.

Download free eBooks at bookboon.com

1 Introduction

1.1 History, present and future of a science and technology

In 1927 the Schlumberger brothers made the first electrical resistivity measurement in an oil well near Pechelbronn/Alsace. They called this new technology "electrical coring" or "electrolog". The fundamental design of this new technology is still valid in our days:

- Create a continuous plot of a measured property (resistivity) as a function of the (measured) depth and call it "the log",
- With the fundamental advantage of representing continuous information this log must be transformed into information for reservoir characterization (porosity, saturation) by a process called interpretation.

For quantitative interpretation petrophysical knowledge is necessary.The first step was done by Archie's famous equations (Archie 1942), describing the correlation between specific electrical resistivities (measured properties), porosity, water saturation (derived properties) and empirical parameters:

$$S_w = \left(\frac{R_o}{R_t}\right)^{\frac{1}{n}}$$

where S_w is water saturation, R_t is the specific electrical resistivity of the formation, R_o is the specific electrical resistivity of the formation at water saturation $S_w = 100\,\%$, and is n Archie's empirical saturation exponent.

A formation or reservoir characterization cannot be derived from one type of logs alone – it needs a combination of various physical parameters in order to derive a consistent model of the formation (complex interpretation).

The historical development of borehole geophysics is therefore characterized by the development of various systems with defined sensitivity. Cornerstones of the first period are:

- Resistivity logs (first commercial logs), directed at water saturation determination for clean rocks,
- Spontaneous Potential log, directed at the separation of sand (clean rock, reservoir) and shale,
- Acoustic log, the only "porosity log" based on Wyllie's equation (Wyllie et al. 1956) in the early days.

Download free eBooks at bookboon.com

With the advent of nuclear tools, a completely new family of logging tools comes to the fore. The Natural Gammalog becomes the log most frequently applied to estimate the shale content. With the Gamma-Gamma-Density- and the Neutronlog two powerful instruments are available to more exactly determine porosity as one of the key parameters. The presence of two (Densitylog and Neutronlog) or three (additionally Acousticlog) "Porosity logs" results in the development of sophisticated combined techniques for a porosity and mineral composition calculation.

On this way all tools have been developed and promoted for elimination of caliper effects, better resolution, and increased depth of investigation. Focusing tools (Laterolog) and Dual-System tools (Density, Neutron) are important levels of development and have been refined – based on the possibilities of digital processing – to different array systems. At the same time new techniques (sensors, data transmission) allow spectral measurements mainly for the nuclear techniques and for full-waveform-registration of acoustic systems.
The increasing amount of input data and advanced data processing are only possible with digital techniques.

With the Nuclear Magnetic Resonance (NMR) technique a major step forward was done in order to derive pore space properties with respect to a permeability estimate and to realize fluid characterization. In the frequently used Coates equation (Coates and Dumanoir 1974; Coates et al. 1999) permeability in md (millidarcy) is derived as follows

$$k_{Coates} = \left(\frac{\phi}{C}\right)^m \cdot \left(\frac{BVM}{BVI}\right)^n$$

where

ϕ is porosity in percent,
BVM is bulk volume fluid movable,
BVI is bulk volume fluid non-movable (irreducible),
m, n are empirical parameters and approximately equal to 4 and 2,
C is also an empirical parameter generally between 6 and 15.

This equation reflects the philosophy of Archie's equation with a simple, physically understandable structure (based on a capillary model) and empirical parameters covering the complicated geometry and structure of the pore space in a fascinating way. And it teaches us that we need laboratory core data in order to determine these empirical parameters for the specific formation, or – with other words – to calibrate our tools.

Download free eBooks at bookboon.com

The long way of this development and the creation of interpretation tools is related to a specific environment: The tool is surrounded by mud in an (open) well; this classic type of logging is called "wireline technique". But also in completed wells investigations are important for example for control of completion and quality (for example cement bond logs) and monitoring fluid saturation (this part of cased hole logging is not subject of this book).

The modern techniques of Measurement While Drilling (MWD) and Logging While Drilling (LWD) reflect the dream to "see" in real-time what is penetrated with the bit; such a measurement is important for an optimized and safe drilling operation also in deviated and horizontal wells.

1.2 Fundamental problems and the way we go

Borehole geophysical measurements are an important group of methods for the solution of fundamental problems in:

a) Hydrocarbon exploration and production,
b) Exploration of water and geothermal resources,
c) Mineral exploration,
d) Geotechnical investigations,
e) And a variety of general problems in earth science.

For the dominant field of hydrocarbon exploration Figure 1-1 defines the fundamental questions with regard to locality, depth and geometry of the reservoir – in most cases this general model is derived from geological, sedimentological and structural studies implementing seismic and other surface geophysical results.

The drilled well gives a possibility to verify the expected geology, to determine exact bed depth and thickness, to indicate the lithology and mineralogy, and to show reservoirs or zones of interest. The step of quantitative determination of key properties (porosity, saturation, permeability) is subject of quantitative log analysis and implements parameters derived from cores.

Of increasing interest are monitoring and observation of changes of properties during the lifetime of a well. This is focused not only on the change of fluid saturation during production, but also directed on mechanical stability and the phenomenon of subsidence.

Download free eBooks at bookboon.com

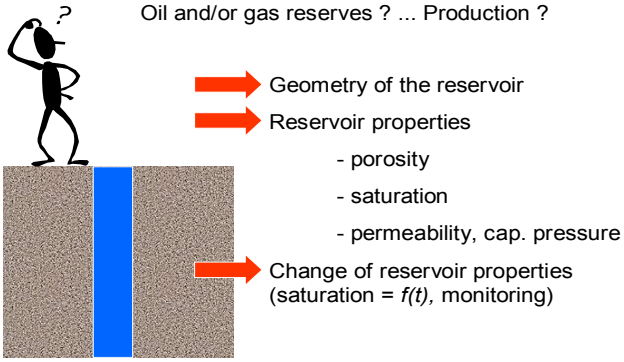

Figure 1-1: The fundamental problems in hydrocarbon exploration – but note: There are also other resources of interest apart from oil and gas, such as for example water or geothermal resources and geotechnical problems.

Borehole geophysics or well logging takes measurements along the borehole in terms of physical properties (log data). The log data present a continuous documentation of the whole profile and give a physical characterization of the individual layers and sections in terms of resistivity, nuclear radiation etc.

Sophisticated interpretation methods transform the measured data into reservoir properties (porosity, saturation, permeability etc.) and other properties of interest.

Thus, there are two types of properties:

1) Properties of primary interest (porosity, saturation, permeability) – reservoir properties,
2) Properties delivered from the well logging tools (resistivity, nuclear cross section, acoustic traveltime or slowness, natural gamma radiation etc.) – log measured properties.

How can we derive equations and algorithms for a transformation of (measured) parameters into reservoir properties?

There are three ways:

1) empirically, using experiments,
2) theoretically, using models,
3) combination of theoretical and empirical results.

Download free eBooks at bookboon.com

Since borehole measurements are realized in a disturbed or inhomogeneous environment (effect of borehole and caliper, invaded zone, layers above or below the measured section, dip of layers etc.), the original measured parameters are "apparent properties" and need a processing to eliminate these effects and to derive "true rock properties". Therefore the whole process of borehole measurement includes the following steps (Figure 1-2):

1) Define the parameters of interest for the lithological type of the section. Design – based on the sensitivity of the individual methods/tools – your logging program.
2) Measure the corresponding logs. The result is a dataset for each method i. With regard to resistivity measurement, this could be Microlog, Laterolog-shallow, and Laterolog-deep.
3) Specific processing algorithms derive a physical model in terms of the measured physical property p_i from these "apparent data". Regarding resistivity measurements this results in the resistivity of the invaded zone R_{xo} and the resistivity of the non-invaded (virgin) zone R_t. This step is called "processing" and has a strong reference to the tool characteristics.
4) Interpretation methods transform measured data into reservoir properties (porosity, saturation, permeability etc.) and other properties of interest. Relationships between measured data and reservoir properties are an instrument of this "interpretation" process. It is important to note that important inputs are necessary for this step (e.g. information about lithology, fluid properties, empirical parameters like Archie's m and n).

SIMPLY CLEVER
ŠKODA
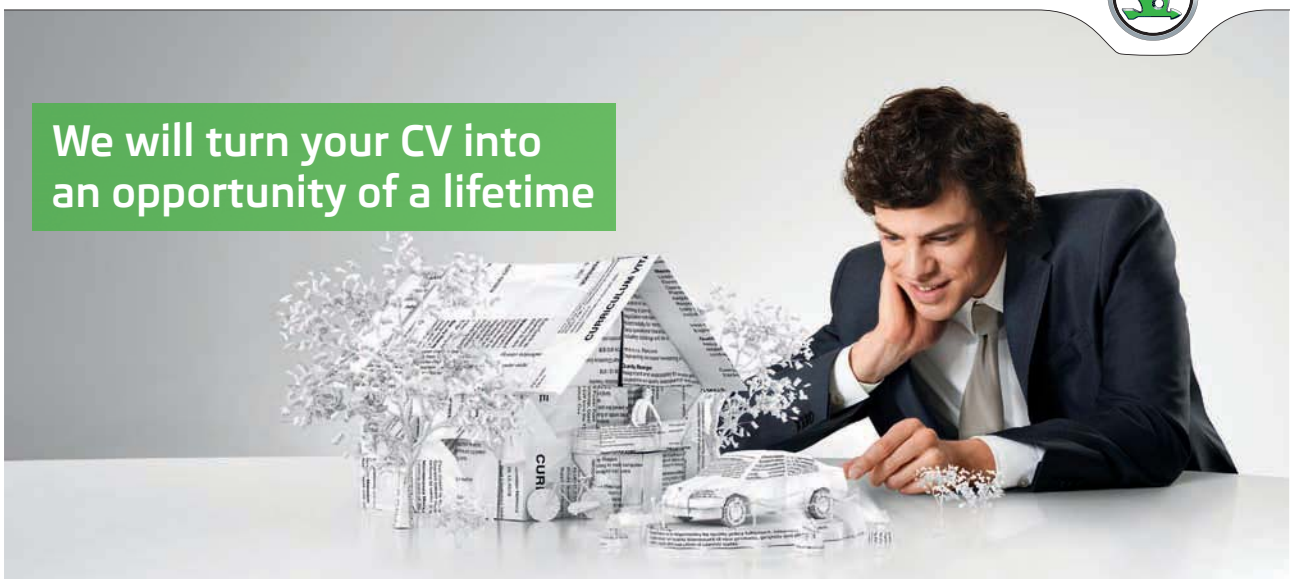

Do you like cars? Would you like to be a part of a successful brand?
We will appreciate and reward both your enthusiasm and talent.
Send us your CV. You will be surprised where it can take you.
Send us your CV on
www.employerforlife.com
Click on the ad to read more

Download free eBooks at bookboon.com

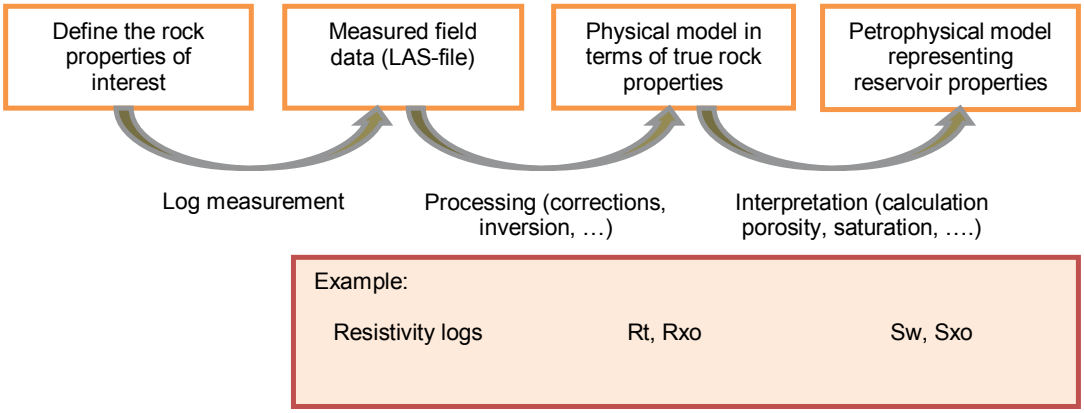

Figure 1-2: Workflow of a "Geophysical Investigation" (Principle).

This workflow determines the way we go in this textbook. We will implement three phases:

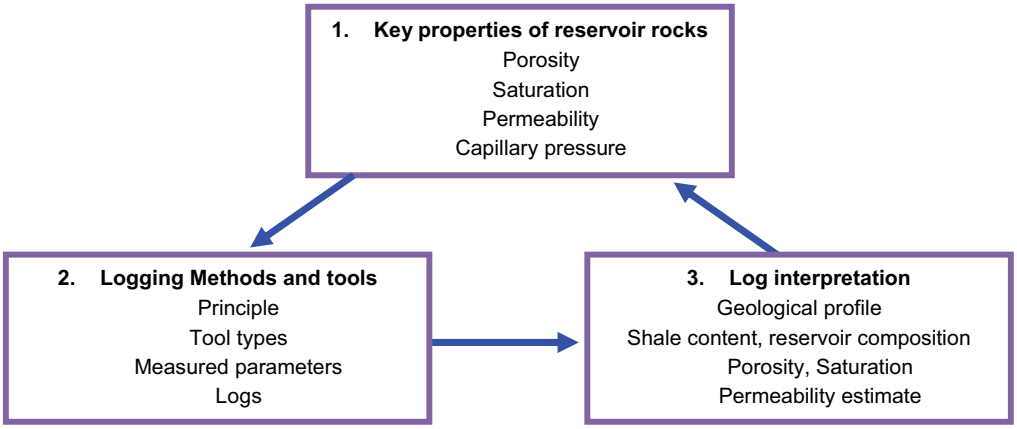

Figure 1-3: Main components of the textbook.

In the next section we will concentrate on phase 1 – the key properties of reservoir rocks – and we will get to know specific characteristics such as porosity, fluid saturation, permeability, and capillary pressure.

Download free eBooks at bookboon.com

2 Reservoir Rocks, Reservoir Properties

This section describes the key properties needed for reservoir characterization of the two dominant lithologic reservoir types sandstone and carbonate rocks. Key properties are porosity, fluid saturation, and permeability. There are two ways of property measurement:

- Direct at cores and plugs (this section)
- Indirect from logs (following sections).

2.1 Reservoir rock types

Fluids (oil, gas, but also water) are accumulated in the pore space of the reservoir rock. Therefore, the fundamental reservoir rock properties are:

- Porosity: How much space is available in the rock?
- Fluid type: Is it oil, gas, or water?
- Saturation: Which volume fraction of the pore space is occupied by oil, gas, and water?
- Permeability: At what rate can I produce a fluid?

For determination and derivation of these reservoir properties, there are two techniques:

Direct: Measurements on samples (cores) in core laboratories. The result refers to a limited volume ("point-information"),

Indirect: Parameters derived from logs (well log measurements, formation analysis). The result is continuous information presented as a curve, but not directly in terms of reservoir properties (porosity, permeability etc.). A transformation (interpretation) into reservoir properties is necessary. This involves a kind of "log calibration" (comparison with laboratory data or tests).

Therefore the combination of both techniques – core and log data – is essential for successful formation evaluation.

Reservoir rocks can be classified into two major types

1) Clastic rocks (sandstone)
2) Carbonate rocks (limestone, dolomite)

Download free eBooks at bookboon.com

The two types have different pore properties, different abundances, and different importance for the world's hydrocarbon production.

For a reservoir the "protecting or sealing formation" (cap rock) is also of critical importance. Thus the main subject of interpretation are the basic lithologies presented in Figure 2-1.

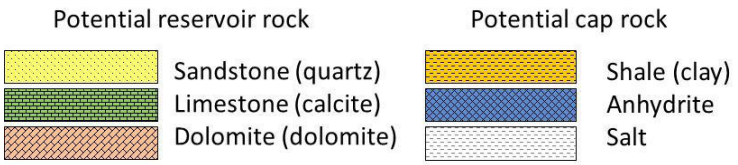

Figure 2-1 Basic lithologies considered in interpretation.

Clastic rocks: Typical members are sandstone, siltstone, claystone, and shale. The parameter used for classification of clastic rocks is grain size (Figure 2-2).

Click on the ad to read more

Download free eBooks at bookboon.com

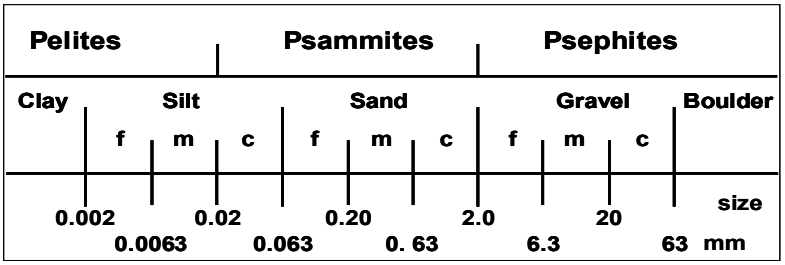

Figure 2-2: Classification of clastic sediments according to grain size; f: fine, m: medium, c: coarse. The terms psephites, psammites, and pelites are defined for more than 50% weight of the corresponding grain size range (Schön, 1996)

Clay has a strong influence on all rock properties; it decreases the effective pore space and reduces permeability.

The terms "clay" and "shale" are a source of confusion; please note:

- Clay is defined as a particle size (< 0.002 mm),
- Clay minerals are a group of phyllosilicates with specific properties (Cation Exchange Capacity CEC),
- Shale is a rock type (high amount of clay minerals, but also fine-grained feldspars and quartz). The clay fraction in shale makes up about 40 … 90%. In many shale physical properties the properties of clay minerals are reflected.

For the effect of clay in a reservoir rock, not only the volume fraction (clay content) and the clay mineralogy, but also the type of clay distribution is important (Figure 2-3):

1) Laminar clay – thin clay layers alternating with sand,
2) Dispersed clay – clay in the pores (also authigenic clay),
3) Structural clay – clay forms grains and is a rock-building component.

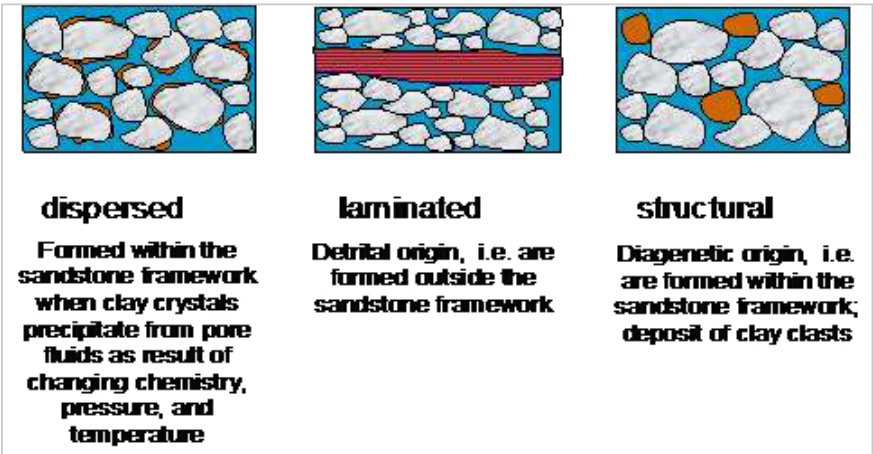

Figure 2-3: Types of clay distribution in sedimentary rocks.

Download free eBooks at bookboon.com

Carbonate: The principal minerals of carbonate reservoir rocks are calcite, dolomite, and minor clay. Secondary minerals are anhydrite, chert, and quartz. The pore space has a very complicated structure.

We distinguish two main carbonate reservoir rock types:

- Limestone is composed of more than 50% carbonates, of which more than half is calcite $CaCO_3$,
- Dolomite is composed of more than 50% carbonates, of which more than half is dolomite $CaMg(CO_3)_2$.

A range of carbonate classification schemes exist: Dunham's Classification of Carbonates is frequently used. It is based on the internal structure of the rock (Akbar et al. 1995, 2000/01).

Table 2-1 shows a petrophysical classification of carbonate pore types (adapted from Lucia 1983, 2007).

Classification (Lucia)		
Interparticle	Vuggy	
	Separate	Connecting
Pore types		
Intergrain intercrystal	Moldic Intrafossil Shelter	Cavernous Fracture Solution-enlarged fracture

Table 2-1 Petrophysical classification of carbonate pore types, adapted from Lucia 1983, 2007.

Valuable information about porosity types in carbonate sections can be derived from acoustic and/or resistivity scans (Figure 2-4).

Download free eBooks at bookboon.com

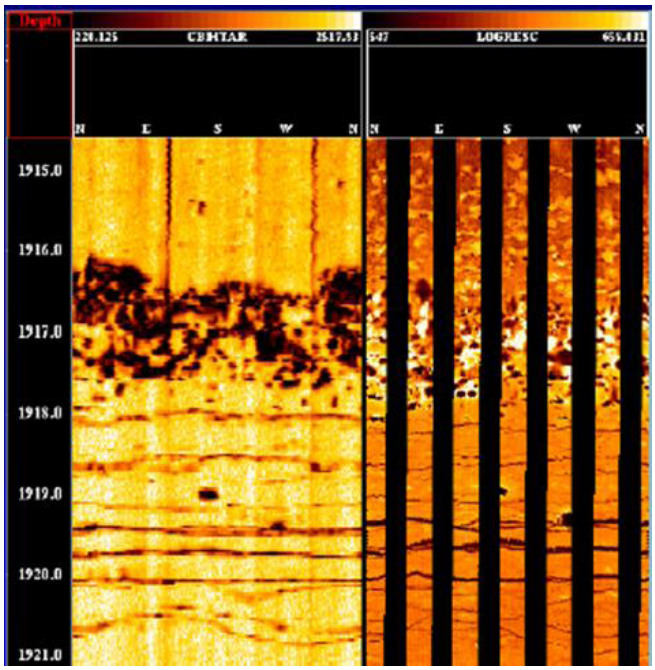

Vuggy porosity

Rotary sidewall cores

Stylolites

Figure 2-4: STAR-images in a complex carbonate section (left acoustic imager, right resistivity image); Baker Atlas (2014).

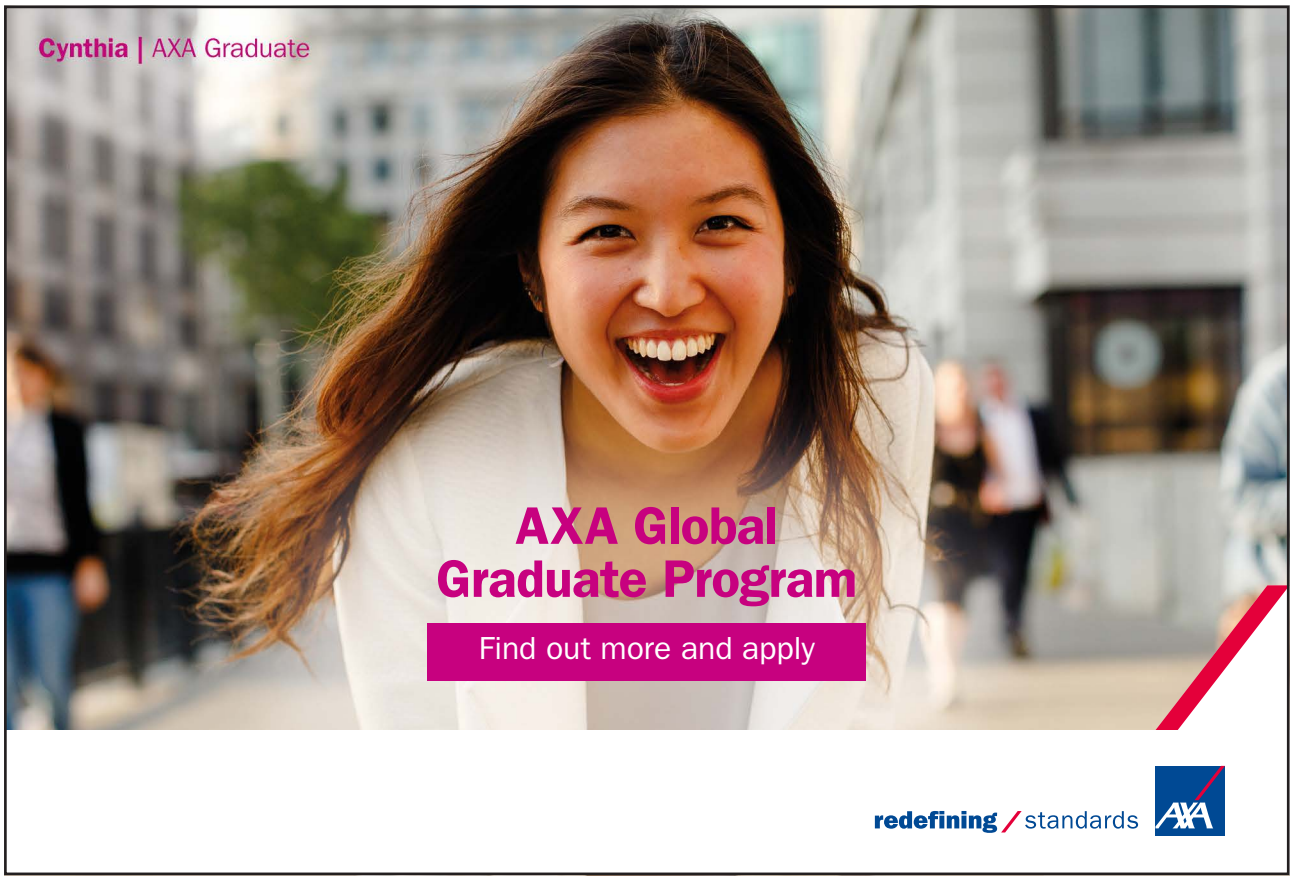

Click on the ad to read more

Download free eBooks at bookboon.com

2.2 Porosity

Porosity is defined as the volume fraction of all pores related to the rock bulk volume (Figure 2-5):

$$porosity = \phi = \frac{volume\ of\ pores}{bulk\ volume} = 1 - \frac{volume\ of\ solid\ minerals}{bulk\ volume}$$

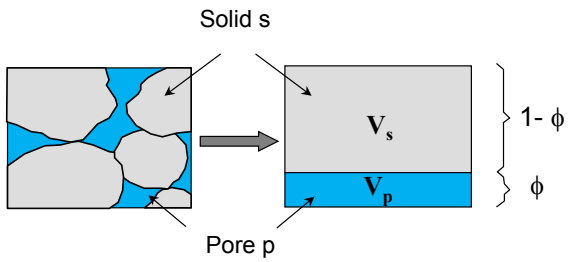

Figure 2-5: Definition of porosity.

Porosity is given as a dimensionless volume fraction or as a percentage.

For reservoir characterization it is important to distinguish between:

1) Total porosity (the fraction of bulk volume occupied by the total pore space or the space not occupied by solid components),
2) Effective porosity (the fraction of bulk volume occupied by interconnected pore space allowing fluid flow). The non-effective part of total porosity is represented in clastic rocks by the clay-bound water and in carbonates by non-connected pores or vugs.

Porosity can be determined:

- Directly at cores, plugs, or samples in the core-laboratory,
- Indirectly from logs (nuclear and acoustic measurements), and by NMR measurements.

2.3 Fluids in the pore space: Saturation and bulk volume fluid

Porosity gives the pore volume related to the bulk rock volume. **Saturation** gives the volume fraction occupied by a fluid related to the pore volume[1]. Thus, saturation S_i describes the volume fraction of a fluid i in a porous rock:

$$S_i = \frac{volume\ of\ fluid\ i}{volume\ of\ pores}$$

Saturation is given as a dimensionless fraction or as a percentage. Saturation theoretically has the lower bound at zero (or 0%) and the upper bound at one (or 100%).
A reservoir hosting the fluids water, oil, and gas is characterized by three saturation terms; their sum must be 1:

$$S_{water} + S_{oil} + S_{gas} = 1$$

Download free eBooks at bookboon.com

Fluid saturation can be determined:

- From cores, plugs, or samples (direct determination by fluid extraction, or capillary pressure measurements),
- Indirectly from logs (resistivity, dielectric, or neutron measurements).

In addition to the parameter "saturation", the parameter "**bulk volume of the fluid**" is used. Bulk volume of a fluid *i* relates the volume of that fluid to the rock bulk volume. The bulk volume of, for example, water is therefore given by:

$$BVW = \frac{volume\ of\ water}{rock\ volume} = \phi \cdot S_w$$

The bulk volume of a fluid theoretically has the lower bound zero and the upper bound given by total porosity.

In a (water wet) porous rock, the water, depending on its interaction with minerals and bonding type, is present as:

- Free movable water in the pore space (bulk volume movable *BVM*),
- Capillary bound water, connected with the grain surface (bulk volume immovable *BVI*), and
- Clay-bound water (*CBW*) with its strong clay-water effects.

The water types have different physical properties and effects (e.g. with respect to permeability or electrical resistivity). Therefore a subdivision into these types is necessary.

Porosity and bulk volume of fluids describe the volumetric composition of a reservoir rock (Figure 26).

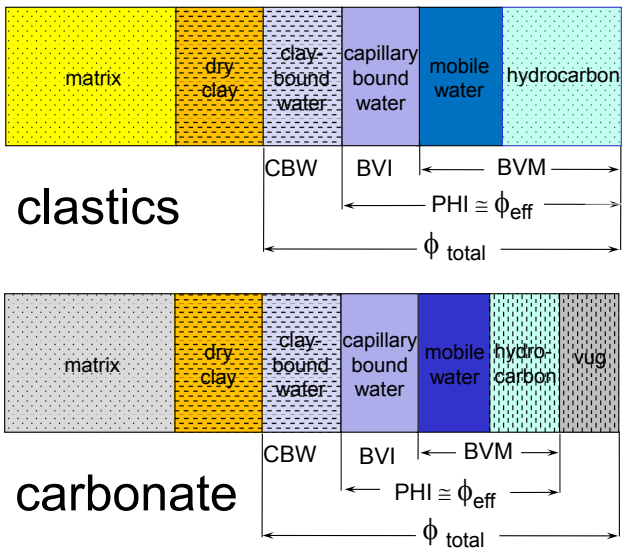

Figure 2-6: Volumetric description of a hydrocarbon-bearing clastic and carbonate reservoir. CBW – clay-bound water; BVI – bulk volume irreducible/non movable water; BVM – bulk volume movable fluids.

Download free eBooks at bookboon.com

2.4 Permeability

Permeability

- characterizes the ability of a rock to transmit a fluid; it connects the fluid flow rate with the applied pressure gradient and the fluid viscosity,
- is controlled by the connected passages of the pore space (pore throats),
- is a tensorial property and exhibits, in many cases, an anisotropy (mostly expressed by horizontal (k_h) and vertical (k_v) permeability[2]).

Methods used to determine permeabilityare:

a) Direct measurements at samples (cores, core plugs),
b) Direct tests: well and drillstem tests, wireline formation testers, pump tests,
c) Indirect methods using grain size parameters and porosity (particularly for unconsolidated sediments),
d) Indirect methods using wireline logs and specific interpretation (NMR, Stoneley wave, or combined techniques implementing irreducible water saturation).

Permeability relates the laminar fluid flow (fluid volume/time) to the macroscopic cross section of the rock, the viscosity of the fluid, and the fluid pressure gradient (Figure 2-7).

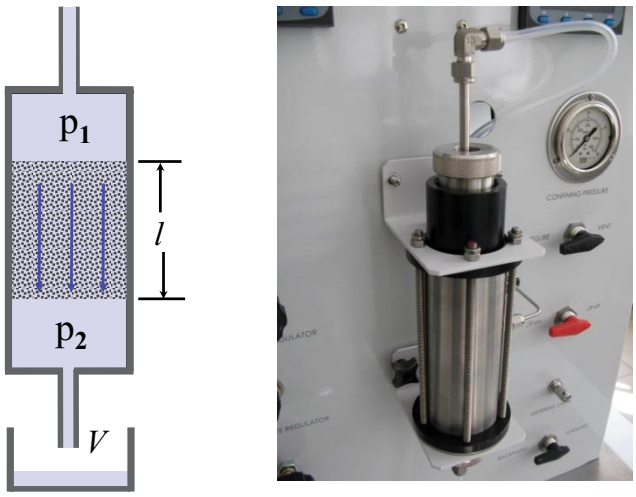

Figure 2-7: Permeability. Left: definition and principle of measurement; right permeameter cell (Vinci technologies)

Permeability results as

$$k = \eta \cdot \frac{u}{grad\ p}$$

Download free eBooks at bookboon.com

where

$u = \frac{V}{t \cdot A}$ is fluid flow (volume V passing a cross section area A in a time t)

η is the dynamic viscosity of the fluid

$grad\ \ p = \frac{p_1 - p_2}{l}$ is the macroscopic fluid pressure gradient[3].

Mobility is the ratio of permeability and fluid viscosity.

Depending on the fluid composition a distinction has to be made:

- Absolute permeability (laminar flow of a single non-reactive fluid),
- Effective permeability (flow of one fluid in the presence of another fluid)
- Relative permeability (ratio of effective to absolute permeability).

The permeability has the unit of an area [m^2] in SI units; this explains permeability as a pore geometrical measure. In the oil industry, Darcy (d) or millidarcy (md) are typical units used with the conversion

$$1\ \text{d} = 0.9869\ 10^{-12}\ \text{m}^2 \quad \text{or} \quad 1\ \text{d} \approx 1\ \mu\text{m}^2$$

Click on the ad to read more

Download free eBooks at bookboon.com

Permeability is a pore space property; main controlling factors are:

1) Porosity (connected porosity),
2) Pore size and fracture width; permeability is proportional to several powers (≈ 2) of pore size or fracture width.

Permeability increases with porosity (see Figure 2-8) and pore (throat) size. If rock contains clay, permeability can decrease by orders of magnitude.

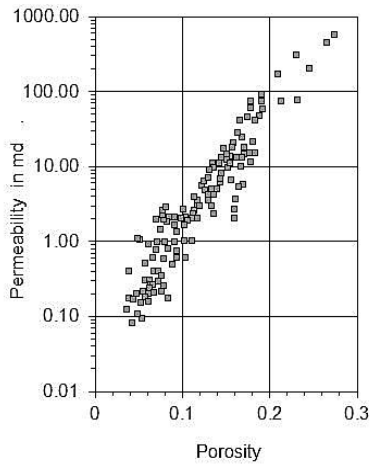

Figure 2-8: Permeability versus porosity (poro-perm correlation) for sandstone

In **clastic sediments**, the correlation between permeability and porosity is one of the most concise tendencies with a high practical importance: Permeability-porosity relationships are a frequent type of predictor. Besides porosity, the pore size has a dominant influence on permeability. Figure 2-9 (left) shows the general tendencies for clastic rocks (sandstone).

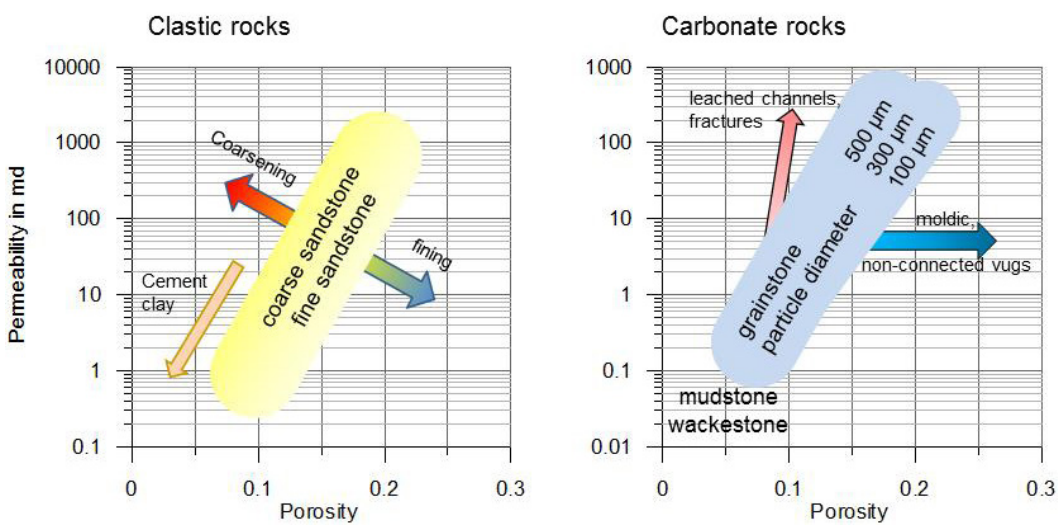

Figure 2-9: Permeability versus porosity – tendencies for clastic and carbonate rocks.

Download free eBooks at bookboon.com

The complex pore structure and diversity of **carbonates** result in problems to derive and correlate permeability with porosity and other parameters (Figure 2-9, right). Reservoir properties are controlled by two basic pore networks (Lucia 1999, 2007):

- Interparticle pore network (intergranular and intercrystalline porosity), and
- Vuggy pore network (pore space larger than or within the particles and commonly present as leached particles, fractures, and large irregular cavities). The effect of vugs on reservoir properties is strongly controlled by the type of interconnection:
    - Separate vugs (only connected via the interparticle pore network, if present), and
    - touching vugs (direct vug-vug contact).

2.5 Core analysis

Core analysis is an important component of reservoir characterization and strongly connected with log analysis. Main tasks are the validation of log-derived reservoir description, determination of critical analysis parameters, and core analysis is the sole source of some petrophysical data. In addition, a reservoir fluid analysis is provided in some cases. Recommended practices for core analysis are compiled by the American Petroleum Institute (API 1998).
Because of the extra rig time involved, cores are expensive – this is why usually only the reservoir interval is cored.

There are two types of core acquisition:

- Conventional (or rotary) cores: Full diameter cores range from 1¾ in (4.5 cm) to 5¼ in (13.5 cm) – Note: Loss of core can indicate good reservoir rock.
- Sidewall core (percussion and rotary sidewall coring).

A full-diameter core is a cylindrical (approximately 1.75 to 5.25 inches in diameter) sample of rock. For laboratory measurements, the core is dissected into multiple plugs (about 1 inch in diameter and 3 inches long). A less expensive option is sidewall coring.

Direct determination of the reservoir properties is subject of core analysis in core laboratories. We distinguish between Routine core analysis (RCAL) and Special core analysis (SCAL); see Figure 2-10.

Download free eBooks at bookboon.com

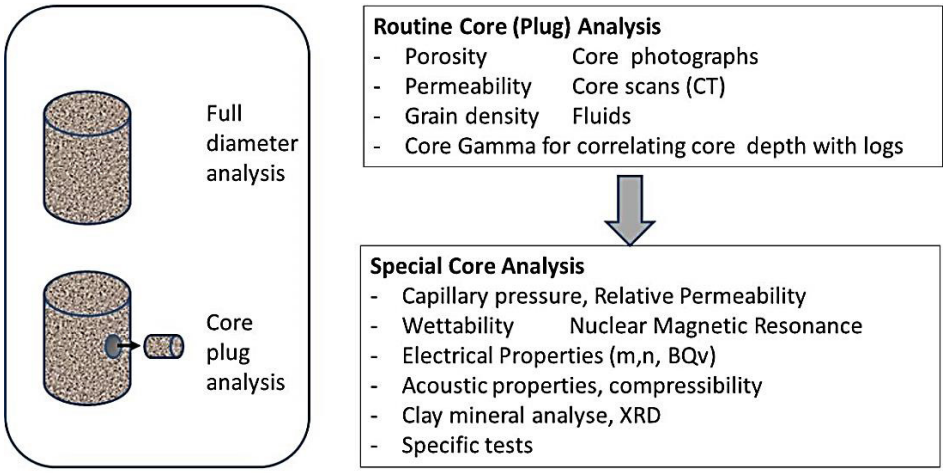

Figure 2-10: Routine and special core analysis.

Cores are therefore essential for:

a) Direct determination of reservoir properties like porosity and permeability (also in order to validate log interpretation),
b) Calibration of log measurement (for example NMR-derived permeability),
c) Determination of fundamental petrophysical properties for log interpretation (for example Archie's parameter *m* and *n*, grain density).

Click on the ad to read more

Download free eBooks at bookboon.com

Limitations and problems of core measurements are:

- Core is only a small section of rock and is not necessarily representative of a reservoir or a large section. This is a question of homogeneity,
- Coring and recovery change stress and temperature and may change rock structure,
- Plugging, cleaning, and drying may change the wettability of plugs.

Andersen, et al. (2013) note: "*The basic description of core material comes from routine analysis. This service includes measurement of porosity, saturation and permeability to answer three fundamental questions about a reservoir. Does the rock contain a fluid-filled space (porosity); does it contain hydrocarbons in that space (saturation); and can those hydrocarbon fluids be produced (permeability)? Core gamma logging provides a link of the core depth to wellbore logging depth, and core computed tomography (CT) scans indicate the core heterogeneity. Core photographs taken in both white and ultraviolet light are used for both documentation and core description.*"

Detailed understanding of a reservoir requires additional measurements obtained in the special core analysis laboratory (SCAL). Electrical measurements obtain Archie exponents for calibrating electrical logging measurements of porosity and saturation and nuclear magnetic resonance (NMR). Core measurements determine a formation-specific cutoff value for the relaxation time from an NMR log. Capillary pressure measurements by mercury injection, centrifuge, or porous plate methods indicate distributions of pore throats and are used to evaluate saturation distribution as a function of height in a formation. Relative permeability determines the multiphase flow character of the formation and can be performed at ambient or elevated conditions of pressure and temperature. Wettability is determined by Amott-Harvey or USBM methods" (see for example Tiab and Donaldson 2014; API 1998).

2.6 Summary

Porosity characterizes the volume of pore space; it is a scalar property. Porosity shows a strong correlation with density (and other properties measured by nuclear, acoustic, or electrical methods).
Permeability expresses the ability of fluid flow and is a tensorial property. Permeability correlates with porosity, but is strongly influenced by pore diameter (or grain size) and pore connectivity. This causes the difficulties in permeability determination.

Porosity, fluid saturation, and permeability are criteria for net pay definition. Some definitions in Figure 2-11 may illustrate this:

- Gross thickness: Refers to a lithological or stratigraphic unit and is not related to the fluids in the formation.
- Net thickness: Represents the total interval of reservoir quality rock within the gross thickness, it will produce fluids, and it must exceed some defined thresholds (cutoffs).

Download free eBooks at bookboon.com

- Net pay: Refers to the total thickness of reservoir quality rock – rock that will flow some amount of hydrocarbons.

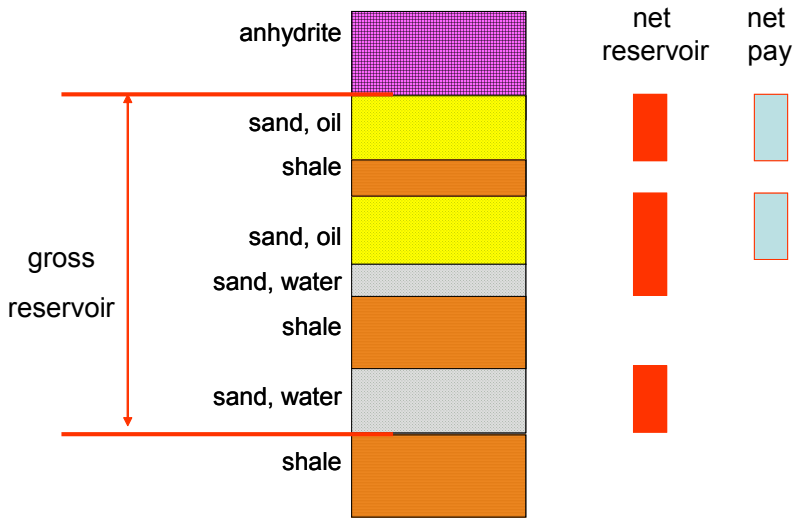

Figure 2-11: Net pay definition (schematic).

Cutoffs are defined in the literature using different criteria. Examples are:

- Bigelow (2002) defined it via cutoffs: $\phi < 15\%$, $V_{sh} > 30\%$, $S_w > 50$ %, $k < 50$ md.
- Darling (2005) formulated the following statement, *"Generally, the cutoff point should be set at a value equivalent to a permeability of 1 md for oil zonesand 0.1 md for gas zones"*.

Download free eBooks at bookboon.com

3 Well Logging – Overview

This section describes the general principles of well logging (open hole), gives a classification of the tools and the main parts of the equipment.

Tools have different responses and realize measurements under the specific condition of a borehole; this results in characteristic radial depth of investigation and the vertical resolution as characteristic properties of the methods.

3.1 Introduction

The general purpose of log measurements is to provide a continuous profile of:

- Lithology with exact depth of formation/rock boundaries,
- Rock properties and rock composition (mineralogy); of special interest are reservoir properties (porosity, saturation, permeability),
- Fractures and tectonic elements,
- Mechanical rock properties for stability, sanding problems, frack operations, etc.,
- Indications or content and properties of other substances than hydrocarbons (water, thermal water, ores, coal, salt, construction materials),
- Seismic-relevant parameters for integrated interpretation of seismic and log measurements,
- Changes of properties; this is important particularly with respect to change of fluid content/ saturation during production (monitoring, time lapse measurements).

Cuttings are a valuable source of information for interpretation of the logs. If no cores are available, cuttings carry the only direct substantial information – they tell us something about the dominant mineral components and matrix porosity, help to establish a "rock model" for multimineral analysis. Mud and cuttings samples are accumulated on a catching board below the shaker screen. Cutting needs a certain time ("lag time") to circulate from the bottom of the well (bit position) to the shaker screens. A rule of thumb (Hyne 2001) is: In an 8-in (20 cm) hole it takes about 10 minutes for mud to circulate each 1000 ft (300 m).Well cuttings are sampled as a composite sample over each 10 ft (3 m) of depth or at shorter interval in the reservoir.

3.2 Principle of log measurement

The wireline logging equipment consists of a set of probes, the cable with winch, a depth sensor, and the surface measuring and control unit.
In the Measurement While Drilling (MWD)/Logging While Drilling (LWD) technique, the measuring elements are part of the drill string; signals are transmitted via mud pulses to the surface unit.

Download free eBooks at bookboon.com

Figure 3-1 shows a wireline logging setup with the main components:

- Tool or probe with sensors, transmitters, sources,
- Cable connected with the probe by a cable-connector. The cable gives depth information about tool position, transmits the energy downwards and the measured data upwards,
- Winch with depth counter,
- Surface unit for controlling the measuring process, visualizing and storing measured data.

Click on the ad to read more

Download free eBooks at bookboon.com

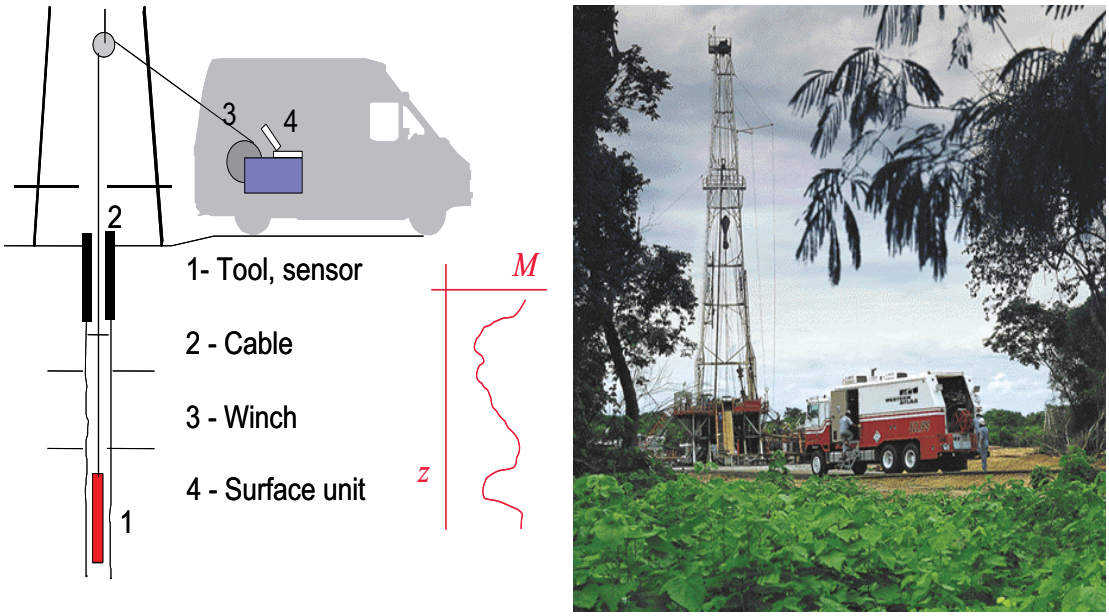

Figure 3-1: The logging unit – principle.

Well logs provide a continuous graph of formation parameters presented versus depth. This result of measurements with a set of methods is called the "log" and includes a number of traces. Each trace shows the variation of the physical parameter measured with the corresponding method as a function of depth (Figure 3-2). The "Art of Formation Analysis" is the extraction of reservoir properties from such a set of logs (Bigelow 2002).

Download free eBooks at bookboon.com

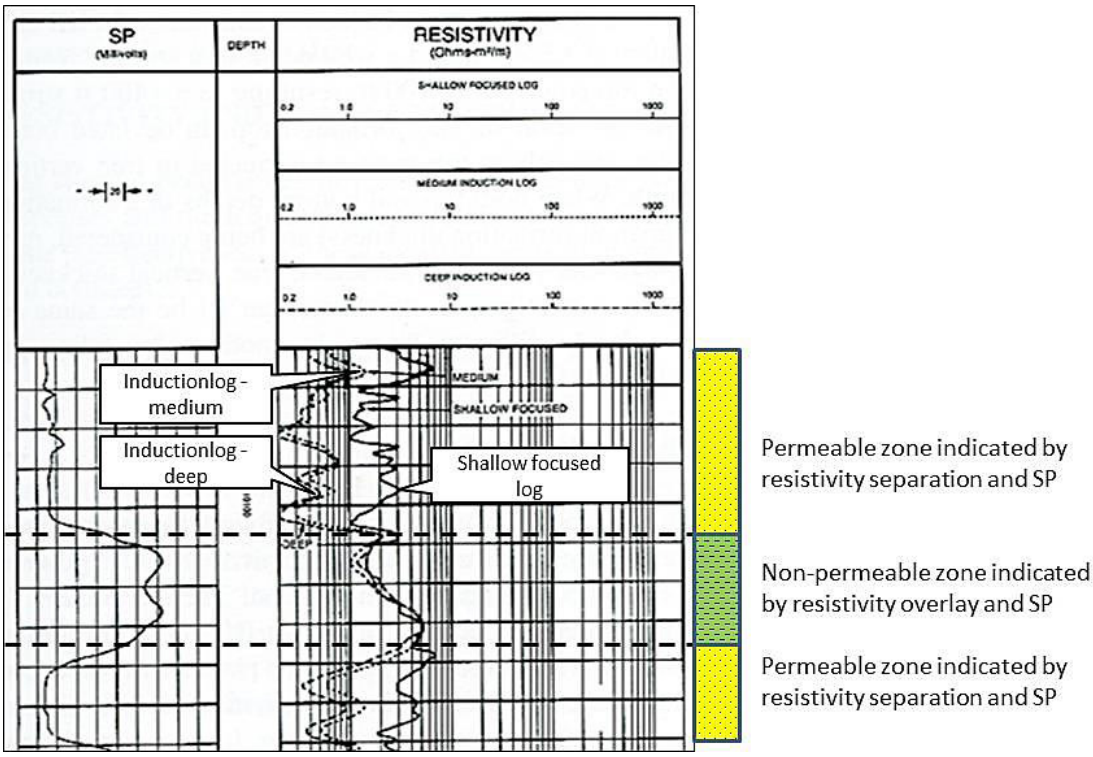

Figure 3-2: The log – each trace shows the variation of a physical parameter as a function of depth (Bigelow, 2002). Left trace: Spontaneous Potential SP in mV; right trace (logarithmic scale): three resistivity curves with different radii of investigation. Separation of the logs results from an invasion effect and indicates permeable zones (sandstone), whereas a fit of the three curves indicates a non-permeable section (shale).

The "Header" (Figure 3-3) on top of the log traces is a part of documentation of the log measurement. Important information from the log header includes:

- Hole location and name,
- Depth – Driller, Depth – Logger, Casing depth, Bit size,
- Logged Interval,
- Fluid Type in Hole, Density/Viscosity, pH/Fluid Loss,
- Fluid resistivities: R_m (mud resistivity) at measured temperature, R_{mf} (mud filtrate resistivity) at measured temperature, R_{mc} (mud cake resistivity) at measured temperature, Source of R_{mf}, R_{mc}
- Temperature: Bottom hole temperature, maximum recorded temperature
- Time since circulation.

Calibration tails are added to the end of log displays to convey the necessary information. Logging tools require shop calibration. Onsite tool calibrations are necessary before the start and after the end of a measurement. They are compared with the shop calibration in order to confirm a proper functionality.

Download free eBooks at bookboon.com

BAKER HUGHES

Baker Atlas

HIGH DEFINITION INDUCTION LOG SM
COMPENSATED Z-DENSILOG SM
COMPENSATED NEUTRON LOG

FILE NO:	COMPANY	ROCK PHYSICS & WELL LOG MEASUREMENTS	
API NO:	WELL	HEADER #1	
	FIELD	TRAINING	
	COUNTY	HARRIS	STATE TEXAS

Ver. 3.71	LOCATION: BAKER ATLAS CENTER	OTHER SERVICES: XMAC, MRIL, HDIP, RCI

PERMANENT DATUM	G.L.	ELEVATION	55 FT	ELEVATIONS:	
LOG MEASURED FROM	K.B.	23 FT	ABOVE P.D.	KB	78 FT
DRILL. MEAS. FROM	K.B.			DF	77 FT
				GL	55 FT

DATE		01-Jan-2000			
RUN	TRIP	1	1		
SERVICE ORDER		123456			
DEPTH DRILLER		9822 FT			
DEPTH LOGGER		9808 FT			
BOTTOM LOGGED INTERVAL		9807 FT			
TOP LOGGED INTERVAL		1232 FT			
CASING-DRILLER		9.625 IN	@1232 FT	@	
CASING LOGGER		1232 FT			
BIT SIZE		8.5 IN			
TYPE OF FLUID IN HOLE		LIGNOSULFONATE			
DENSITY	VISCOSITY	11.6 LB/G	50 S		
PH	FLUIDLOSS	10	8 C3		
SOURCE OF SAMPLE		FLOW LINE			
RM AT MEAS. TEMP.		0.4 OHMM	@94 DEGF	@	
RMF AT MEAS. TEMP.		0.2 OHMM	@94 DEGF	@	
RMC AT MEAS. TEMP.		0.7 OHMM	@94 DEGF	@	
SOURCE OF RMF	RMC	MEAS	CALC		
RM AT BHT		0.22 OHMM	@178 DEGF	@	
TIME SINCE CIRCULATION		7			
MAX. RECORDED TEMP.		178 DEGF			
EQUIP. NO.	LOCATION	9999	HOUSTON		
RECORDED BY		A. TEACHER			
WITNESSED BY		T.H.E. CLASS			

Figure 3-3: Log header (example), Baker Atlas.

All log measurements mostly deliver "indirect" information – and therefore need a transformation into reservoir properties (interpretation, formation analysis). But on the other hand – and compared with the direct core measurement – they deliver continuous information on the vertical profile without any "core loss". For computer-supported interpretation the quantitative nature of information is a high benefit. And finally log data have no information loss or change with time (alteration etc.) and allow a "reinterpretation" also after years.

Download free eBooks at bookboon.com

3.3 Logging methods – Classification

Wireline logging methods can be classified following the (physical) principle of measurement as shown in Figure 3-4. There are two fundamental types:

1) Passive tools measure properties or parameters delivered by the formation or by interaction of the formation and the borehole-fluid without any source (e.g. natural Gamma-measurement/ Gammalog, Spontaneous Potential/Self Potential).
2) Active tools measure the "answer" to a signal, pulse, radiation, current, i.e. the result of an interaction with the formation in the vicinity of the tool. Typically they have a source and one or more detectors (e.g. Gamma-Gamma-Log, Acousticlog, Resistivitylogs).

Click on the ad to read more

Download free eBooks at bookboon.com

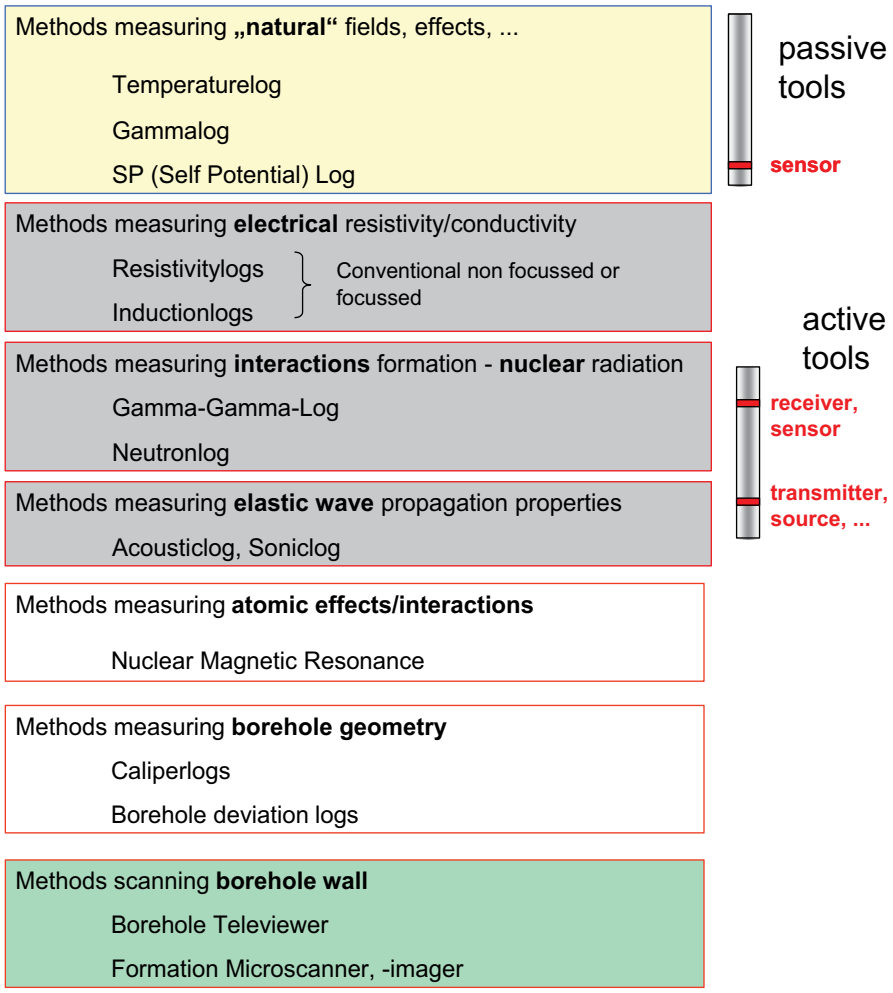

Figure 3-4: Logging methods – overview.

Directions of development in well logging are characterized by:

- Digital devices, with onsite plotting and interpretation,
- Combined tools (save time and costs, increase accuracy),
- Logging programs as a combination of methods for typical subjects of evaluation (e.g., sand-shale profile, carbonate reservoirs),
- Special tools for deviated and horizontal wells and hostile environments,
- Development of “Measurement While Drilling methods” (MWD) and “Logging While Drilling methods” (LWD).

Download free eBooks at bookboon.com

Measurement While Drilling (MWD) and Logging While Drilling (LWD) realize measurements simultaneously to the drilling process using special measuring systems as part of the drill string near the bit. In a modified technique nearly all wireline methods are realized. Data are transmitted to the surface unit by coded pressure pulses through the mud in real time. Large data files can be stored in the memory for later transmission and recovery. Thus, the MWD/LWD components are:

a) Downhole sensor system and telemetry,
b) Transmission system and medium,
c) Surface system (decoding/display/archival).

Measurement While Drilling (MWD) primarily assists drilling in order to optimize drilling process – the first objective is to steer the well optimally. Formation evaluation and reservoir measurements are an "extra". Benefits of these techniques are (after Baker Atlas, 2014):

- Safety – early detection of problems,
- Saving rig time, data are logged while drilling progresses,
- Optimizing the drilling process, geosteering to enhance well positioning (Figure 3-5),
- Capability for better measurements, longer logging time – better statistics, closer to the borehole wall, less time for invasion.

American online
LIGS University
is currently enrolling in the
Interactive Online BBA, MBA, MSc,
DBA and PhD programs:

- enroll by September 30th, 2014 and
- save up to 16% on the tuition!
- pay in 10 installments / 2 years
- Interactive Online education
- visit www.ligsuniversity.com to find out more!

Note: LIGS University is not accredited by any nationally recognized accrediting agency listed by the US Secretary of Education.
More info here.

Click on the ad to read more

Download free eBooks at bookboon.com

Logging While Drilling (LWD) is focused on gathering formation evaluation data (shale content, porosity, saturation, …).

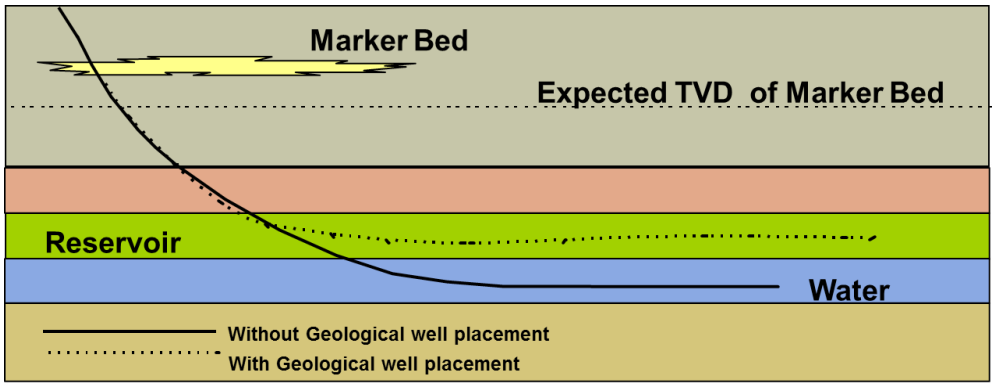

Figure 3-5: Benefit of MWD for optimized geological well placement.

3.4 The tool (probe) and the environment of measurement

Logging tools measure certain physical properties; resistivity tools, for example, measure the electrical resistivity of the formation. The measured magnitude is representative for a defined volume of response in a radial distance from the tool axis. The response of a tool is controlled by the design of its elements (e.g., electrode array) and expressed as "tool characteristic".

All borehole measurements are realized in a non-homogeneous environment:

- The well itself originates an inhomogeneity effect. This effect must be "corrected" for determination of "true" formation properties. Therefore caliper and mud properties influence the measured property and are necessary for correction.
- Infiltration creates additional inhomogeneity in radial direction. In porous, permeable rocks infiltration forms a typical radial profile (Figure 3-2, Figure 3-6). In the invaded zone much of the original fluid is replaced by the mud filtrate (sometimes the invaded zone is subdivided into a flushed and a transition zone). In the uninvaded or virgin zone – in greater distance from borehole wall – original fluids are not contaminated by mud filtrate.
- Vertical inhomogeneity is (depending on the vertical resolution) originated by the thickness of layers. It results in, for example, the "shoulder bed effect" of resistivity measurements.

Download free eBooks at bookboon.com

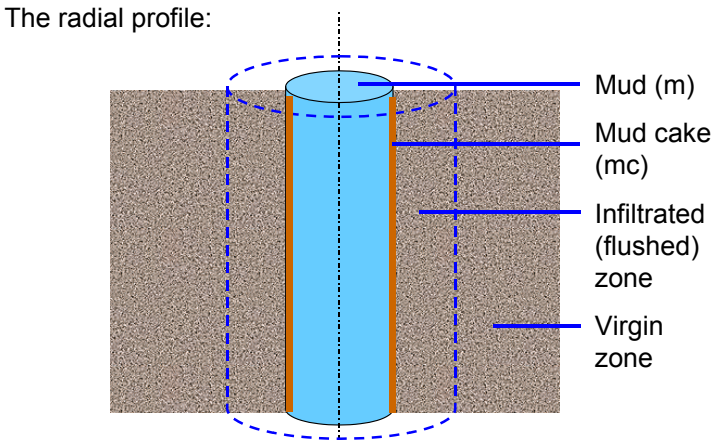

Figure 3-6: Invaded and virgin zone in a permeable section of a borehole.

For the ratio d_i/d_h, i.e. the ratio of the diameter of the invasion d_i to the diameter of borehole d_h (see also Figure 4-6), Asquith and Krygowsky (2004) give the following values as orientation:

$d_i/d_h = 2$ for high porous rocks
$d_i/d_h = 5$ for intermediate porous rocks
$d_i/d_h = 10$ for low porous rocks

In case of inhomogeneity, measured data represent averaged or "apparent" properties (controlled by the response function of the tool). But for quantitative formation characterization the "true" physical properties of the uninvaded (virgin) formation as well as of the invaded zone are necessary.

The tool characteristics are described by its response function and/or its vertical resolution, and the radius (depth) of investigation. Figure 3-7 schematically shows the radial response function for a simple transmitter – receiver tool. The differential response g(r) gives the normalized contribution of a cylinder with radius r to the measured signal. Therefore the maximum can be considered as the radial distance with the strongest influence on the measured magnitude. As cumulative presentation the integral response G(r) describes the radial buildup of the total measured signal. For tool characterization the radius of G(r) = 0.5 (50%) is frequently used as "radius of investigation 50%". Radius of investigation 50% (r_{50}) means that 50% of the total signal response is originated in a radial distance below r_{50}, and 50% originates from the space outside this cylinder.

Download free eBooks at bookboon.com

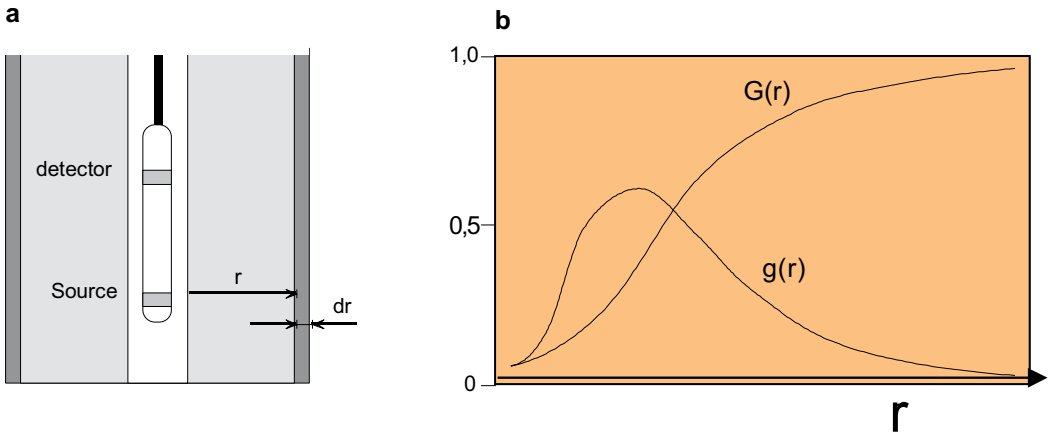

Figure 3-7: Radial characteristic and response, after Tittman (1986) (g(r) Differential Response; G(r) Integral Response).

Besides the depth or radius of investigation, tools have a specific vertical resolution – it describes the ability to detect and separate thin layers individually (Table 3-1).

Click on the ad to read more

Download free eBooks at bookboon.com

Tool	Vertical resolution 90%	Radius of investigation 50%
Gammalog	18…36 in	4 in
Density	33 in (5.5 enhanced processing)	1.5 in
Neutron (th)	36 in (20 enhanced processing)	6 in
Acoustic/Sonic	12 in (depends on spacing)	about 6 in
Inductionlog		
Deep	24	91 in
Medium	24	39 in
Shallow	<17	17 in
Laterolog		
Deep	24	60…84 in
Shallow	24	24…36 in
MFSL	3	1…3 in

Table 3-1: Vertical resolution of some tools (Asquith and Krygowski, 2004).

In permeable zones – depending on the radial characteristic of the tool and the depth of invasion – the device measures contributions from the invaded and non-invaded zone. Figure 3-8 schematically shows the radius of investigation of some tools.

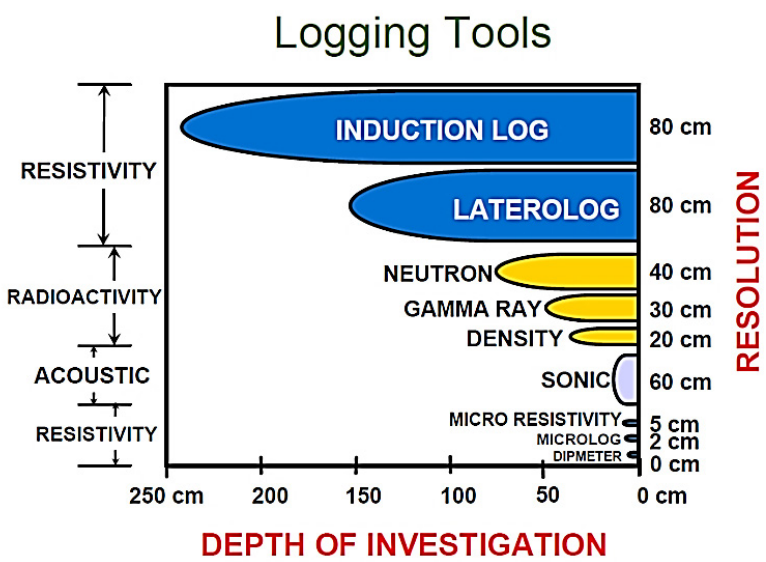

Figure 3-8: Depth of investigation and vertical resolution of some tools (Torres-Verdin, 2004).

The transformation of the processed "true" properties into reservoir properties (porosity, saturation) is the following step of interpretation (Figure 3-9). Some standard techniques are discussed in chapter 5.

Download free eBooks at bookboon.com

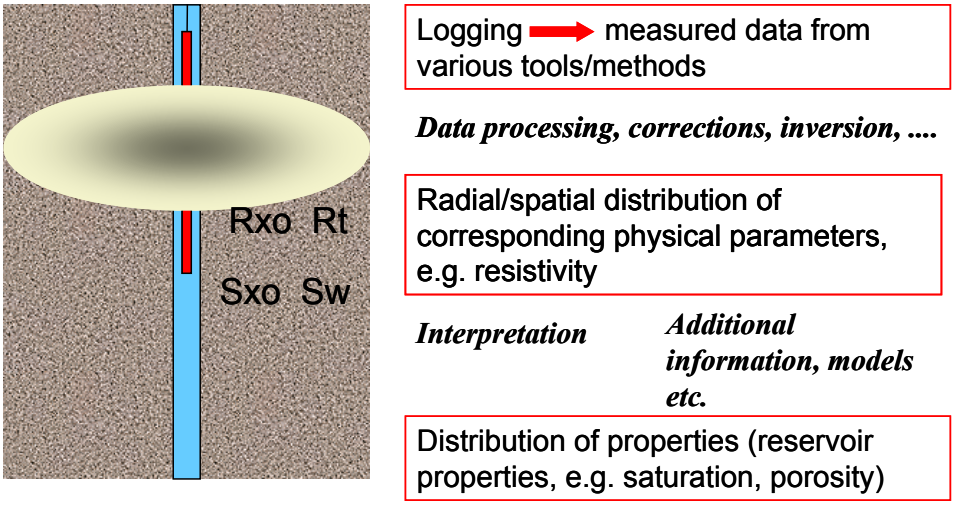

Figure 3-9: Formation evaluation by well logging – the steps "processing" and "interpretation".

Click on the ad to read more

Download free eBooks at bookboon.com

4 Well Logging – The Methods

This section describes the most applied logging methods and tools without technical details. For each method the physical principle and the main applications are discussed.

This section compiles the "toolbox" for a combined application and for interpretation.

A detailed description of the different tools, the physical principles, and applications are given in various textbooks (for example Asquith and Krygowski, 2004; Ellis and Singer, 2007; Darling, 2005) and the companies' manuals and chartbooks (see Recommended books and sources).

4.1 Borehole geometry

The geometry of a borehole is given by the geometry of the well trajectory and the diameter of the well as a function of the depth.

The geometry of the trajectory is determined by azimuth and inclination of the well sections as a function of the depth. By convention

- inclination is defined as angle (in degrees) between the local vertical gravity vector and the tangent to the well bore axis at a particular point: 0° is vertical and 90° is horizontal.
- azimuth of a borehole at a point is the direction of the borehole on the horizontal plane. Azimuth is measured as a clockwise angle (0°–360°) from the North reference.

Inclination is necessary for transformation of "measured depth" MD to the "true vertical depth" TVD:

- Measured Depth (MD) is the distance measured along the borehole from the surface reference point.
- True Vertical Depth (TVD) is the distance measured vertically from the surface reference point.

Tools mostly work on the basis of gyro systems; older tools with magnetic systems are known as "single shot and multiple shot" instruments.

The diameter of the borehole as a function of the depth is measured with a Caliper log. There are two principles:

a) Mechanical systems (Figure 4-1): One or more pads are pressed against the borehole wall during upward motion. The angle between pad mechanism and tool axis is a measure of the pad distance from the tool axis. 2-arm, 3-arm, 4-arm and 6-arm caliper tools are in use. Sophisticated tools deliver the diameter in different azimuths with orientation from a gyro system. Frequently the pad holds other measuring systems (for example microresistivity).

Download free eBooks at bookboon.com

b) Acoustic systems: Ultrasonic Caliper or Acoustic borehole televiewer (see section 4.6) deliver a circular two-way travel time from the rotating transmitter-receiver-system to the borehole wall. Conversion into a distance via mud wave velocity gives a detailed azimuthal caliper.

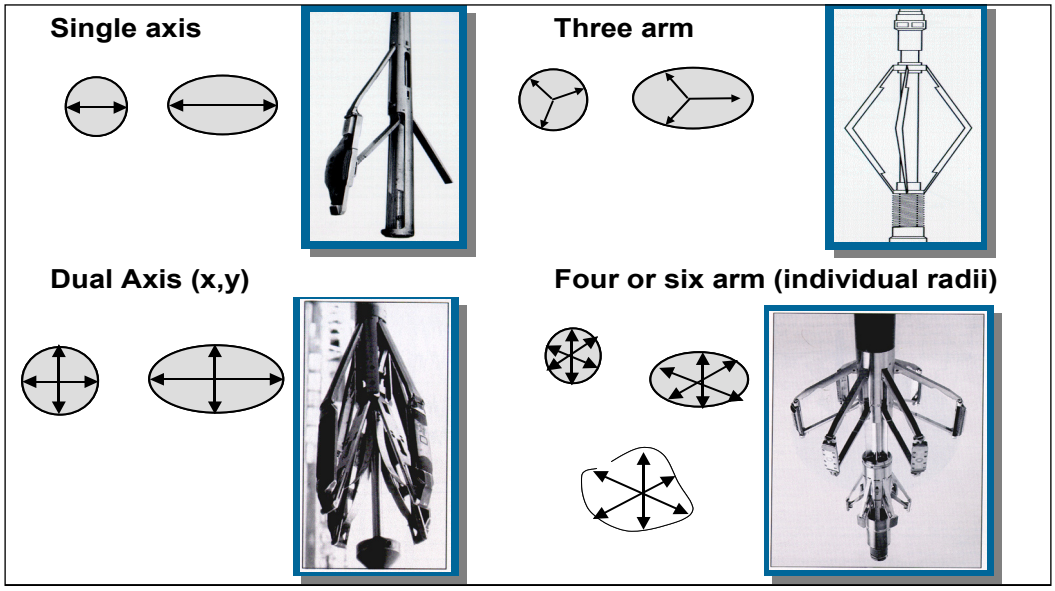

Figure 4-1: Different types of (mechanical) caliper tools (Bigelow 2002).

Caliper measurements can be done in open and cased wells with all borehole fluids (gas or air, water, water or oil-based mud).

The most important applications of caliper logs are:

- Borehole geometry and stability, breakouts,
- Indication of permeable zones (mud cake),
- Thickness of mudcake,
- Indication of fractured zones,
- Borehole volume (for cementation operations).

The caliperlog delivers very important input for caliper-correction of many borehole measurements, for quality control, and for identification of "bad hole situation". Therefore caliper logs are auxiliary to the other measurements.
The caliperlog is part of a graphic log presentation (mostly left trace). It is mostly named CAL or CALI and presented in inch or cm.

Download free eBooks at bookboon.com

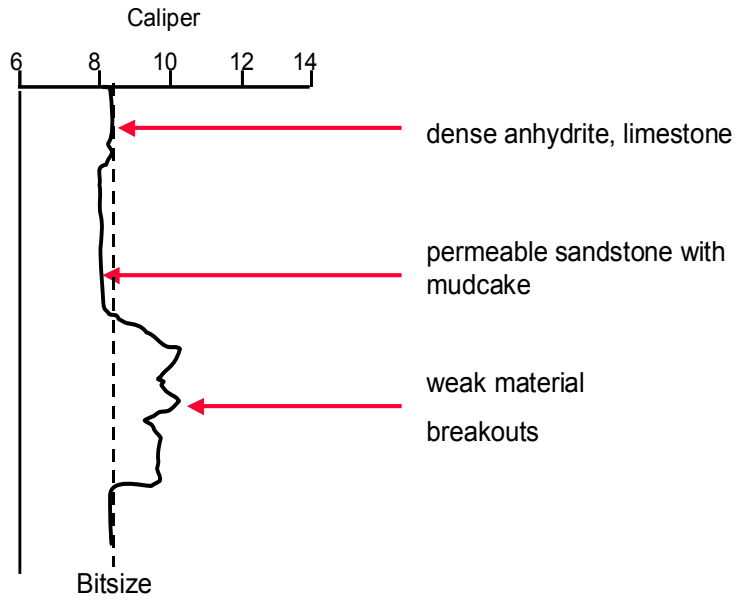

Figure 4-2: Caliperlog in different formations.

Maastricht University Leading in Learning!

Join the best at the Maastricht University School of Business and Economics!

Top master's programmes
- 33rd place Financial Times worldwide ranking: MSc International Business
- 1st place: MSc International Business
- 1st place: MSc Financial Economics
- 2nd place: MSc Management of Learning
- 2nd place: MSc Economics
- 2nd place: MSc Econometrics and Operations Research
- 2nd place: MSc Global Supply Chain Management and Change

Sources: Keuzegids Master ranking 2013; Elsevier 'Beste Studies' ranking 2012; Financial Times Global Masters in Management ranking 2012

Maastricht University is the best specialist university in the Netherlands (Elsevier)

Visit us and find out why we are the best!
Master's Open Day: 22 February 2014

www.mastersopenday.nl

Click on the ad to read more

Download free eBooks at bookboon.com

4.2 Electrical and electromagnetic logs

In 1927 the Schlumberger brothers started the development of well logging with the first electrical resistivity measurement. In 1942 Archie published the fundamentals of interpretation of electrical resistivity logs with his famous equations. Both – resistivity measurement and Archie-based interpretation – are also today's cornerstones of well logging particularly for determination of water saturation.
The resistivity of a formation is a key parameter in determining hydrocarbon saturation. Electricity can pass through a clean formation only because of the conductive water it contains.

Electrical (galvanic) and electromagnetic (inductive) logs measure the electrical resistivity or conductivity of the formation as a function of the depth.

Measurements are possible in open holes.

- Galvanic resistivity measurements using electrodes are possible only in conductive water-based mud,
- Inductive conductivity measurements using antennas are possible in non-conductive oil-based mud or dry wells and also in water-based mud.

Tools have different radial depth of investigation, are influenced by invaded and non-invaded zone in different ways and indicate permeable, invaded zones by log separation. Processing delivers resistivity of invaded and of non-invaded zone. Sophisticated array tools deliver a dataset for detailed inversion techniques.

Application:

- Determination of water saturation (Archie equations),
- Characterization of the invasion process.

4.2.1 Specific electrical resistivity of rocks

Formation resistivity covers a broad range of magnitudes from about 0.1 to 1000 Ohm-m, depending on porosity, water saturation, salinity, and shalyness. Resistivities higher than 1000 Ohm-m are typical of impervious, very low-porosity formations (e.g., evaporates).

Clean rocks – Archie's (1942) equations:

In a "clean porous rock" (for example sandstone without clay and/or other conductive solid components), the formation water is the only electrically conductive component, because matrix (quartz) and hydrocarbons or air in the pore space are insulators. In this case the specific resistivity of the rock is proportional to the specific resistivity of the pore water.

Download free eBooks at bookboon.com

The specific resistivity of the formation water is a function of salinity (concentration of dissolved salts) and temperature (see nomogram Figure 4-3).

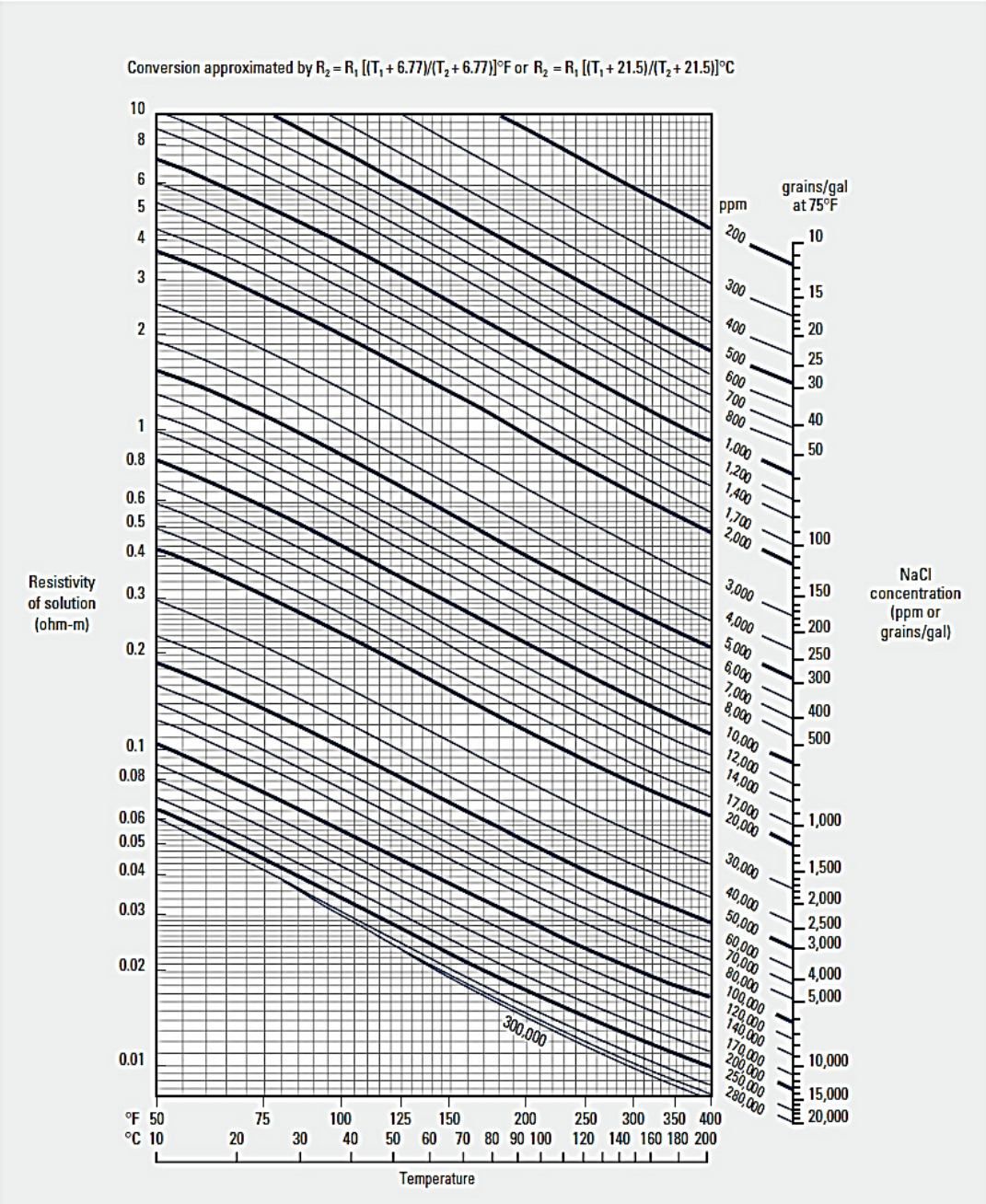

Figure 4-3: Schlumberger Log Interpretation Charts (2000 Edition)

The temperature-dependence of NaCl-based water can be described by Arps' equation (Arps, 1953)

$$R_w(T_2) = R_w(T_1) \cdot \frac{T_1 + 21.5}{T_2 + 21.5}$$

Download free eBooks at bookboon.com

where temperatures T_1 and T_2 are in °Celsius, or

$$R_w(T_2) = R_w(T_1) \cdot \frac{T_1 + 6.77}{T_2 + 6.77}$$

where temperatures T_1 and T_2 are in °Fahrenheit.

The proportionality between rock resistivity and formation water resistivity is the fundamental idea of Archie's (1942) equations which describe the relationship of rock resistivity to porosity and water saturation:

For a water-saturated porous rock ($S_w = 1$) the specific rock resistivity R_o is controlled by the resistivity of the pore water R_w

$$R_o = F \cdot R_w$$

The introduced formation resistivity factor F depends on porosity:

$$R_o = \frac{1}{\phi^m} \cdot R_w$$

Click on the ad to read more

Download free eBooks at bookboon.com

Where the exponent m is the cementation exponent (empirical) and is in the order of 2 for sandstones. In a plot of F versus porosity ϕ with logarithmically scaled axes this is represented as a straight line with the slope m (Figure 4-4).

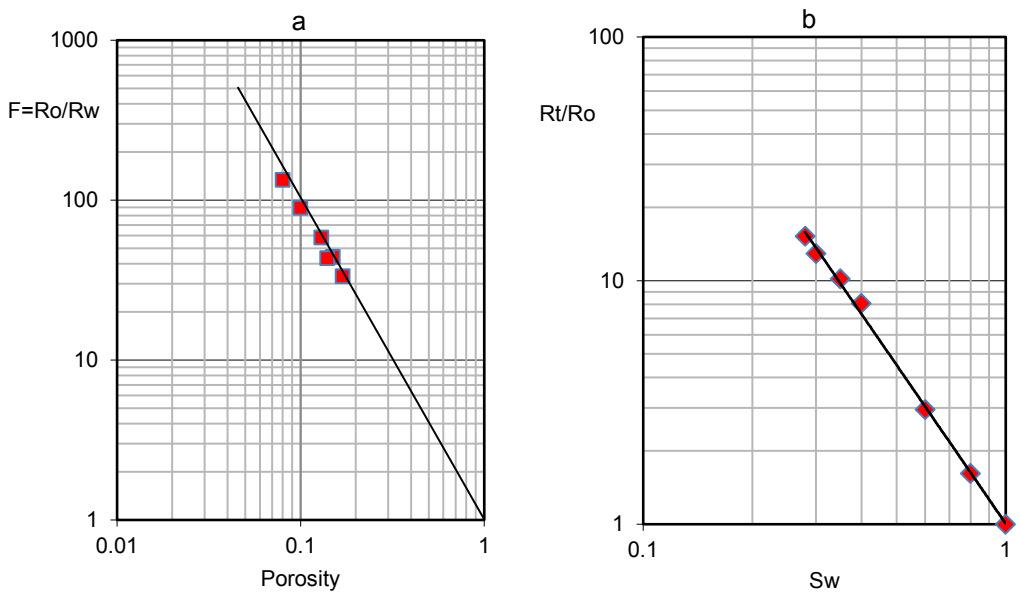

Figure 4-4: Archie's relationships (experimental data from Darling 2005):

a) Formation factor versus porosity; slope gives $m = 2.00$
b) esistivity index versus saturation (porosity = 0.17); slope gives $n = 2.16$.

For partial water saturation S_w, the specific rock resistivity R_t increases with decreasing water saturation. Archie (1942) formulated this by introducing a "resistivity index I" and referenced the rock resistivity R_t at any water saturation S_w to the rock resistivity at total water saturation R_o:

$$R_t = I \cdot R_0 = R_o \cdot S_w^{-n}$$

n is the empirical saturation exponent.

In a plot I versus water saturation S_w with logarithmically scaled axes (Figure 4-4), this is represented also by a straight line with the slope n.

Thus,

- the formation factor F expresses the magnification of the rock resistivity (compared with water resistivity) as result of the non-conductive solid minerals.
- the resistivity index I expresses the magnification of the rock resistivity (compared with water-saturated rock resistivity) as result of the non-conductive fluid components (oil, gas).

Download free eBooks at bookboon.com

The relationships deliver Archie's fundamental equation for water saturation calculation (see also examples, chapter 7):

$$S_w = \left(\frac{R_o}{R_t}\right)^{\frac{1}{n}} = \left(\frac{R_w}{R_t} \cdot \frac{1}{\phi^m}\right)^{\frac{1}{n}}$$

The two Archie exponents m and n are empirical rock parameters controlled by the geometry of the pore network and subject of special core analysis. Figure 4-5 describes the tendency of m for clastic and carbonate rocks.

Need help with your dissertation?

Get in-depth feedback & advice from experts in your topic area. Find out what you can do to improve the quality of your dissertation!

Get Help Now

Go to www.helpmyassignment.co.uk for more info

Helpmyassignment

Click on the ad to read more

Download free eBooks at bookboon.com

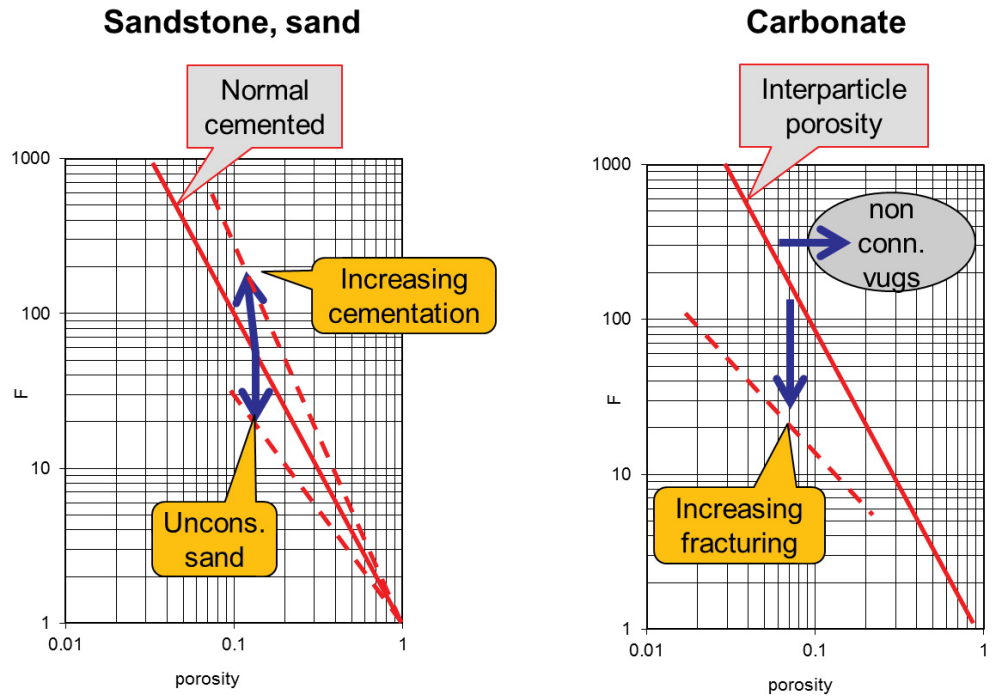

Figure 4-5: Formation factor versus porosity – tendencies for clastic (left) and carbonate (right) rocks.

In many cases (and if no other information is available) $m \approx n \approx 2$ is recommended for a first orientation. In this case the equation results in:

$$S_w = \sqrt{\frac{R_o}{R_t}} = \frac{1}{\phi} \cdot \sqrt{\frac{R_w}{R_t}}$$

Equation shows that for saturation calculation, the following input is necessary:

- The measured formation resistivity R_t,
- The formation resistivity at total water saturation R_o, or
- The porosity ϕ and water resistivity R_w.

The formation resistivity R_o at $S_w = 1$ can be

- estimated for a quick-look interpretation from a water zone in the same reservoir
- calculated from Archie's first equation with water resistivity R_w, an independent porosity determination (for example density, neutron, or acoustic measurements), and the exponent m (see examples chapter 7)

Download free eBooks at bookboon.com

In a permeable porous formation Archie's equation can be applied (compare Figure 4-6):

a) On the non-invaded zone in order to determine the water saturation S_w from formation resistivity R_t.

$$S_w = \left(\frac{R_o}{R_t}\right)^{\frac{1}{n}} = \left(\frac{R_w}{R_t} \cdot \frac{1}{\phi^m}\right)^{\frac{1}{n}}$$

The difference $(1 - S_w) = S_{hy}$ gives the hydrocarbon saturation.

b) On the invaded zone in order to determine the mud filtrate saturation S_{xo} from the resistivity of the invaded zone R_{xo} using mud filtrate resistivity R_{xo} as resistivity of the conductive fluid with the saturation equation in the form:

$$S_{xo} = \left(\frac{R_{mf}}{R_{xo}} \cdot \frac{1}{\phi^m}\right)^{\frac{1}{n}}$$

The difference $(1 - S_{xo}) = S_{hy,non-mov}$ gives the non-moveable (residual) hydrocarbon saturation (part of original fluid which is not displaced by infiltration). The fluid displacement is an indication of fluid mobility.

The terminology for resistivity and saturation is given in Figure 4-6.

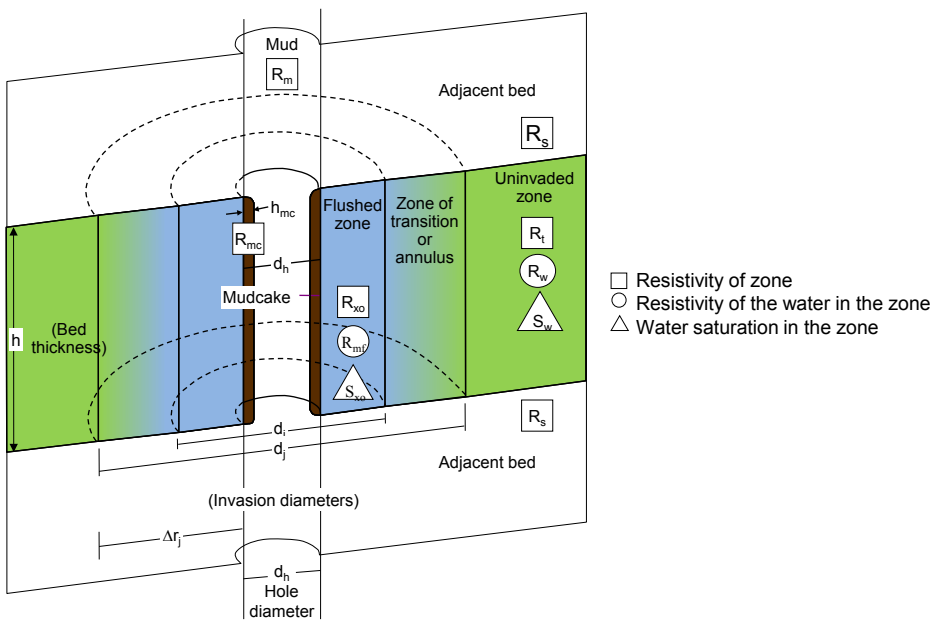

Figure 4-6: Symbols used in log interpretation (Schlumberger, 2000).

Download free eBooks at bookboon.com

Shaly rocks:

The presence of shale results in a decrease of reservoir quality (porosity, permeability) and "disturbs" traditional interpretation algorithms and techniques – particularly Sw determination using Archie's equation. Shale in the formation is a second conductivity component in addition to the formation water. "Shale conductivity" results from interface effects of clay minerals and adjacent electrolyte (formation water). Frequently this effect is described by the cation exchange capacity (CEC) of clay. Neglecting this conductivity contribution of shale to the measured conductivity (= resistivity^{-1}) results in an overestimate of the calculated water saturation. Some shaly sand equations eliminating this effect are discussed in section 5.6.2.

4.2.2 Electrical log measurement – Principles

In well logging a diversity of tools are applied to deliver a resistivity model of the formation mostly in terms of resistivity of the non-invaded (virgin) zone, resistivity of the invaded zone, and depth of invasion.

Electrical properties are measured in the open hole

- with galvanic tools (resistivity logs): Current is introduced via electrodes and the voltage is measured also via electrodes within a conductive (water-based) mud.
- with induction tools (induction logs): An electromagnetic field is introduced and measured via antennas which is also possible in non-conductive (oil-based) mud.

With different geometries of the electrodes and antennas the response of the tool can be directed to different radial zones (invaded zone, shallow-, medium-, and deep-reading tools).

In the MWD/LWD-technique specific high frequency propagation tools are used.

4.2.3 Resistivity tools

The first resistivity tools used 4 electrodes (current electrodes A and B, voltage electrodes M and N) in different geometry called Normal tool (Figure 4-7); a second 4 electrode type is the Gradient tool.

Download free eBooks at bookboon.com

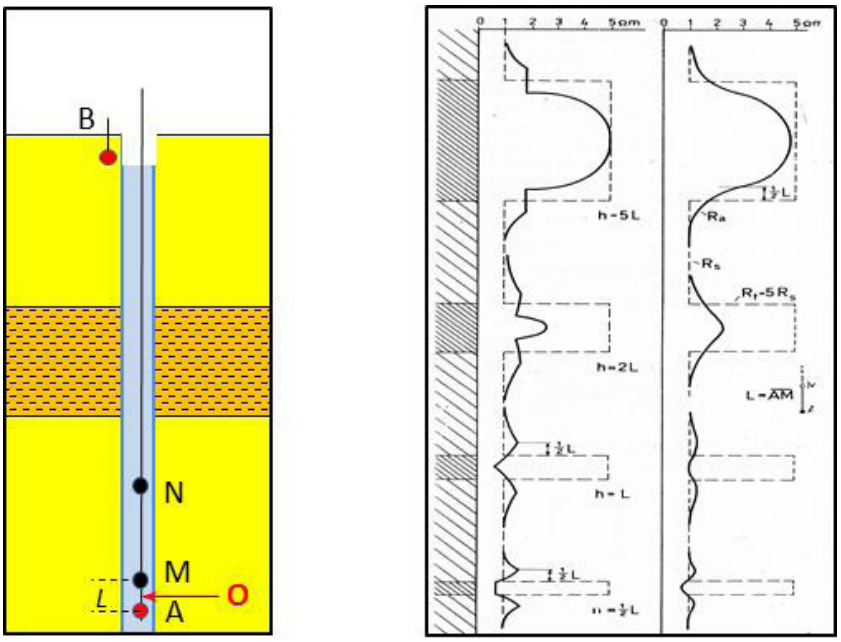

Figure 4-7: Left: Electrode configuration of a potential sonde (Normal); Right: Shape of resistivity curves (Normal) and influence of spacing *L* and bed thickness *h*. Left trace without mud influence, right trace with mud influence (Lehnert and Rothe, 1962; Fricke and Schön, 1999)

Click on the ad to read more

Download free eBooks at bookboon.com

Measured electrical parameters are the current I_{AB} and the Voltage U_{MN}. Then the resistance is U_{MN}/I_{AB}. The specific electrical resistivity of the formation R_t is connected with a factor k characterizing the geometry of the current distribution

$$R_t = \frac{U_{MN}}{I_{AB}} \cdot k$$

For the simple situation of the 4-electrode tool in a homogeneous medium this factor is

$$k = 4\pi \cdot \left(\frac{1}{\overline{AM}} - \frac{1}{\overline{BM}} - \frac{1}{\overline{AN}} + \frac{1}{\overline{BN}}\right)^{-1}$$

If the electrode B of a potential sonde is placed at a large distance from the other electrodes, the equation gets

$$k = 4\pi \cdot \left(\frac{1}{\overline{AM}} - \frac{1}{\overline{AN}}\right)^{-1}$$

The distance $\overline{AM} = L$ is called the "spacing". The red point O is the reference point of the electrode array: The measured magnitude is referenced to the depth of this position.

There are two standard configurations of 4-electrode normal tools:

a) Short Normal with the spacing L = 16 inch ≈ 0.40 m,
b) Long Normal with the spacing L = 64 inch ≈ 1.60 m.

Conventional 4-electrode tools have a moderate depth of investigation (depth increases with spacing) and no sharp vertical resolution (vertical resolution decreases with spacing). Figure 4-7b shows how the ratio of bed thickness h to spacing L controls the logged resistivity curve; there is no sharp step at the boundary but a smoothed shape called "shoulder bed effect".

Particularly in highly resistive formations the current from the electrode A has the tendency to miss the formation and prefer adjacent better conductive zones and the mud column. As a "hardware solution" of this problem[4], focusing electrode-systems or laterologs have been developed (Figure 4-8): Additional bucking or guard electrodes above and below the measuring current electrode A emit a current to focus the measuring current laterally into the formation. The guard current is regulated electronically in such a kind, that there is no potential difference between additional monitoring electrodes (focusing condition). With this technique three goals are attained:

a) Focused measuring current flow perpendicular to the tool,
b) Deep penetration of the focused current (into the uninvaded zone) and simultaneously,
c) Sharp vertical resolution.

Download free eBooks at bookboon.com

Non-focusing tool (normal device):

For non-focusing tools the "free current flow" avoids the highly resistive layer and takes the way of "lowest resistivity".

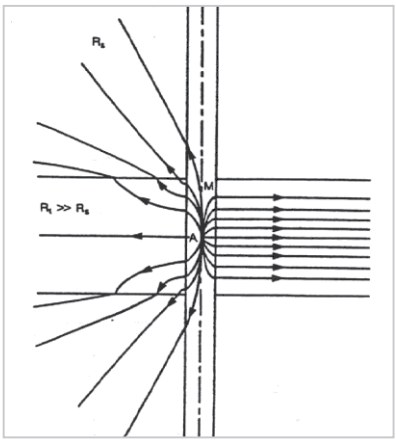

Focusing tool (Laterolog):

The additional bucking current from the guard electrodes presses the measuring current into the highly resistive formation.

Figure 4-8: Current lines in a highly resistive bed for conventional, non-focusing (left) and focusing (right) tools. Schlumberger (1989).

There are various devices in application; typical examples are:

- Dual Laterolog (with Deep and Shallow Laterolog),
- Laterolog 3 (uses cylindrical guard electrodes).

Figure 4-9 shows the Dual Laterolog with Deep and Shallow Current Patterns.

Focusing resistivity logs (Laterolog) and focusing induction logs (see next section) are powerful instruments for determination of the specific resistivity of the non-invaded formation R_t.

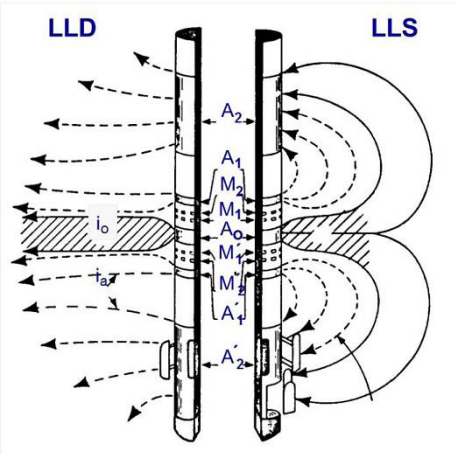

Figure 4-9: Dual Laterolog system with current pattern: Ao: Measurement current electrode, A1, A1', A2, A2': Bucking current electrodes, M1, M1', M2, M2': Monitoring electrodes (Baker Atlas, course material 2014).

Download free eBooks at bookboon.com

For investigation of the invaded zone (and the determination of R_{xo}) another tool type is applied – the family of micrologs. The electrode system is fixed on a pad and pressed against the borehole wall. The electrodes have a very short distance (microlog 2.5 cm) and therefore they are characterized by:

- Extreme vertical resolution, able to detect thin layers, but also fractures,
- Extremely small depth of investigation (R_{mc}, R_{xo}).

There are unfocussed systems (classic Microlog ML), as well as focussed systems (for example Microlaterolog MLL, MicroSphericalFocusing Log MFSL).

4.2.4 Induction tools (Inductionlogs)

Induction tools are developed for measurement of formation resistivity in boreholes containing oil-based muds and in air-drilled boreholes. Electrode devices did not work in these non-conductive muds.

Induction tools measure the formation conductivity (= specific resistivity^{-1}). An electromagnetic field with frequencies in the order of 20 kHz is transferred into the formation and measured on the basis of an electromagnetic coupling via antennas or coils (Maxwell's equations apply) instead of the galvanic coupling via electrodes in case of resistivity tools. Therefore induction tools also work in case of non-conductive mud or borehole fluid (oil-based mud or dry well).

TURN TO THE EXPERTS FOR
SUBSCRIPTION CONSULTANCY

Subscrybe is one of the leading companies in Europe when it comes to innovation and business development within subscription businesses.

We innovate new subscription business models or improve existing ones. We do business reviews of existing subscription businesses and we develope acquisition and retention strategies.

Learn more at linkedin.com/company/subscrybe or contact
Managing Director Morten Suhr Hansen at mha@subscrybe.dk

SUBSCRYBE - to the future

Click on the ad to read more

Download free eBooks at bookboon.com

Figure 4-10 illustrates the principle:

- A high-frequency alternating current of constant intensity is sent through the transmitter coil and generates an alternating primary magnetic field.
- This alternating primary magnetic field induces a circular alternating voltage and a current flow in the formation (the loop is coaxial with the transmitter coil) which is controlled by the conductivity of the formation.
- The current causes an alternating secondary magnetic field which is sensed by the receiver coils as an induced voltage.
- Thus, the measured signal is controlled by the tool parameters and formation conductivity.

Because the alternating current in the transmitter coil is of constant frequency and amplitude, the ground loop currents are directly proportional to the formation conductivity. The voltage induced in the receiver coil is proportional to the ground loop currents and thus also to the conductivity of the formation.

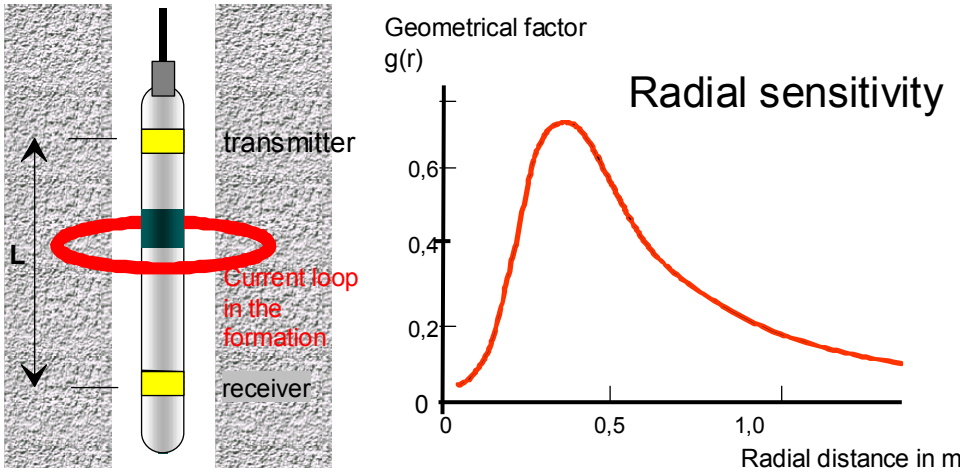

Figure 4-10: The Inductionlog – principle.

Focussing tools with different characteristics increase the vertical resolution and monitor different depths of investigation (deep and medium induction tool). Some typical induction tools are the Dual Induction Log and the Dual Phase Induction Tool (uses R- and X-signals). The Phasor-Induction SFL tool uses a conventional dual induction-SFL array to record resistivity data at three depths of investigation:

- Spherically focused log: Shallow-reading device affected mainly by the flushed (R_{xo}) zone (radial distance about 30 cm).
- Medium induction (ILM): Depending on the invasion diameter and profile the ILM may be influenced by the R_{xo} or R_t zones or both; (radial distance about 60…80 cm).
- Deep induction (ILD): Mostly affected by Rt, unless invasion is very deep.

Download free eBooks at bookboon.com

A specific tool type are induction tools with orthogonal transmitter-receiver systems (Section 4.2.6).

Since both types – resistivity and induction tools – can be used in water-based holes, some "rules of thumb" were formulated (Asquith and Krygowski, 2004; Schlumberger, 1989) for detection of hydrocarbons in exploration wells:

- For $R_{mf} < 2\ R_w$ use laterolog,
- For $R_{mf} > 2\ R_w$ use inductionlog.

The inductionlog gives a direct reading of R_t under conditions of fresh mud with $R_{mf}/R_w > 3$, shallow invasion and low formation resistivity.

4.2.5 Determination of true resistivity (Rxo and Rt)

In a water-bearing formation with low formation water resistivity R_w, the infiltration of the mud-filtrate with higher resistivity R_{mf} results in an increase of rock resistivity in the infiltrated (R_{xo}) zone compared with the non-invaded zone (R_o).

In a hydrocarbon-bearing formation the resistivity R_t is relatively high as result of lower water saturation S_w. Infiltration displaces a part of the original fluid (water and hydrocarbon) and results in a decrease of rock resistivity in the infiltrated zone (R_{xo}). This is illustrated in Figure 4-11). Two notes are important:

- The R_{xo}-level in the hydrocarbon-bearing formation is somewhat higher than the corresponding level in the water-saturated formation. This is the effect of a residual hydrocarbon volume $(1 - S_{xo})$ in the pore space which is not totally displaced by the mud filtrate. This gives important information about the moveable part of hydrocarbon.
- The magnitude of R_t in the hydrocarbon-bearing formation is controlled by porosity, water saturation, and formation water saturation. Therefore R_t can be low for highly saline formation water also in case of high hydrocarbon saturation.

Download free eBooks at bookboon.com

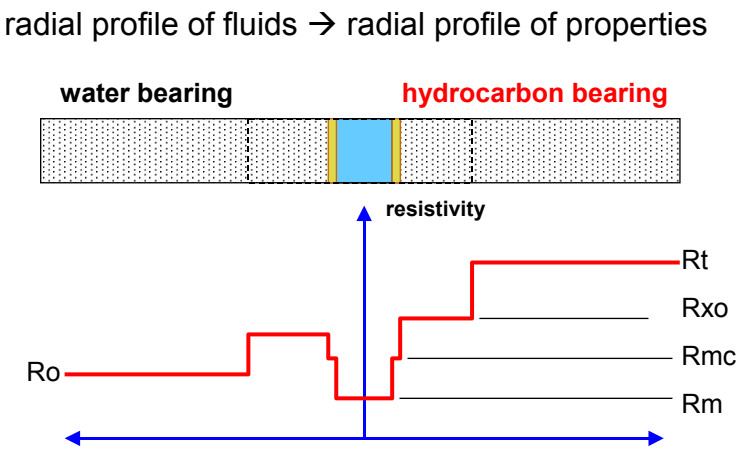

Figure 4-11: Resistivity profile for water-bearing (left) and a hydrocarbon-bearing (right) zones.

The different types of classic resistivity logs cover preferentially the following zones of a formation:

- The resistivity of the flushed zone R_{xo} controls dominantly Microlog (ML), Microlaterolog (MLL), Microsperically Focused log (MSFL).
- The resistivity of the non-invaded zone R_t controls dominantly Laterolog deep (LLD), Laterolog-3 (LL 3), Inductionlog deep (ILD). But all "deep-reading tools" are also influenced by the flushed zone, because current crosses this zone. Laterolog shallow (LLS) and Inductionlog medium (ILM) read a somewhat mixed effect of the non-invaded zone and the invaded zone.

The mission of resistivity measurements is the determination of R_t and R_{xo} for saturation calculation (S_w, S_{xo}). For a "Quick-look" estimate of R_{xo} a microresistivity tool is used in many cases and R_t is approximated by a "deep-reading" focused tool (e.g. LLD). A more exact technique is based on a graphic or numerical solution of the problem to derive "true resistivities" R_t,R_{xo} and d_i from a set of measured "apparent resistivities" (for example RMLL, RLLS and RLLD).

The principle can be demonstrated by application of the so called "tornado charts": Tornado charts are the result of a forward modeling of the response answer of tools with different formation resistivity models (given in terms of R_t, R_{xo}, d_i). Figure 4-12 shows the chart for a dual Laterolog-Rxo device combination for thick beds and 8 inch borehole.

The charts are plotted in logarithmic scale for resistivity ratios in general:

- The x-axis shows the ratio of the forward calculated ratio R_{LLD}/R_{LLS} and the y-axis the forward calculated ratio R_{LLD}/R_{xo},
- The parameter of the individual curves correspond to the model input (ratio R_t/R_{xo}, ratio R_t/R_{LLD}, and depth of invasion d_i) attributed to the calculated curves.

Download free eBooks at bookboon.com

The application includes the following steps (see example in Figure 4-12):

1. Take the measured resistivities R_{xo}, R_{LLS} and R_{LLD},
2. Calculate the ratios R_{LLD}/R_{LLS} and R_{LLD}/R_{xo},
3. Enter the abscissa and ordinate and plot the ratios on the chart.
4. The intersection of the lines is the solution of the problem in terms of R_t/R_{LLD}, R_t/R_{xo} and d_i.
5. Calculate the true resistivities R_t and R_{xo}.

Example:

We read from the log: R_{LLD} = 16 Ohmm	R_{LLS} = 10 Ohmm	R_{MSFL} = 4.5 Ohmm
Calculate the ratios:	R_{LLD}/R_{MSFL} = 3.56	R_{LLD}/R_{LLS} = 1.60
At the intersection we read:	R_t/R_{LLD} = 1.33	R_t/R_{xo}= 4.7 d_i = 36 inch
Therefore the result is:	R_t = 21.3 Ohmm	R_{xo} = 4.53 Ohmm

Please note:

a) The true resistivity of the non-invaded formation R_t = 21.3 Ohmm is distinctly higher than the measured resistivity of the deepest reading tool R_{LLD} = 10 Ohmm. This results from the influence of the lower resistivity (4.53 Ohmm) of the invaded zone (d_i = 36 inch). Neglecting this effect would result in an overestimate of S_w.
b) The true resistivity of the invaded zone R_{xo} = 4.53 Ohmm is close to the measured resistivity of the micro tool R_{MSFL} = 4.5 Ohmm.

Download free eBooks at bookboon.com

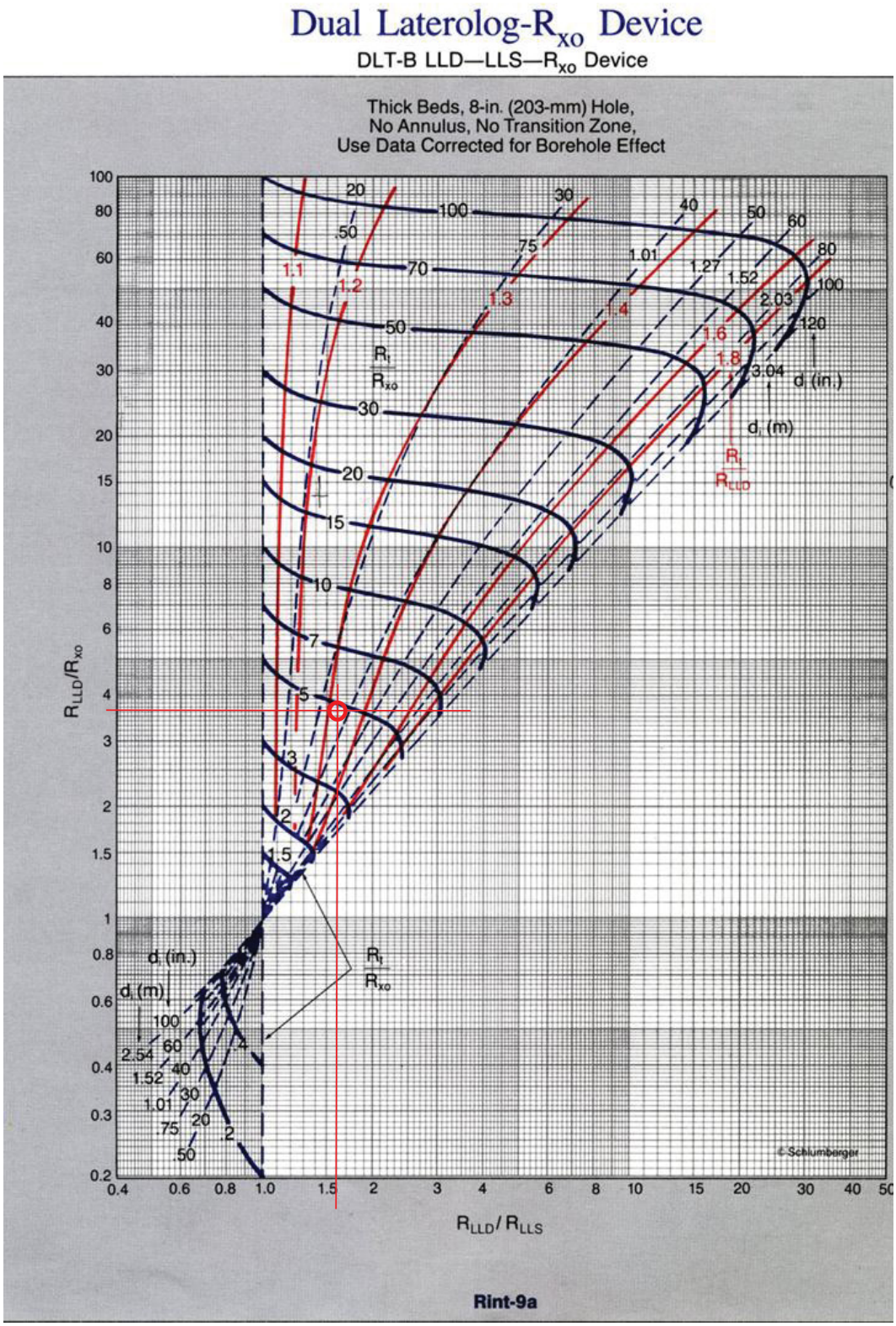

Figure 4-12: Tornado Chart for a Dual Laterolog-Rxo device combination with an example; Chart: Schlumberger (2000).

Download free eBooks at bookboon.com

4.2.6 Some sophisticated tools and methods

Resistivity calculation by an inversion process: The principle of this modern technique (see Figure 4-13) is:

1. Measure a set of resistivity/conductivity data with various electrode or antenna combinations (array configuration) with different spatial response,
2. Derive (computer-supported) an initial resistivity/conductivity earth model,
3. Run a forward calculation with this information to get the response for your individual array configurations,
4. Compare forward-calculated data with measured data and run an iteration process in order to get the best fit resistivity/conductivity model as result.

Prominent examples for this technology are:

High-Resolution Laterlog Array HRLA (Schlumberger): The tool has five independent, actively focused, depth- and resolution-matched measurements. These measurements, with a 2D earth model and inversion scheme, simultaneously account for borehole, shoulder-bed and invasion effects and gives an accurate, more robust R_t.

Click on the ad to read more

Download free eBooks at bookboon.com

Array Induction Imager Tool AIT (Schlumberger): The AIT sonde contains eight induction arrays with spacings ranging from several inches to several feet. A single transmitter operates simultaneously at three frequencies, with adjacent frequency pairs utilized by six of the arrays. – In-phase (R) and quadrature (X) signal components are measured for each array and each frequency to provide 28 induction-array measurements acquired at 3-inch depth intervals. – The 28 array conductivity measurements are borehole-corrected and combined using functions weighted in both the r (radial) and z (depth) directions to produce a set of five logs. The logs have median depths of investigations of 10, 20, 30, 60 and 90 inch from the center of the borehole. The deep-reading logs are quite insensitive to the borehole and the near-wellbore region.

Azimuthal Resistivity Imager ARI (Schlumberger): The ARI makes directional deep measurements around the borehole with high vertical resolution. Tool uses 12 azimuthal electrodes (incorporated in a dual laterolog array) and results in an azimuthal resistivity display.

Click on the ad to read more

Download free eBooks at bookboon.com

Orthogonal systems: Tool examples are 3DEX (Baker Atlas) and Rt Scanner (Schlumberger). Motivation for these tools are mainly laminated reservoirs: Since the tool cannot resolve the individual layer, the measured parameter represents an "averaged" value, depending on the response characteristic of the tool. Measurements in different directions result in different resistivities ("macroscopic anisotropy"). Derivation of a horizontal and a vertical resistivity allows a more precise determination of the resistivity of the sand fraction (reservoir component) and detects anisotropy in general (Mollison et al., 1999; Schoen et al., 1999, 2000).

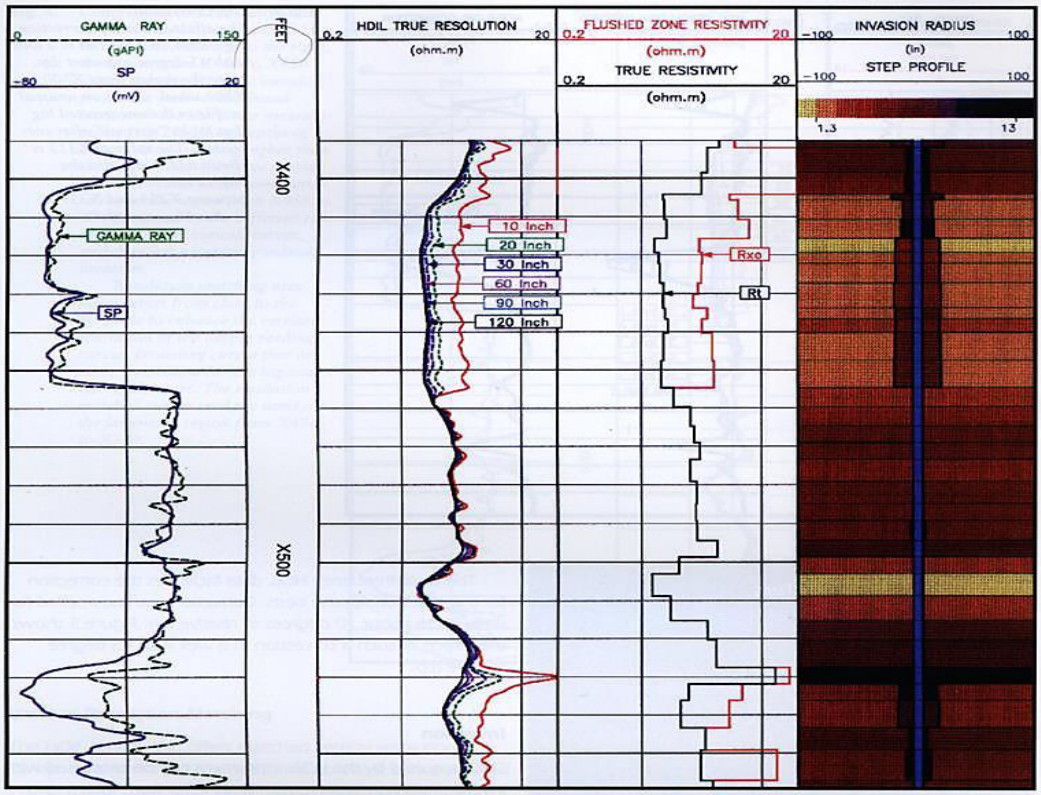

Fig. 6. *Inversion Results*
The radius of invasion can be seen in this two-dimensional color image where the colors represent resistivity values. In this case the inversion only needed one radial boundary to match the log data. If more complex invasion profiles are indicated, the inversion scheme will add more boundaries.The inversion process searches for a two-dimensional model of the formation which is consistent with the acquired data. If more than one model is possible, this particular inversion scheme will choose the simplest, or the one with the least number of boundaries. We can use the resistivity of the regions furthest from the borehole as an estimate of true virgin formation resistivity, and we can use the resistivity of the regions closest to the borehole as an estimate of the resistivity of the zone fully flushed with mud filtrate.

Figure 4-13: Derivation of a resistivity model by an inversion process; data are measured using an multielectrode resistivity device. – Inversion result: The radius of invasion can be seen in this two-dimensional color image where the colors represent resistivity values. In this case the inversion only need one radial boundary to match the log data. We can use the resistivity of the regions furthest from the borehole as an estimate of true virgin formation resistivity, and we canuse the resistivity of the regions closest to the borehole as an estimate of the resistivity of the zone fully flushed with mud filtrate (Baker Atlas Document, course material 2014).

Download free eBooks at bookboon.com

4.2.7 Spontaneous potential (SP)

Spontaneous potential SP is a natural electrical potential (very small voltage, given in mV) observed in a water-based mud-filled borehole. This voltage is measured by a downhole electrode relative to a reference electrode. The SP is measured mostly simultaneously with the resistivity log in an open hole with water-based mud.

The origin of spontaneous potential (Figure 4-14) is a charge exchange process driven by the difference of concentration (salinity) between formation water C_w and the mud filtrate C_{mf}. The concentration difference (in most cases is $C_w > C_{mf}$) results in an ion motion controlled by the electrochemical properties of the

- permeable sandstone creating a negative diffusion potential E_D as result of the higher mobility of the positive Na-ions
- non-permeable shale creating a positive membrane potential E_M as result of the anion-blocking (ion-selectivity) of the clay minerals.

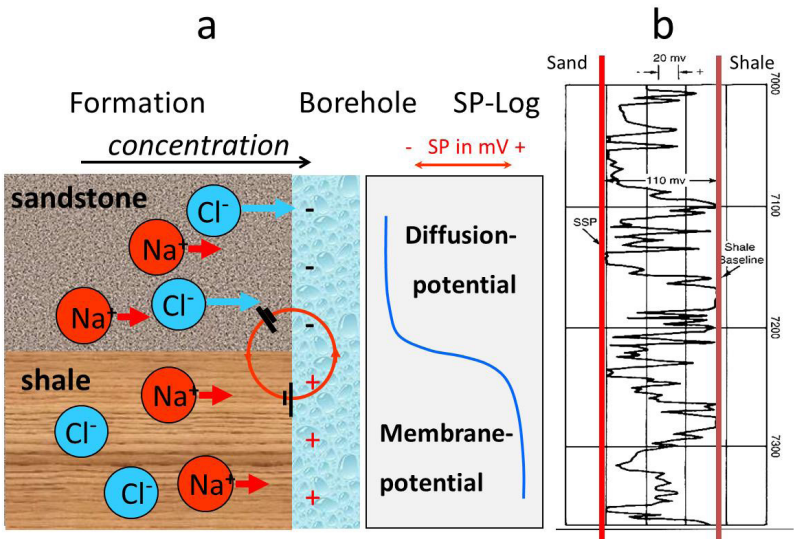

Figure 4-14: The Spontaneous Potential: a) Origin as result of an electrochemical interaction of formation water and mud/mud filtrate; b) Log example (sand-shale section).

SP as a relative measurement combines the effect of both components. The maximum difference between the most negative and the most positive level is called static spontaneous potential *SSP*

$$SSP = |E_D| + |E_M| = k_{SP} \cdot \log\left(\frac{C_w}{C_{mf}}\right)$$

Download free eBooks at bookboon.com

The parameter k_{SP} is controlled by temperature, type of dissolved salts (electrolyte), and membrane activity of shale; it is about 71 mV at 25 degrees Celsius (or degrees Fahrenheit) for NaCl. For practical application, the following empirical equation can be used (Desbrandes, 1985):

$$k_{SSP}(in\ mV) = 65 + 0.24\ \cdot T\ (in\ °C)$$

$$k_{SSP}(in\ mV) = 61 + 0.133\ \cdot T\ (in\ °F)$$

The SP-curve is influenced by several effects (correction charts eliminate most effects; see for example Schlumberger, 1989):

- Bed thickness and borehole size,
- Depth of invasion (correction charts),
- Hydrocarbons: $S_w < 1$ causes a reduced magnitude of the SP in the reservoir zone.

Frequently a "shale baseline shift" can be observed as result of a change of clay mineralogy, water mineralization and/or temperature with depth.

Click on the ad to read more

Download free eBooks at bookboon.com

There are two main applications of the SP-log:

1. Lithologic profile, sand – shale discrimination, and detection of permeable zones: The deflection of the SP-curve from a relatively stable "shale baseline" in a reservoir zone is negative if $R_{mf} > R_w$, positive if $R_{mf} < R_w$, and zero if $R_{mf} = R_w$.

   An estimate of the shale content is also possible with the following relationship

   $$V_{shale} = \frac{SP_{clean} - SP_{log}}{SP_{clean} - SP_{shale}}$$

   where
   SP_{clean} is the maximum SP deflection in a clean zone (wet) near the zone of interest,
   SP_{shale} is the SP magnitude of the shale base line,
   SP_{log} is the SP in the zone of interest (log).

2. R_w calculation: Since the electrolytes' specific electrical resistivity and concentration are inverse with a good approximation, the ratio C_w/C_{mf} can be replaced by the ratio R_{mf}/R_w

   $$SSP = k_{SP} \cdot \log\left(\frac{C_w}{C_{mf}}\right) = k_{SP} \cdot \log\left(\frac{R_{mf}}{R_w}\right)$$

   The resistivity of the formation water R_w is a fundamental input for calculation of water saturation. The equation offers the possibility of a determination from the SP-log at formation temperature without a water sample:
   For R_w determination, R_{mf} – the mud filtrate resistivity (at formation temperature), SSP – the difference between the SP level in a clean zone and the shale baseline, and T – the formation temperature are used as input.
   For R_w determination a nomogram is frequently used (see example 7.1 Oil-bearing Sandstone).

4.3 Nuclear logs

- Three main types of measurements: Gammalog, Gamma-Gammalogs, Neutronlogs.
- Measurements are possible in open and cased boreholes.
- For all nuclear measurements borehole corrections are necessary (e.g. caliper and mud correction).

Download free eBooks at bookboon.com

4.3.1 Introduction – Overview and fundamentals

Nuclear logs are an important group of log measurements using nuclear radiation. Measurements are possible in open hole and cased hole. Basic types of nuclear methods are

- Measurement of the natural gamma radiation of the formation (Gammalog)
- Measurement of the radiation as result of an interaction of the source-emitted radiation with the formation
    - Gamma-Gamma-logs (uses a gamma source),
    - Neutronlogs (uses a chemical neutron source or neutron generator).

Some fundamentals regarding the atomic structure, some terms and the statistic nature of the nuclear or radioactive processes will help to understand the function of the tools:

Interactions of radiation with the target material (formation) are processes connected with the atomic structure. Some properties and magnitudes of important with regard to these processes are summarized in Table 4-1.

	Mass	Electrical charge
Proton p^+	$1.67 \cdot 10^{-27}$ kg	$+1.602 \cdot 10^{-19}$ C
Neutron n	$1.67 \cdot 10^{-27}$ kg	neutral, ± 0
Electron e^-	$9.11 \cdot 10^{-31}$ kg	$-1.602 \cdot 10^{-19}$ C

Table 4-1: Atomic properties for nuclear measurements.

Radiation energy is given in Electronvolt (eV): 1 eV is the energy needed to move one electron with the charge of 1.6 10^{-19} C (Coulomb) through a potential difference of 1 Volt.

Nuclear processes are statistically determined. The statistical variation obeys a Poisson distribution with the standard deviation σ equal to the square root of the total number of counts N

$$\sigma = \sqrt{N}$$

It follows that the precision of a nuclear measurement depends on the number of counts recorded – therefore statistical precision can be improved by logging slowlier and/or using sensors with high sensitivity.

Download free eBooks at bookboon.com

4.3.2 Natural gamma measurement – Gammalog

Natural radioactivity is the spontaneous decay of a certain isotope into another isotope, characterized by emission of radiation. The three types of radiation (α, β, γ) have different ability to penetrate a material:

α, β : are particle radiation with a very shallow penetration or high absorption,
γ: is an electromagnetic wave with high penetration.

Therefore γ-radiation (gamma radiation) is preferred for practical application.

Natural gamma activity of minerals and rocks is originated by

- Uranium-radium series (half-life time of $4.4 \cdot 10^9$ years)
- Thorium series (half-life time of $1.4 \cdot 10^9$ years)
- Potassium K^{40} (half-life time of $1.3 \cdot 10^9$ years).

The result of emission at discrete energies for U- and Th-series and the monoenergetic radiation from K is a spectrum of radiation.

Occurrence and behavior of the three components in rocks are different. The abundance of these elements or isotopes in a formation controls the intensity of detectable natural radioactivity.

Click on the ad to read more

Download free eBooks at bookboon.com

Table 4-2 shows the mean content of K, U, and Th for some minerals.

Mineral	K in %	U in ppm	Th in ppm	Ref.
Plagioclase	0.54	0.02 … 5.0	… 3.0	BA
$NaAl/CaAl_2\ Si_2O_8$	0.54	0.2 … 5.0	0.5 … 3.0	Sch
Orthoclase	11.8 … 14.0	0.2 … 3.0	0.01 … 7.0	BA
$KAlSi_3O_8$ – monoclinic	11.8[a] (14 ideal)	0.2 … 3.0	3 … 7	Sch
Biotite	6.2 … 10.1 [8.5]	1 … 40	0.5 … 50	Sch
$K(Mg,Fe)_3(AlSi_3O_{10})(OH,F)_2$	6.7 … 8.3		< 0.01	BA
Muscovite	7.9 … 9.8		< 0.01	BA
$KAl_2(AlSi_3O_{10})(OH,F)_2$	7.9 (9.8 ideal)	2 … 8	10 … 25[b]	Sch
Illite	3.5 … 8.3 [6.1]	1.5	10 … 25	Sch
Kaolinite	0.42	1.5 … 3	6 … 19	BA
	0 … 0.6[d] [0.35]	1.5 … 9	6 … 42	Sch
Chlorite	0 … 0.35 [0.1]		3 … 5	Sch
Smectite	0 … 1.5	1 …. 21	6 … 44	Hu
Montmorillonite	0 … 4.9[c] [1.6]	2 … 5	10 … 24	Sch
Bauxite		3 … 30	10 … 132	Sch
Bentonite		1 … 36	4 … 55	Sch
Glauconite	3.2 … 5.8 [4.5]		< 10	Sch
Sylvite KCl	52.4			Sch
Carnallite $KCl\ MgCl_2(H_2O)_6$	14.1			Sch

a – Corresponds to beginning alteration.

b – Pure muscovite has no Th content. In sedimentary rocks, however, the deposition of muscovite (or micas) is generally accompanied by deposition of finer heavy minerals which are Th- and U-bearing.

c – Some montmorillonites might correspond to imperfectly degraded muscovite or to an incomplete transformation into illite by diagenesis.

d – Kaolinite sometimes contains more K due to imperfectly degraded feldspars. Authigenic kaolinite does not contain K and Th (Schlumberger 1989).

Table 4-2 K, U, and Th content of some minerals; values in [ ] are averages; Schön, 2011. Reference key: BA: Baker Atlas (1985); Sch: Schlumberger (1989).

Some accessory minerals have high U and Th content as for example Monazite with U = 500 … 3000 ppm and Th = (2.5 … 20) · 10^4 ppm.

Download free eBooks at bookboon.com

Table 4-2 shows

- Typical minerals forming the "clean" reservoirs (quartz, calcite, dolomite) have no gamma activity,
- Clay minerals in general are characterized by a higher content with a big scatter and different content of individual clay types,
- Mica and K-feldspar also show high concentration creating natural gamma radiation.

The spectral character of decay results in two techniques of measurement:

- Integral measurement – measures all incoming counts above an energy-threshold
- Spectral measurement – measures in energy-windows and delivers count rates (and concentration) for the three components K (in %), U and Th (in ppm).

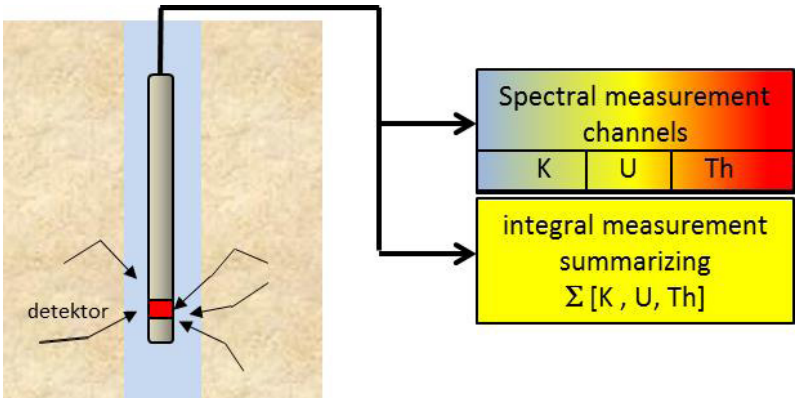

Figure 4-15: Gamma measurements – Principles.

Table 4-3 gives some technical parameters of Gammalogs.

Radius of investigation	4 in = 10 cm (50%) 11 in = 28 cm (90%)
Precision	± 4 … 5 API
Vertical resolution	18 … 36 in = 46 … 91 cm; 12 in = 30 cm enhanced resolution processing
Logging speed	< 10 feet/min = 3 m/min

Table 4-3 Gammalog – Some tool properties; Halliburton spectral gamma ray tool CSNG (after Asquith and Krygowsky, 2004)

Download free eBooks at bookboon.com

The following corrections are necessary:

- Absorption of radiation in the borehole fluid: influence of caliper and mud density,
- Tool position (centralized or sidewall): centralizing the tool decreases count rate,
- Mud type: KCl muds increase potassium count rate,
- Logging speed: influences statistics and vertical resolution.

Further details are presented for example in the companies' chart books.

Integral Gamma Measurement

With an integral gamma measurement (Gammaraylog GR) the summarized contributions of all three origins K (in %), U (in ppm), and Th (in ppm) are measured:

$$I_{GR} = k \cdot (a \cdot K + U + b \cdot Th)$$

The counts originated by each source-element are converted into equivalent U concentration by factors a and b.k is a factor characterizing the sensitivity of the sonde (determined by calibration).

Click on the ad to read more

Download free eBooks at bookboon.com

In most cases the "API-unit" (American Petroleum Institute) is applied as measurement unit. The API calibration facility is constructed of concrete with an admixture of radium to provide U decay series, monazite ore as a source of Th, and mica as a source of K. Figure 4-16 shows the general tendency of natural Gamma activity and Table 4-4 gives some mean magnitudes in API.

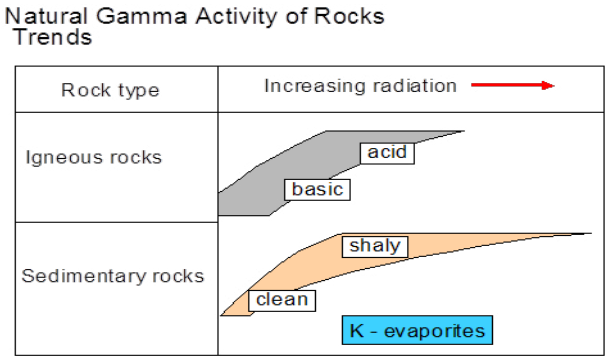

Figure 4-16: Radioactivity of Rocks – General tendency (Schoen 1989).

Material	Gamma in API
Quartz, calcite, dolomite (clean)	0
Plagioclase (albite, anorthite)	0
Alcali feldspar	≈ 220
Muscovite	≈ 270
Biotite	≈ 275
Kaolinite	80 …130
Illite	250 …300
Chlorite	180 … 250
Montmorillonite	150 … 200
Sylvite	500 +
Carnallite	≈ 220

Table 4-4: Mean API values for gamma activity; taken from Schön (2011; data from Schlumberger 2000).

Applications of the (integral) Gammalog are:

- Design of a lithological profile, particularly sand-shale separation, localization of "clean zones",
- Estimate of shale content,
- Depth adjustment: This processing step removes depth discrepancies between the different logging runs. Discrepancies are caused for example by cable stretch. One Gammalog is chosen as reference log for data quality. The other gamma logs are matched to the reference using an automatic routine. Resulting depth shifts are applied to the other logs on the tool strings.
- Lithological correlation from well to well if a number of wells is logged in a field.

Figure 4-17 shows an example for a sand-shale profile.

Download free eBooks at bookboon.com

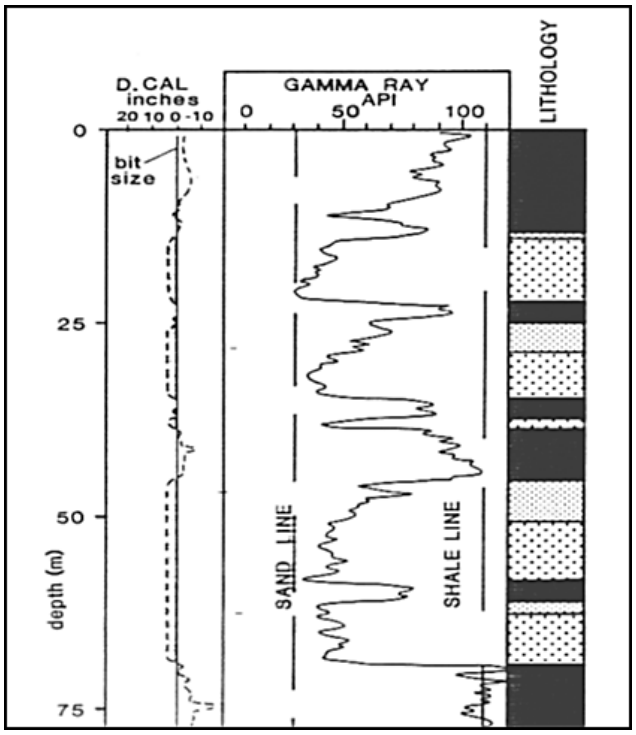

Figure 4-17: Sand-Shale Separation: It is recommended to plot a "Sand Line" first, connecting the minima of GR, then to plot a "Shale Line" as second step, connecting the maxima. By interpolation a qualitative lithological column can be plotted. sand layers as potential reservoir zones are clearly visible. Please consider also the effect at thin layers: Adjacent beds influence the "true" level of a thin layer.

In the first trace the difference of the bit size minus measured Caliper is plotted. Sandy zones show positive difference indicating the presence of mud cake. Thus, there are two completely different indicators for reservoir zones: Low gamma based on low shale content, and mud cake indicating permeability.

Another important application of the Gammalog is **calculation of the shale content** based on the correlation between shale content and gamma activity. It implements the assumption that only shale contains radioactive components in a rock and no other radioactive minerals (for example K-feldspar) are present.

Steps of shale content calculation are (see Figure 4-18 and Figure 4-19):

1) Analyzing the Gammalog and definition of the minimum level representing clean zones GR_{cn} and the maximum level representing pure shale GR_{sh}
2) Calculation of the "Gamma Ray Index" with the measured gamma values

$$I_{GR} = \frac{GR - GR_{cn}}{GR_{sh} - GR_{cn}}$$

Download free eBooks at bookboon.com

where

GR_{cn} is the log response in a clean zone – no shale

GR_{sh} is the log response in a shale zone

GR is the log response in the zone of interest.

This normalization of the logs results in $I_{GR} = 0$ for clean rocks (0% shale) and $I_{GR} = 1$ for pure shale (100% shale).

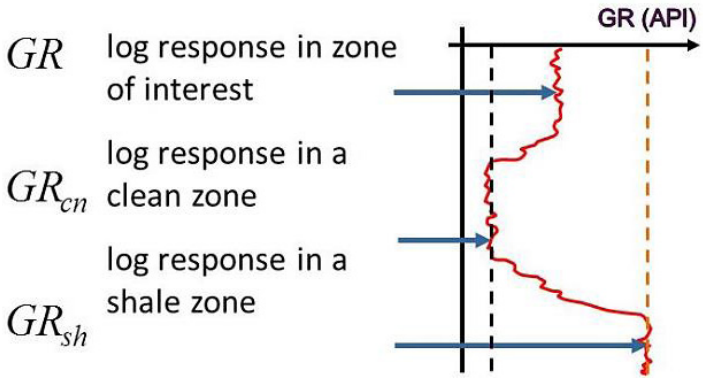

Figure 4-18: Derivation of the Gamma Ray Index – Principle.

3) an empirical equation is recommended in most cases because the Gamma Ray Index is not identical with the volumetric determined shale content (core analysis) (see also the nomogram in Figure 4-19):

$V_{sh} = I_{GR}$	Linear relationship (upper limit)
$V_{sh} = 0.083 \cdot \left(2^{3.7 \cdot I_{GR}} - 1\right)$	Tertiary clastics (Larionov, 1969)
$V_{sh} = 0.33 \cdot \left(2^{2.0 \cdot I_{GR}} - 1\right)$	Mesozoic and older rocks (Larionov, 1969)

Download free eBooks at bookboon.com

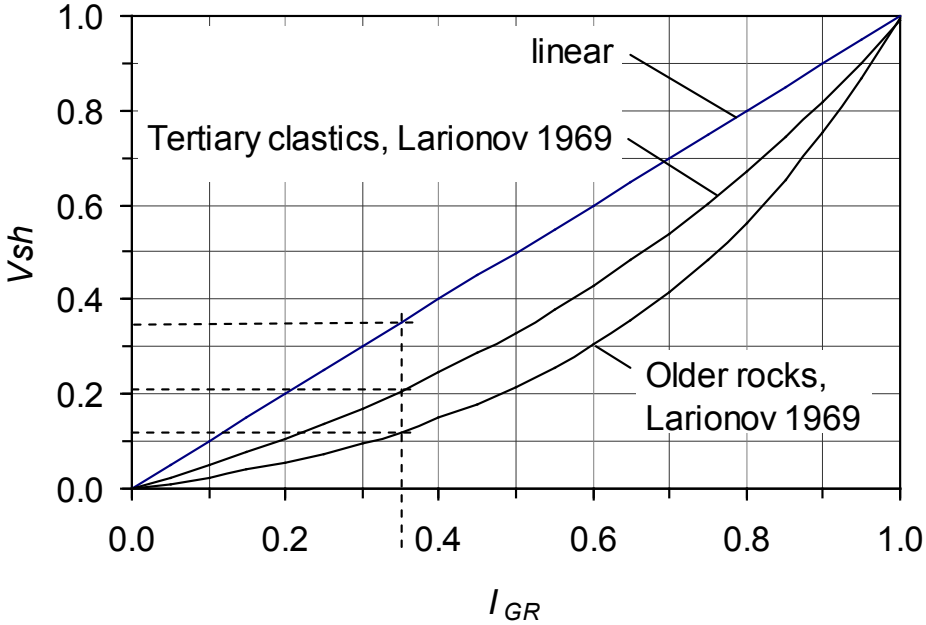

Figure 4-19: Determination of the shale content from Shale Index – Relationships between Gamma Ray Index I_{GR} and shale content V_{sh}.
Example: I_{GR} = 0.35 (dotted line) results in a V_{sh} = 0.35 for the linear equation, V_{sh} = 0.21 for Larionov equation/Tertiary clastics, and V_{sh} = 0.12 for Larionov equation/Mesozoic and older clastics.

Deloitte.

Discover the truth at www.deloitte.ca/careers

© Deloitte & Touche LLP and affiliated entities.

Click on the ad to read more

Download free eBooks at bookboon.com

If a spectral gamma measurement is available, it is recommended to use a Gamma Ray Index calculated only from K and Th. These two components are dominated by the mineral composition, whereas U is controlled more by the environment of sedimentation and organic components (Schön, 2011). Spectral measurement also helps to detect K-feldspar, mica or glauconite as origin of high radiation.

Particularly in carbonate series, the integral gamma intensity is very often a poor clay indicator, because the measured value is not related to clay content, but to the presence of uranium. A spectral measurement therefore gives more information. Typical cases are

- Pure carbonate (chemical origin) which has a thorium and potassium level near zero. If uranium is zero too, this carbonate was precipitated in an oxidizing environment.
- If there is variable uranium content, the carbonate can either have been deposited in a reducing environment, or it corresponds to a carbonate with stylolithes or to phosphate-bearing layers.
- If thorium and potassium are present along with uranium, this indicates a certain clay content of the carbonate.
- If potassium is present with or without uranium it can correspond to a carbonate of algal origin or a carbonate with glauconite (Schlumberger, 1982).

Figure 4-20 presents these tendencies for carbonate.

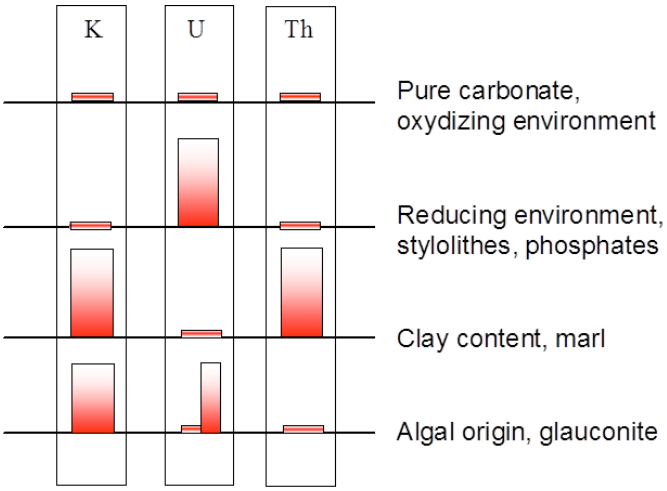

Figure 4-20: Gamma components in carbonates.

A kind of "clay mineral typing" is possible because clay minerals show different Th/K ratio (Figure 4-21).

Download free eBooks at bookboon.com

The high Uranium content of organic components is an indicator for source rocks and gives a link to TOC (Total Organic Content). – As rule of thumb, the Th/U ratio is recommended as an indicator for environment (Fertl, 1979):

Th/U > 7	continental, oxidizing
Th/U < 7	marine, grey…green shales
Th/U < 2	marine, black shales, phosphates.

Extremely high concentrations are observed in stagnant, anoxic waters with low rates of sediment deposition as they are typical of black shales (North Sea Jurassic "hot shales").

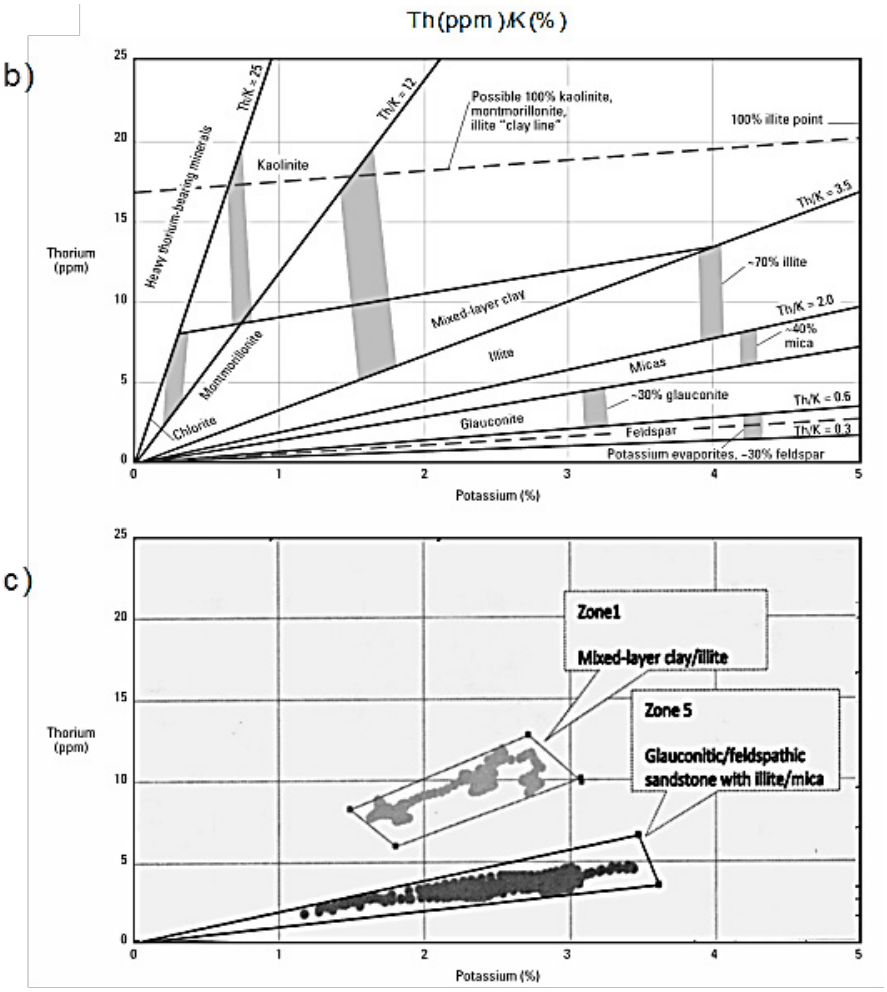

Figure 4-21: K vs. Th plot for clay mineral estimate from spectral Gammalog (Schlumberger, 2000, with permission). Data from spectral Gammalog in two zones in a Th vs. K plot with identified clay types (Mohammadlou et al., 2010).

Download free eBooks at bookboon.com

4.3.3 Gamma-Gamma-logs

Gamma-Gamma-methods use the interaction of gamma radiation produced by a source (as part of the tool) with the formation. The main components of a Gamma-Gamma-probe are (Figure 4-23):

- Gamma source (Cs or Co),
- One or more gamma detectors detecting the backscattered radiation,
- A shield between source and detectors to supress direct radiation.

There are three effects with regard to gamma material interaction:

1. Photoelectric effect,
2. Compton effect,
3. Pair production.

The probability of interaction depends on the energy of the gamma radiation and the atomic number of the target material (Figure 4-22). For most rock-forming elements and the commonly used Cs or Co source the Compton effect dominates. Observation of low energy components also controls the Photoelectric effect.

SIMPLY CLEVER
ŠKODA

Do you like cars? Would you like to be a part of a successful brand?
We will appreciate and reward both your enthusiasm and talent.
Send us your CV. You will be surprised where it can take you.
Send us your CV on
www.employerforlife.com
Click on the ad to read more

Download free eBooks at bookboon.com

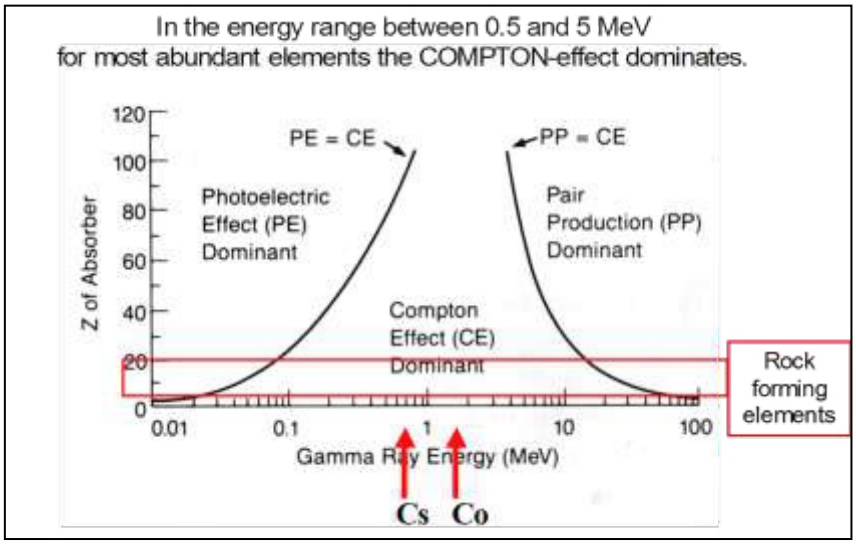

Figure 4-22: Gamma ray absorption effects (Hearst and Nelson 1985).

Interactions result in absorption of radiation and can be characterized by an absorption coefficient as a material property. The absorption coefficient is connected with the absorption cross section of the target material and related to the type of interaction. Thus there is an absorption coefficient for the Photoelectric effect and one for the Compton effect.

The **photoelectric** cross section shows a strong correlation to the atomic number *Z*. On this basis an effective photoelectric index *PE* (average photoelectric cross section per electron) is defined:

$$PE = (Z/10)^{3.6}$$

PE has the unit b/e (barns per electron).
The index *PE* strong depends on the on elemental composition and is therefore a typical characteristic of various minerals (Table 4-5). This presents a possibility for identification of rock types. *PE* can help to discriminate between quartz, calcite, and dolomite, and is extremely sensitive to barite (mud).

In case of several minerals in a formation, the photoelectric index is not a linear function of the *PE*-values of the mineral components, a second parameter *U* (volumetric photoelectric absorption index) was introduced

$$U = PE \cdot \rho$$

In a multimineral lithology this index is the volume weighted sum of the individual contributions.

Download free eBooks at bookboon.com

The **Compton Effect** is a scatter reaction with the orbiting electrons of the target material. Therefore the probability of an interaction is controlled by the number of electrons, which is equal to *Z*. For the most common earth minerals, the ratio *Z / A* is constant (Table 4-5).
Since rock bulk density ρ_b is dominated by atomic mass *A*, the following relationship connects the "electron density" ρ_e as seen by the Compton effect via this ratio:

$$\rho_b = 2 \cdot \left(\frac{Z}{A}\right) \cdot \rho_e \approx \rho_e$$

Mineral, fluid	ρ	$(Z/A)_{eff}$	ρ_{GG}	Pe	U
Quartz	2,654	0,499	2,650	1,81	4,79
Calcite	2,710	0,500	2,708	5,08	13,77
Dolomite	2,850	0,499	2,864	3,14	9,00
Anhydrite	2,960	0,499	2,957	5,05	14,95
Gypsum	2,320	0,511	2,372	3,42	8,11
Halite	2,165	0,479	2,074	4,65	9,65
Montmorillonite	2,12	0,500	2,12	2,04	7,28
Illite	2,65	0,496	2,63	3,55	10,97
Kaolinite	2,44	0,500	2,44	1,84	6,14
Barite	4,50	0,446	4,01	267	1070
Water (fresh)	1,000	0,555	1,110	0,36	0,40
Water (120000 ppm)	1,086	0,545	1,185	0,81	0,96
Oil (mean)	0,850	0,558	0,948	0,12	0,11

Table 4-5: Mean values for density ρ in 10^3 kg m^{-3} , electron density or Gamma-Gamma-density $\rho_e = \rho_{GG}$ in 10^3 kg m^{-3}, effective ratio Z/A, Photoelectric Absorption Index PE in barn/electron and volumetric photoelectric absorption index U in barn/cm^3 (data after Schlumberger, 1989; Hearst and Nelson, 1985; Schön, 1996)

Gamma-Gamma-probes (Figure 4-23) have two detectors with different spacing (distance between source and detector). For both spacings a different calibration function results. If irregularities of the borehole (rugosity etc.) exist, the short-spaced measurement is influenced more strongly than the long-spaced one and a correction or compensation of these effects is possible. The information delivered by these measurements are the corrected density (RHOB) and the applied density correction (DRHO).

DRHO is a significant measure of log quality (QC):

- Correction curve DRHO should be near zero in smooth holes,
- DRHO > 0.05: Data quality may be questionable due to loss of pad contact,
- DRHO > 0.10: Indicates that the density value is not reliable.

(adapted after Asquith and Krygowski, 2004).

Download free eBooks at bookboon.com

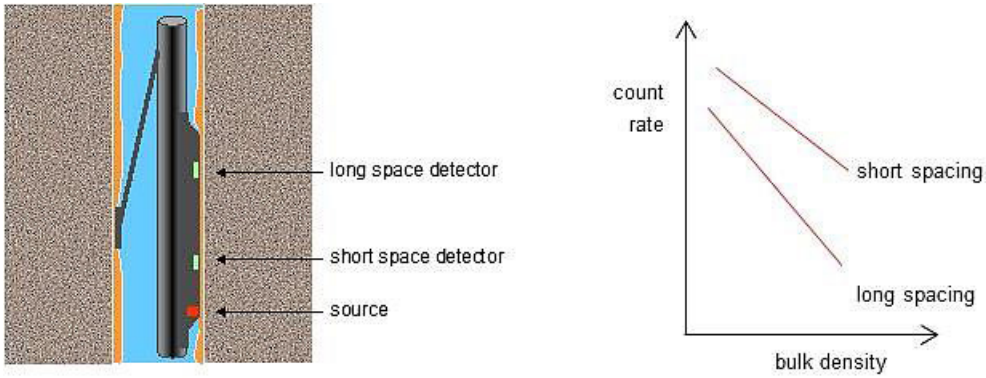

Figure 4-23: Compensated Density Tool (left) and calibration curves (right).

Table 4-6 gives some data for Gamma-Gamma-tools; please note the very small depth of investigation.

	Density	PE
Depth of investigation	1.5 in = 3.8 cm (50 %)	0.5 in = 1.3 cm (50 %)
Vertical resolution	33 in = 84 cm; 5.5 in = 14 cm enhanced resolution processing	33 in = 84 cm; 2 in = 5.1 cm enhanced resolution processing
Precision	± 0.01 g cm³	± 5 %
Logging speed	< 60 feet/min = 18 m/min lower for enhanced resolution processing	

Table 4-6: Gamma-Gamma-log – some data (after Asquith and Krygowsky, 2004; Halliburton spectral density tool (SDL)).

The following applications of Gamma-Gamma-Densitylogs are of special interest:

1. Determination of porosity (see below) from GG-Densitylog
2. Derivation of porosity and mineralogy from combined interpretation of Gamma-Gamma-density and Neutronlog (see section 5) or/and PE-measurement)
3. Density determination for general rock characterization and as input for seismic processing techniques (synthetic seismograms).

Porosity determination from density measurement is based on a volumetric model (Figure 2-6). The measured bulk density of a porous rock is

$$\rho_{GG} = \rho_b = (1 - \phi) \cdot \rho_{matrix} + \phi \cdot \rho_{fluid}$$

and the porosity results as

$$\phi = \frac{\rho_{matrix} - \rho_b}{\rho_{matrix} - \rho_{fluid}}$$

Download free eBooks at bookboon.com

Thus, for porosity calculation from GG-density two input parameters are necessary:

1. Matrix density (or an information about mineralogy),
2. Fluid density: The depth of investigation for GG-measurements is very shallow (Table 4-6); thus, the measurement is controlled by the flushed zone in most cases and the density of mud filtrate can be used. Only in case of shallow gas invasion density is lowered; for calculation an average fluid density of 0.7 g/cm^3 is recommended (see Asquith and Krygovsky, 2004).

4.3.4 Neutron methods

Neutron methods use the interaction of neutron radiation from a source (as part of the tool) and the formation. The main components of a neutron probe are: The neutron source (chemical source or neutron generator), one or more detectors (neutron and gamma) detecting neutron radiation after slowing down processes and induced gamma radiation, and a shield between source and detectors to supress direct radiation.

Neutrons are classified by their energy:

- Fast neutrons > 500 keV,
- Intermediate neutrons 500 … 1 keV,
- Slow neutrons < 1 keV (epithermal 1 … 0.1 keV, thermal < 0.1 keV).

Click on the ad to read more

Download free eBooks at bookboon.com

Neutrons as a particle radiation (a neutron has approximately the same mass as a proton) react with the nuclei of the target material. There are different types of interaction:

1. Moderating interactions result in an energy decrease (slowing down effect)
   a) Inelastic scattering
   b) Elastic scattering
2. Capturing interactions.

Figure 4-24 illustrates the processes during the life of a neutron and will be described from the high to the low energy level in the following section.

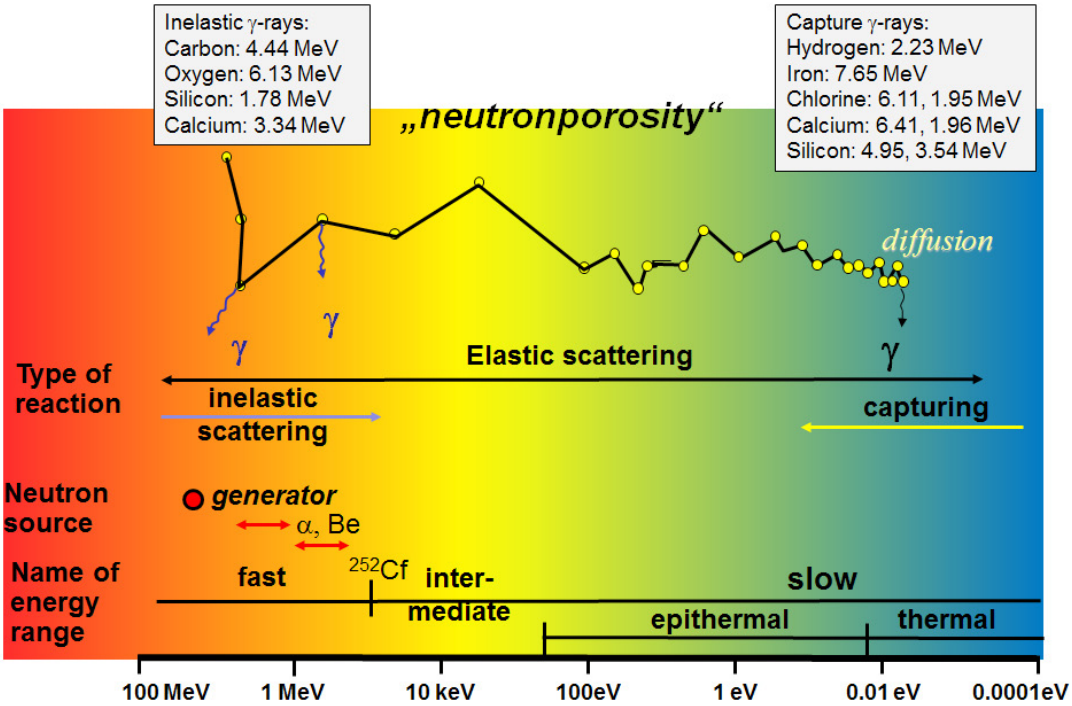

Figure 4-24: Neutron phenomena as a function of energy (in MeV). The neutron sources and the energy regions are indicated at the bottom. At the top are the types of reactions and processes plotted (adapted after a figure from Hearst and Nelson, 1985).

Inelastic Scattering:

Neutrons collide with a nucleus and transfers a fraction of their kinetic energy to the nucleus, which results in the nucleus' excitation, followed by the emission of a characteristic gamma photon (de-excitation). The emitted gamma radiation is characteristic for the target element (see Table 4-7). An application is the Carbon/Oxygen log.

Download free eBooks at bookboon.com

Elastic Scattering:
Neutrons collide with the atomic nucleus and lose kinetic energy. The maximum energy loss results for a target material with the same atomic mass as the neutron; this is the case for hydrogen. The other rock forming elements have a lower slowing down effect and are different (see Table 4-8). This leads to the conclusion:

- Elastic scattering is dominated by Hydrogen in the formation; therefore a strong contribution is expected from the liquids with a high H-concentration (water and oil) and a somewhat lower contribution from gas with a some lower H-concentration. In general, elastic scattering is dominated by pore fluids.
- Other elements have a distinctly smaller effect; but this effect is different for each element. Therefore a different neutron response for different minerals (quartz, calcite, and dolomite) is expected.

Element	Gamma energy in MeV - inelastic scattering -	Gamma energy in MeV - capturing -
H		2.2
O	6.1, 7.0	
C	4.43	
Si	1.78	3.5, 4.9
S	2.2	3.2, 4.9, 5.4
Ca	3.7	2.0, 4.4, 6.4
Al	2.2	7.7
Mg		3.9
Fe		6.0, 7.3, 7.6

Table 4-7: Inelastic scattering and capturing—Some characteristic energies of emitted gamma radiation (Hearst and Nelson, 1985; Schön, 2013).

Element	n	Element	n
H	19	Al	290
C	112	Si	297
O	154	Cl	343
Mg	235	Ca	380

Table 4-8: Averaged number of collisions *n* required to thermalize a 14-MeV neutron (Hearst and Nelson, 1985).

Neutrons can be captured when they are thermalized. With this process a compound nucleus in an excited state is formed. When it returns to the ground state, it and emits gamma radiation with an exactly defined energy (see Table 4-7). The capturing effect is used with the TDT Log (Thermal neutron diffusion/decay measurements).

Download free eBooks at bookboon.com

Neutronlog for porosity determination – Tools and calibration

For neutron porosity measurement elastic scattering is applied using the dominant effect of hydrogen as component of pore fluids. The relationship between measured neutron readings and porosity is determined by calibration. Most tools are "limestone-calibrated" (Figure 4-25). Therefore the calibration curve relates the neutron reading (response) to the porosity of a fresh water saturated limestone. Different mineral composition and different pore fluids result in a deviation from the porosity defined as the ratio of pore volume divided by sample volume.

Tool examples are the SNP – Sidewall neutron porosity tool (Schlumberger) – and the CNL – Compensated Neutronlog (Schlumberger).

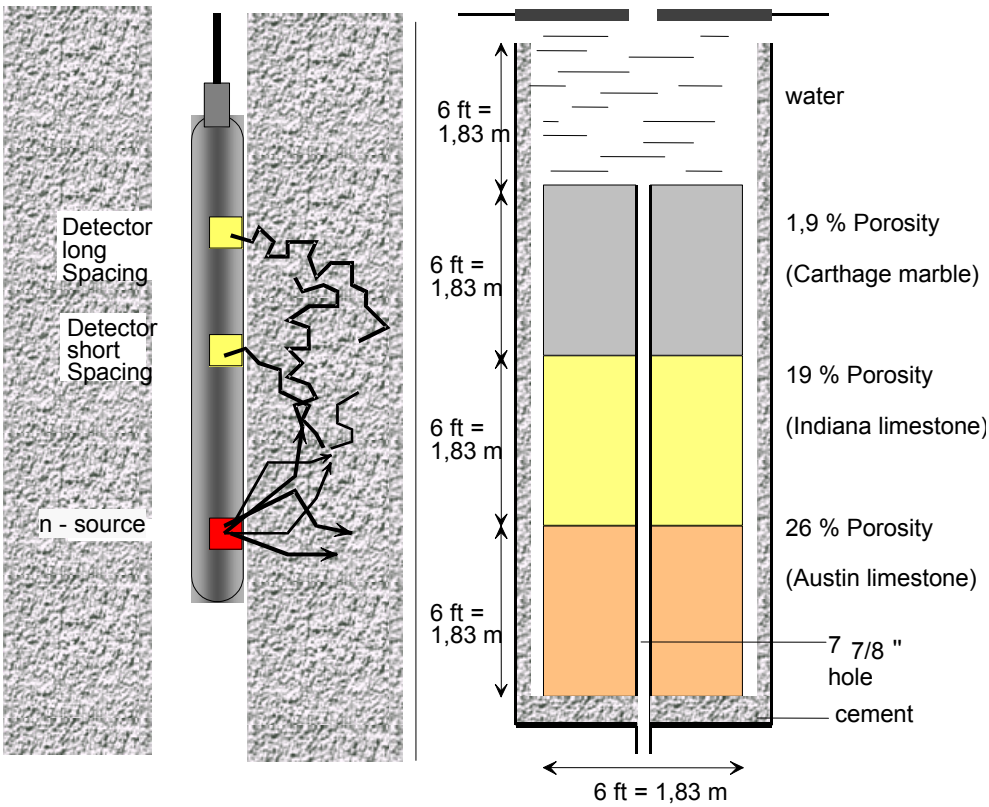

Figure 4-25: Neutronlog – Principle of tool and calibration facility.

	thermal	epithermal	neutron-gamma
Radius of investigation	6 in = 15 cm (50 %)		8 in = 20 cm (50 %)
Vertical resolution	36 in = 84 cm; 20 in = 51 cm enhanced resolution processing	30 … 44 in = 76 … 112 cm	20 in = 51 cm
Precision	0.4 p.u	1 p.u.	
Logging speed	< 60 feet/min = 18 m/min Lower for enhanced resolution processing		

Table 4-9: Neutronlog – Some data (after Asquith and Krygowsky, 2004; Halliburton neutron tool (DSN-II)

Download free eBooks at bookboon.com

Since the neutron tool is calibrated for a limestone matrix and fresh water as the pore fluid, only for this situation, the measured neutron porosity is exactly the true porosity. For a different formation and/or pore fluids, corrections are necessary:

- Other matrix materials (sandstone, dolomite) have a different neutron effect in comparison with limestone;
- Particularly shale has a high amount of H and this results in a high neutron porosity → a shale correction is necessary; the Neutronlog can be used as a shale indicator.
- Other pore fluids than fresh water have a different H-concentration. This is expressed by the "hydrogen index" (Table 4-10).

Figure 4-26 shows a simplified picture of a porous rock with the various solid and fluid components. As a general rule the different responses indicate that:

- For a water- or oil-saturated rock, the neutron response reflects mainly porosity, whereas gas (with a lower H-content/volume) has a lower neutron effect.
- The solid minerals in general have a small – but not negligible – influence ("matrix effect").
- Shale with a high amount of bound water can have a strong effect.

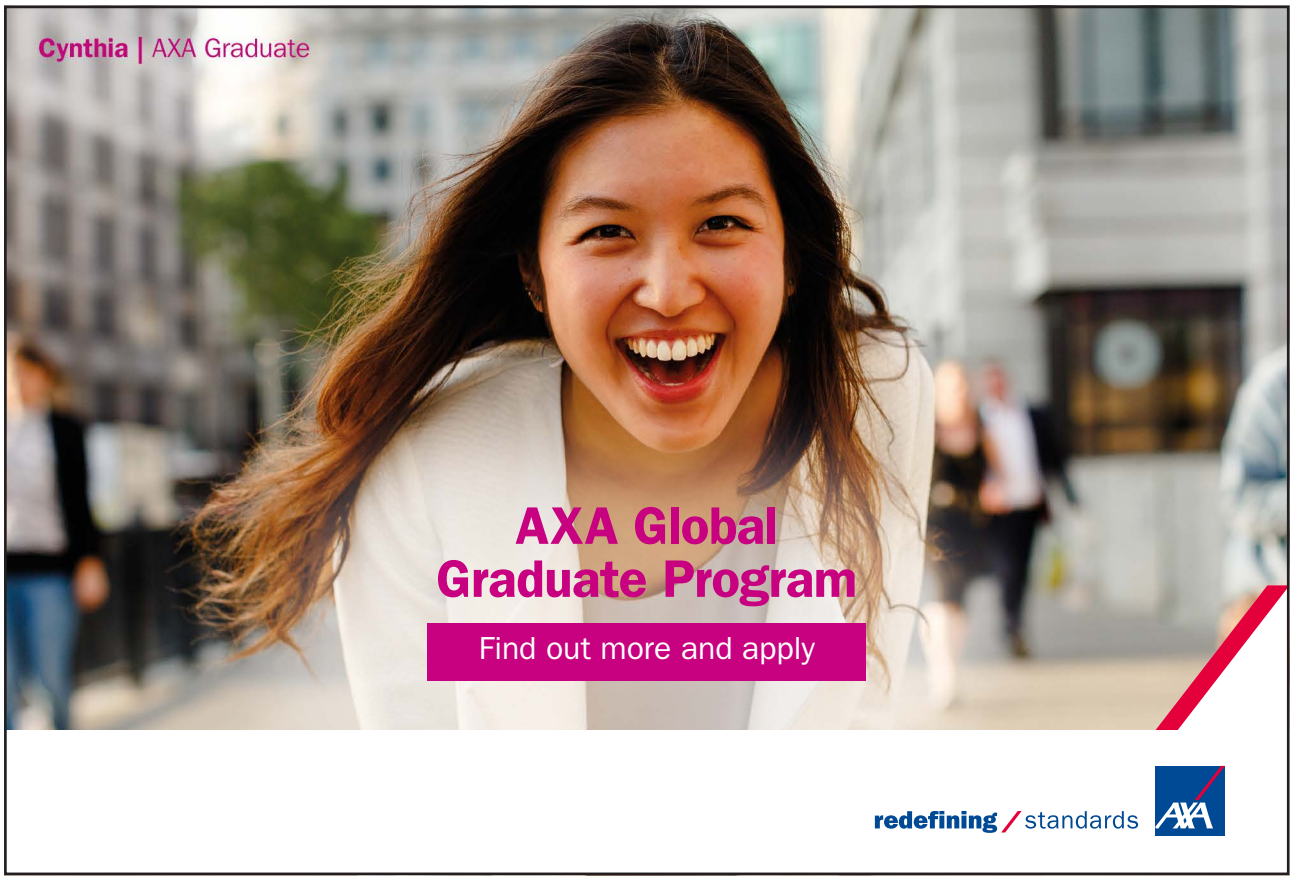

Click on the ad to read more

Download free eBooks at bookboon.com

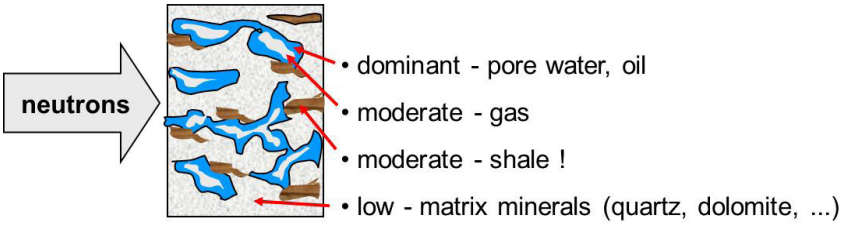

Figure 4-26: Neutron response in a porous rock.

Component	ϕ_N	Component	ϕ_N
Water, fresh	1	Calcite	0
Water, 200 000 ppm NaCl	0.9	Dolomite	0.01 … 0.02
Oil, average	0.96 … 1.02	Quartz	– 0.02
Gas, average, 15 °C, 0.1 MPa	0.0017	Gypsum	0.49
Gas, average, 93 °C, 48 MPa	0.54	Shale, average	0.2 … 0.4

Table 4-10: Neutron response of some rock components, expressed as neutron porosity ϕ_N (after Baker Atlas 2002; Schlumberger 2000; Fricke and Schön, 1999).

For any porous rock composed of different mineral components, shale, and fluids, the porosity derived from a limestone-freshwater calibrated device results as

$$\phi_N = \phi \cdot \phi_{N,\,fluid} + (1 - \phi) \cdot \lfloor (1 - V_{shale}) \cdot \phi_{N,matrix} + V_{shale} \cdot \phi_{N,shale} \rfloor$$

where
ϕ is the rock porosity
ϕ_N is the measured neutron porosity
$\phi_{N,\,fluid}$ is the neutron response of the fluid
$\phi_{N,matrix}$ is the neutron response of the matrix
$\phi_{N,shale}$ is the neutron response of the shale
V_{shale} is the shale content.

The cartoon in Figure 4-27 demonstrates the effect of different mineralogy, different pore fluid, and the presence of shale.

Download free eBooks at bookboon.com

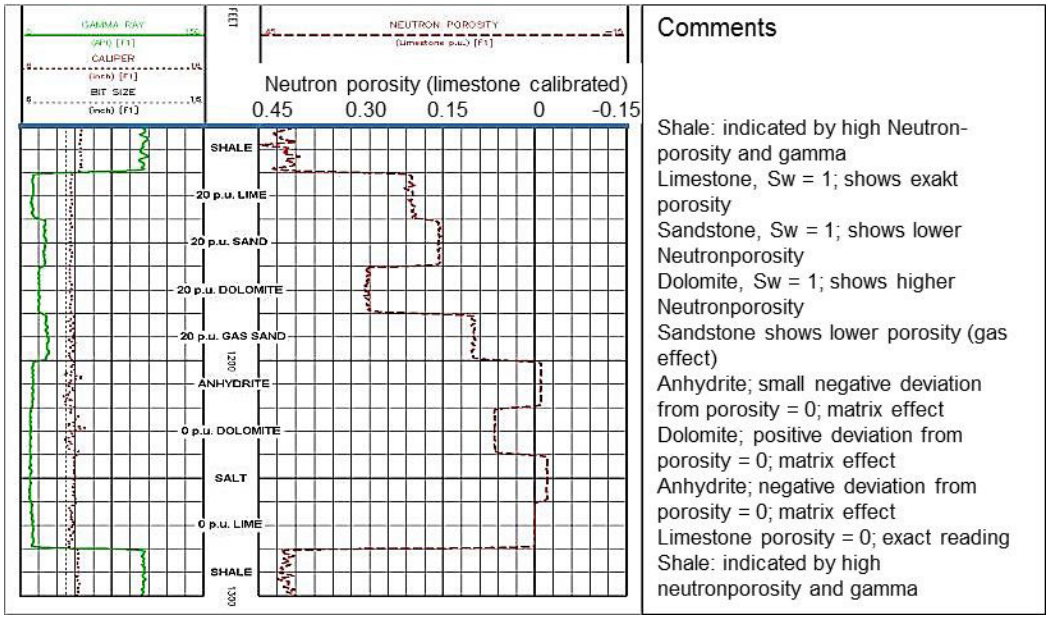

Figure 4-27: Neutron response – Influence of mineralogy and pore fluid (Baker Atlas, 2014).

Particularly the transformation from a limestone calibration to a sandstone or dolomite referenced scale is implemented in software packages and also graphically presented in the companie's chart books (see Figure 4-28).

Click on the ad to read more

Download free eBooks at bookboon.com

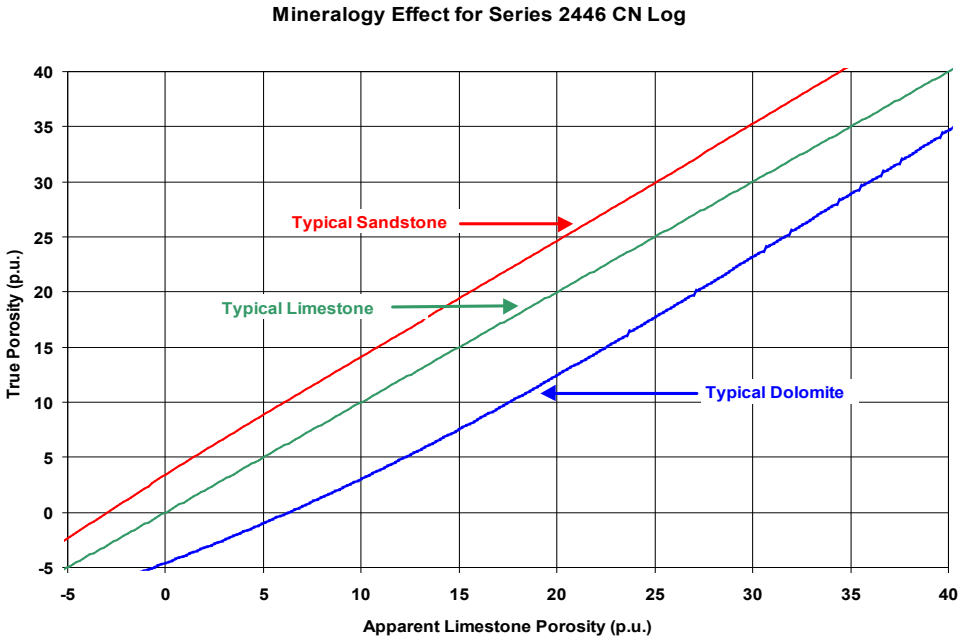

Figure 4-28: Neutron response to different minerals (Baker Atlas, Chart book 2003). X-axis shows the measured porosity using a limestone-calibrated tool. If the logged formation is a limestone, then this is identical true rock porosity (y-axis). If the logged formation is a dolomite, then measured limestone-referenced porosity (for example 20 p.u. represents only 12.5 p.u. true rock porosity (y-axis). If the logged formation is a sandstone, then measured limestone-referenced porosity (for example 20 p.u.) represents about 25 p.u. true rock porosity (y-axis). Note that such charts are referenced to a specific tool series.

4.3.5 Application of nuclear measurements for mineral analysis

Traditional nuclear measurements (natural Gammalog, Gamma-Gamma-log, Neutronlog) offer possibilities for an initial classification using defined characteristic values or tendencies. Examples are:

- Shale indication from a Gammalog and a combination Gamma-Gamma-density and Neutronlog,
- Carbonate detection (limestone, dolomite) using neutron-density cross plots (see chapter 5),
- Identification of dolomite and/or limestone supported by photoelectric cross section (PE) measurement,
- Identification of anhydrite by extremely high density (2.96 g cm^{-3}), supported by PE measurement.

For a more detailed and reliable characterization of the mineralogical composition, elemental analyses based on spectral nuclear measurement have been developed. The physical processes of nuclear measurements are directly connected with the reaction of certain elements and their components.

Neutron gamma spectrometric methods using pulsed neutron generators can deliver information about the concentration of various elements from gamma rays produced either by inelastic scattering or by in neutron capture events. Elements occurring in different rock components are listed in Table 4-11.

Download free eBooks at bookboon.com

Detected element	Found in
H	water, hydrocarbons, clay
Ca	calcite $CaCO_3$, dolomite $CaMg(CO_3)_2$, anhydrite $CaSO_4$
Si	quartz SiO_2, clay
Cl	rock salt NaCl
S	anhydrite $CaSO_4$
Fe	pyrite FeS_2, clay
C	hydrocarbons, calcite $CaCO_3$, dolomite $CaMg(CO_3)_2$

Table 4-11: Occurrence of elements detected by gamma spectrometry in rocks and fluids (Schlumberger, Gamma Ray Spectrometry Tool, 1983).

In carbonate formations neutron capture spectroscopy (Schlumberger, 2008) can be used to detect Ca, Mg, and S, and therefore to discriminate dolomite $CaMg(CO_3)_2$ from calcite $CaCO_3$ and provide accurate estimates of anhydrite volumes ($CaSO_4$).
Modern methods and tools like "Elemental Capture Spectroscopy Sonde ECS" and "EcoScope" (Schlumberger) and the "Formation Lithology eXplorer (FLeX)" (Baker Atlas) determine certain elemental concentrations and calculate mineral composition based on a model assumption. Fundamental papers were written, for example, by Hertzog et al. 1987, Gilchrist et al. 1999, 2000, Pemper et al. 2006, and Han et al. 2009.

Neutron capture spectroscopy is an integrated component of the Schlumberger "Carbonate Advisor" (www.slb.com/carbonates). For carbonates the measurement of magnesium and sulphur can be used for discrimination of calcite and anhydrite and for anhydrite volume estimate (underestimating anhydrite content results in underestimation of grain density and underestimation of total porosity). The brochure gives an example and demonstrates that "*incorporation of neutron spectrometry in the lithology-porosity analysis identifies anhydrite and improved the porosity estimates, which are up to 2 p.u. (porosity units) higher than the porosity derived from triple-combo logs alone*".

4.4 Acousticlog, Sonic log

Acoustic logs or Sonic logs measure the velocity of elastic waves (or slowness, the inverse property) of the formation. Therefore in general elastic properties of the formation are investigated with the measurement. Results give information about porosity, lithology, and supports seismic exploration.

4.4.1 Elastic properties

In an elastic material two body wave types propagate:

- Compressional wave with the velocity v_p
- Shear wave with velocity v_s.

Download free eBooks at bookboon.com

As boundary wave in a borehole Stoneley and Rayleigh waves additionally travel along the borehole wall.

Wave velocities can be expressed in terms of the elastic moduli and the density of the rock:

Compressional wave: $$v_p = \sqrt{\frac{M}{\rho}} = \sqrt{\frac{E}{\rho} \cdot \frac{1-\nu}{(1+\nu)\cdot(1-2\nu)}} = \sqrt{\frac{k + \frac{4}{3}\cdot\mu}{\rho}}$$

Shear wave: $$v_s = \sqrt{\frac{\mu}{\rho}} = \sqrt{\frac{E}{\rho} \cdot \frac{1}{2\cdot(1+\nu)}}$$

where

E	Young's modulus, defined as ratio of stress to strain in a uniaxial stress state,
M	Compressional wave modulus, defined as the ratio of stress to strain in an uniaxial strain state,
k	Bulk compressional modulus, defined as the ratio of hydrostatic stress to volumetric strain,
μ	Shear modulus, defined as the ratio of shear stress to shear strain,
ν	Poisson's ratio, defined as the ratio of lateral strain to axial strain (uniaxial stress state),
ρ	Bulk density.

Instead of the velocity the slowness Δt is frequently used; it is the reciprocal of velocity:

Compressional slowness: $\Delta t_p = v_p^{-1}$

Shear slowness: $\Delta t_s = v_s^{-1}$

Units:

Velocity: SI-unit is m s^{-1}, other frequently used unit is ft s^{-1}

Conversion: 1 m s^{-1} = 3.2808 ft s^{-1} or 1 ft s^{-1} = 0.3048 m s^{-1}

Elastic moduli (E, μ, …): SI-unit is Pa (Pascal); other units are kp cm^{-2} and psi.

Conversion: 1 Pa = $1.0197 \cdot 10^{-5}$ kp cm^{-2} = $1.4504 \cdot 10^{-4}$ psi or 1 psi = 6895 Pa.

Poisson's ratio is dimensionless.

Slowness: SI-unit is μs m^{-1} other unit is μs ft^{-1}

Conversion: 1 μs m^{-1} = 0.3048 μs ft^{-1} or 1 μs ft^{-1} =3.2808 μs m^{-1}.

Download free eBooks at bookboon.com

The velocity of elastic waves in rocks – particularly in reservoir rocks – shows a complex dependence on various influences. This is subject of special literature (e.g., Schön, 1999, 2011). The following dependencies are of interest for practical application:

1. Velocities v_p and v_s decrease with increasing porosity (porosity effect; see Figure 4-29),
2. Different lithology (sandstone, limestone, dolomite) show different magnitudes of velocity for same porosity value (matrix effect),
3. A change of pore fluid from gas to water results in a strong increase of v_p but a small decrease of v_s (pore fluid effect),
4. Velocities increase nonlinearly with increasing effective pressure (pressure effect).

Click on the ad to read more

Download free eBooks at bookboon.com

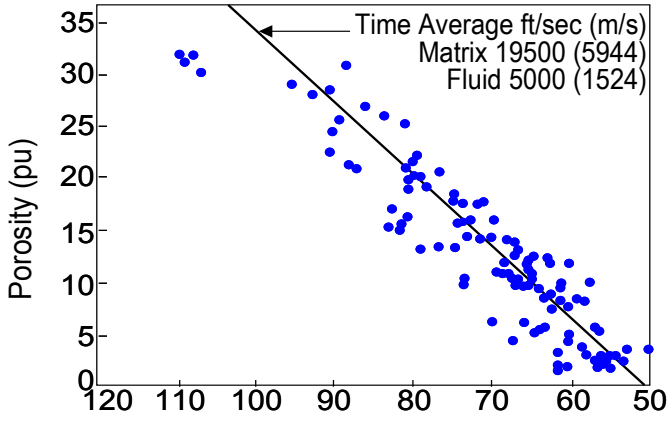

Figure 4-29 Explanation of Wyllie's equation "Time Average Relationship" (Wyllie et al. 1956).

From the strong correlation between compressional wave slowness and porosity (Figure 4-29), Wyllie et al. (1956) derived their famous time-average equation. Written in terms of slowness, the equation is

$$\Delta t_p = (1-\phi)\cdot \Delta t_{p,ma} + \phi \cdot \Delta t_{fl}$$

where

Δt_p is the compressional wave slowness of the porous rock

$\Delta t_{p,ma}$ is the compressional slowness of the matrix material

Δt_{fl} is the compressional slowness of the pore fluid (mostly assumed water)

ϕ is the porosity.

Rearranging the linear relationship between measured compressional wave slowness Δt_p and porosity results in the equation

$$\phi = \frac{\Delta t_p - \Delta t_{p,ma}}{\Delta t_{fl} - \Delta t_{p,ma}}$$

The porosity calculation based on slowness Δt_p requires the two "material properties" $\Delta t_{p,ma}$ and Δt_{fl} as input. Table 4-12 gives some mean values for the components.

Rock type	$\Delta t_{p,ma}$ µs/ft	$\Delta t_{p,ma}$ µs/m	Fluid	Δt_{fl} µs/ft	Δt_{fl} µs/m
Sandstone $\phi > 0.1$	55.5	182	fresh water mud filtrate	189	620
Sandstone $\phi < 0.1$	51.2	168			
Limestone	47.6	156	Saltwater mud filtrate	185	607
Dolomite	43.5	143			

Table 4-12: Mean input parameters $\Delta t_{p,ma}$ (matrix slowness) and Δt_{fl} (slowness of pore fluid) for application of Wyllie's equation; Reference: Asquith and Krygowski (2004).

Download free eBooks at bookboon.com

The equation works best for water-saturated and well-compacted porous rocks, particularly sandstones. Presence of gas can give erroneous results (Asquith and Krygowski, 2004).

Poor consolidation or low effective stress results in high slowness values and therefore an overestimate of porosity. In this case a "compaction correction" is recommended: The slowness in an adjacent shale bed is used as "compaction reference". If measured slowness is $\Delta t_{shale} > 100\ \mu$s/ft, the following equation for a compaction-corrected Wyllie porosity is recommended (see for example Asquith and Krygowski, 2004):

$$\phi_{corrected} = \phi_{Wyllie} \cdot \frac{1}{C_p} = \frac{\Delta t - \Delta t_{ma}}{\Delta t_{fl} - \Delta t_{ma}} \cdot \frac{100}{\Delta t_{shale}}$$

For carbonates with intergranular porosity Wyllie's equation can be applied. For carbonates with secondary porosity, vugs, fractures with much larger dimensions than primary pores the wave propagation is still controlled mainly by primary porosity. Therefore the equation results in porosities which are too low by the amount of secondary porosity. Thus, an estimate of secondary porosity ϕ_{sec} can be given by the difference between total porosity (from density or neutron) ϕ_t and sonic-derived porosity ϕ_{SV} based on Wyllie's equation $\phi_{sec} = \phi_t - \phi_{SV}$ (Asquith and Krygovski, 2004; see also Lucia 2007).

In deep and medium invaded reservoir zones (and in water zones) compressional wave propagation is controlled by mud filtrate as pore fluid and the magnitude of Δt_{fluid} is approximated by water slowness. For hydrocarbon-bearing zones at shallow invasion an empirical correction is recommended (Asquith and Krygovski, 2004):

$\phi_{corr} = \phi_{wyllie} \times 0.7$ for gas $\qquad$ $\phi_{corr} = \phi_{wyllie} \times 0.9$ for oil.

4.4.2 Acousticlog/Soniclog measurement – Principles

Figure 4-37 shows the simplest configuration of an Acousticlog probe. The ultrasonic transmitter generates a compressional wave, which is transmitted through the mud and hits the formation at the borehole wall. From this boundary incident wave propagates as reflected and refracted waves. The Acousticlog uses the refracted wave. If the wave velocity of formation > wave velocity of mud, the refraction wave moves in the direction of the boundary. At the so called critical angle a refracted wave propagates with the velocity of the formation along the borehole. The wave generates secondary waves passing the mud and arriving at the two receivers. Difference of the arrival time divided by receiver distance gives the slowness of the formation (if the tool is centered)[5].

The right part of the figure shows the wave traces with first arrival for compressional wave, second arrival for shear wave. A third arrival (not marked) is the Stoneley wave.

Download free eBooks at bookboon.com

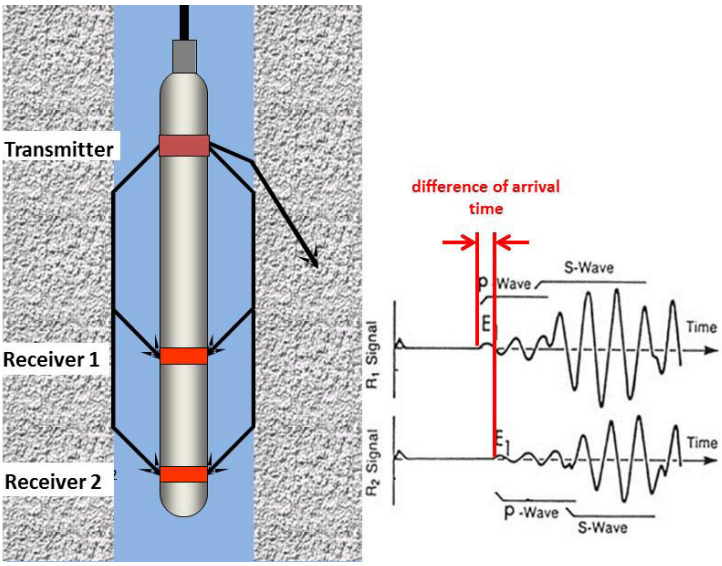

Figure 4-30: Sonic log/Acousticlog – Principle.

Radius of investigation	≈ 6 in = 15 cm (50 %)
Precision	± 1 µs/ft
Vertical resolution	12 in = 30 cm depends on receiver spacing
Logging speed	< 60 feet/min = 18 m/min; array tools slower

Table 4-13: Acousticlog – some data (after Asquith and Krygowsky, 2004; Halliburton Full Wave Sonic tool).

Click on the ad to read more

Download free eBooks at bookboon.com

For Quality Control you may check DT values in anhydrite (50 µs/ft = 164 µs/m) or casing (57 µs/ft = 187 µs/m).

"Compensated" tools use multiple transmitter-receiver pairs in order to minimize the borehole effect. "Array" tools have many receivers. Data from all receivers are processed for a precise and robust determination of wave arrivals (compressional, shear, Stoneley); see Figure 4-31. A powerful part of these sophisticated systems is the application of correlation techniques (Semblance technique).

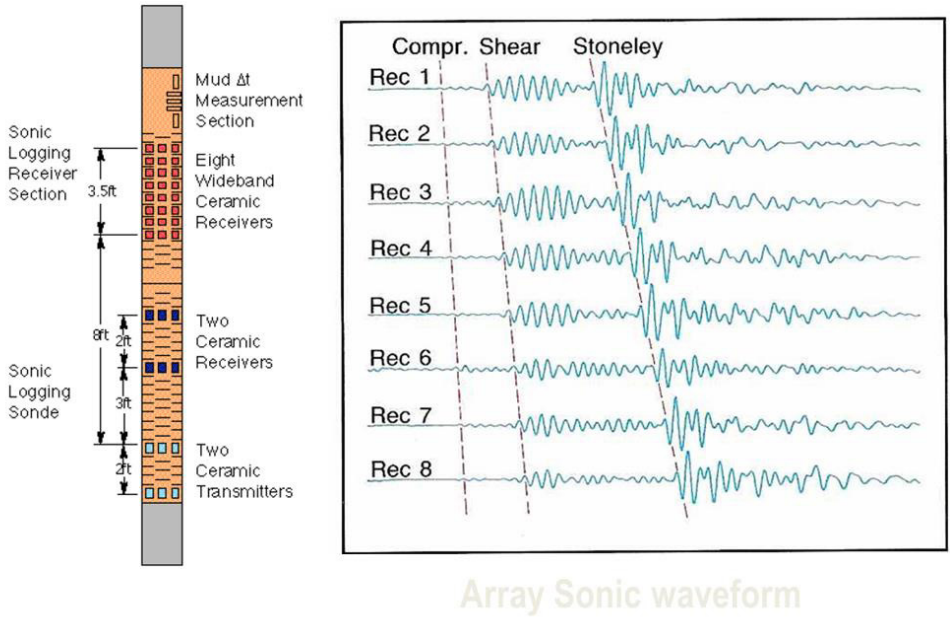

Figure 4-31: Modern digital sonic tools (left) offer the possibilities of a signal correlation (right)

An important part of the tool is the transmitter. Particularly in so-called "slow formations" where the shear wave velocity of the formation is lower than the compressional wave velocity in the mud no refracted shear wave can be observed. In such cases a special transmitter (dipole-shear) creates a shear wave in the formation. Sophisticated tools work with a simple monopole transducer, dipole and/or quadrupole transducers to initiate all wave types.

Main applications of acoustic/sonic logs are:

- Support for seismic interpretation (velocity-depth function, synthetic seismograms),
- Porosity determination based on Wyllie's equation or other empirical equations,
- Porosity and lithology determination (combination with neutron and gamma-gamma-density log (cross plots etc.),
- Derivation of elastic rock properties (Poisson's ratio, Youngs modulus),
- Permeability estimate from Stoneley wave analysis (Tang and Patterson 2004),

Download free eBooks at bookboon.com

A special application in completed wells is Cementation Control (Cement bond log). In order to control if the cement is adhering solidly to the outside of the casing the log uses the variations in the amplitude of an acoustic signal traveling down the casing wall between a transmitter and receiver to determine the quality of cement bond on the exterior casing wall. The fundamental principle is that the acoustic signal will be attenuated more strongly in the presence of cement than in uncemented casings. The newer versions, called cement evaluation logs, along with their processing software, can give detailed, 360-degree representations of the integrity of the cement job, whereas older versions may display a single line representing the integrated integrity around the casing (Schlumberger Oilfield Glossary).

4.5 NMR measurements

Nuclear Magnetic Resonance (NMR) measurements use the interaction of hydrogen nuclei with an external magnetic field. Hydrogen nuclei (protons) have a magnetic and an angular momentum. In an external magnetic field interaction results in a precessing motion with a typical frequency (Larmor frequency):

$$f_0 = \left(\frac{\gamma}{2\,\pi}\right) \cdot B_0$$

where B_0 is the strength of the external magnetic field and γ is the gyromagnetic ratio which is typical for the substance (Table 4-14). Hydrogen nuclei are a component of fluid molecules of water and hydrocarbons in the pore space.

Nucleus	$\gamma/2\pi$ in MHz/Tesla
^{1}H	42.6
^{13}C	10.7
^{23}Na	11.3

Table 414: Gyromagnetic ratio.

The measurement consists of a series of steps (Figure 4-32) – called CPMG (Carr, Purcell, Meiboom and Gill) sequence – using two magnetic fields:

- B_0 – the external static field which controls the Larmor frequency
- B_1 – the "tipping" field (RF-pulse). It is applied perpendicular to the B_0 field (90°RF pulse) and creates coherency of the spinning protons.

In certain time steps *TE* so-called 180°RF pulses repeat the polarization and create an echo of the signal. Irreversible interactions result in a decrease of the echo amplitude and describe the signal decay.

Download free eBooks at bookboon.com

The relaxation (and built up) process can be described by exponential functions with the two relaxation time terms:

- T_1- longitudinal, or spin-lattice relaxation time,
- T_2- transverse, or spin-spin relaxation time.

Two pieces of information are extracted from the spin echo sequence:

1) Initial signal amplitude: The initial signal amplitude is controlled by the number of hydrogen nuclei associated with the pore fluids in the measurement volume – thus, it gives the porosity.
2) Signal amplitude decay: The amplitude decays exponentially with time and is characterized by the decay time T_2.

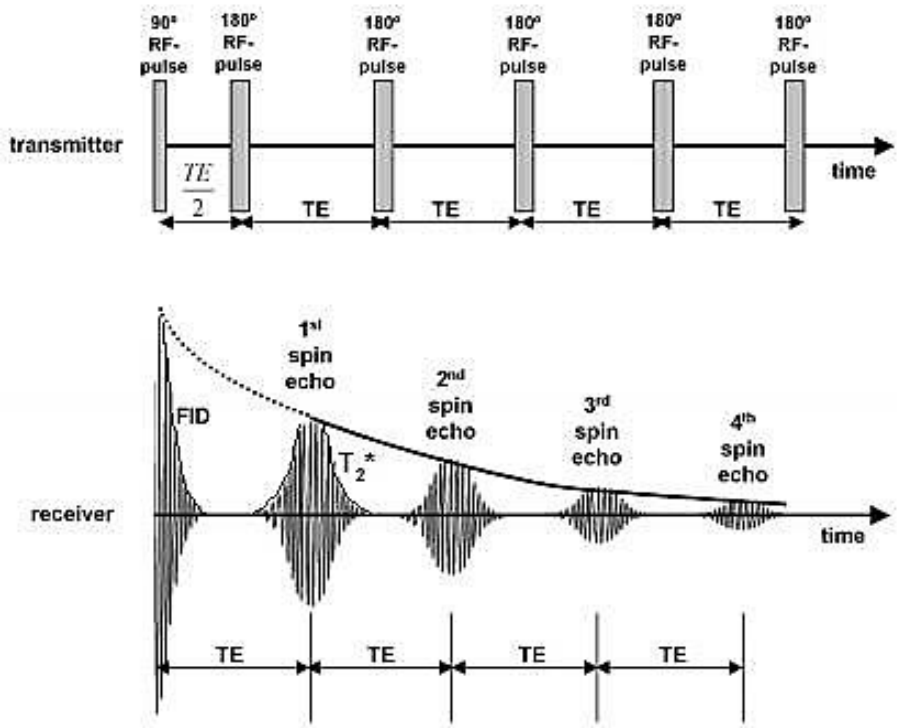

Figure 4-32: Carr-Purcell-Meiboom-Gill (CPMG) sequence: Timing of the RF-pulses transmitted into the formation, and Free Induction Decay (FID) and spin echoes detected by the receiver. The envelope of the spin echo maxima decays exponentially with the time constant T_2. The extrapolation of the spin echo envelope to time zero yields the net magnetization. After calibration, the net magnetization is a direct measure of formation porosity (Appel 2004).

Figure 4-33 shows the principle of an NMR borehole tool. The static magnetic field B_0 is a function of the radial distance from the tool axis and exactly known. For a given magnitude of the field, the Larmor frequency is defined. Realizing the measurements within this frequency band relates the measurements to an exactly defined radial distance (response space, sensitive volume).

Download free eBooks at bookboon.com

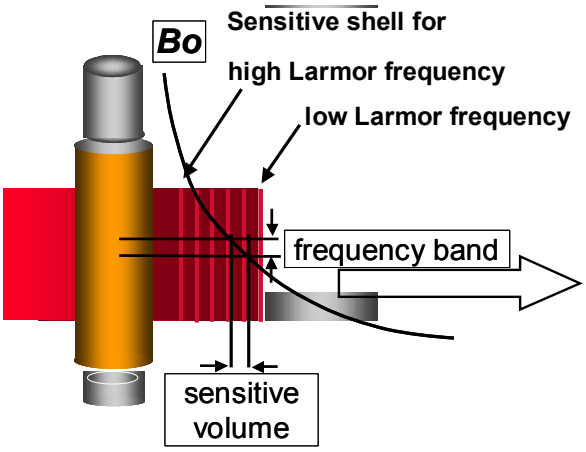

Figure 4-33: NMR Tool – the principle (Baker Atlas document).

In a porous rock protons in the fluid relax differently with respect to their "bonding properties". There are independent mechanisms (see Figure 4-34) described by a T_2-decay time:

- $T_{2,bulk} = T_2$ relaxation time of the pore fluid as it would be measured in a container.
- $T_{2,surface} = T_2$ relaxation time of the pore fluid resulting from surface relaxation.
- $T_{2,diffusion} = T_2$ relaxation time of the pore fluid as induced by diffusion in the magnetic field gradient.

Superposition of the effects results in the observed relaxation process:

$$\frac{1}{T_2} = \frac{1}{T_{2,bulk}} + \frac{1}{T_{2,surface}} + \frac{1}{T_{2,diffusion}}$$

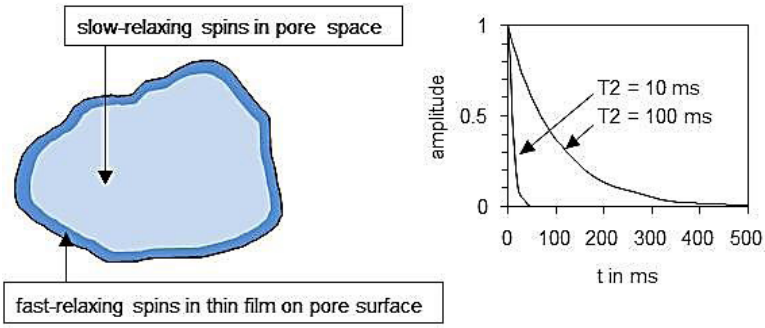

Figure 4-34: Bulk and surface contributions of transverse relaxation in a water-filled pore. The diagram on the right-hand side shows relaxation curves calculated for T_2 = 10 ms (surface relaxation) and T_2 = 100 ms (bulk relaxation).

Download free eBooks at bookboon.com

In general the decay covers the sum of relaxation contributions from clay bound water, capillary bound water (irreducible water), free movable water, and diffusion if gas is present and can describe it as a sum of exponential terms with different relaxation time and magnitude.
The processing extracts a distribution of T_2 (Echo Data Inversion) from the decay curve (see Figure 4-35). So called cutoffs separate the regions:

- CBW/BVI: about 1 … 5 ms (clay minerals).
- BVI/BVM: faster decaying clastics about 33 ms – slower decaying carbonates about 92 ms.

Click on the ad to read more

Download free eBooks at bookboon.com

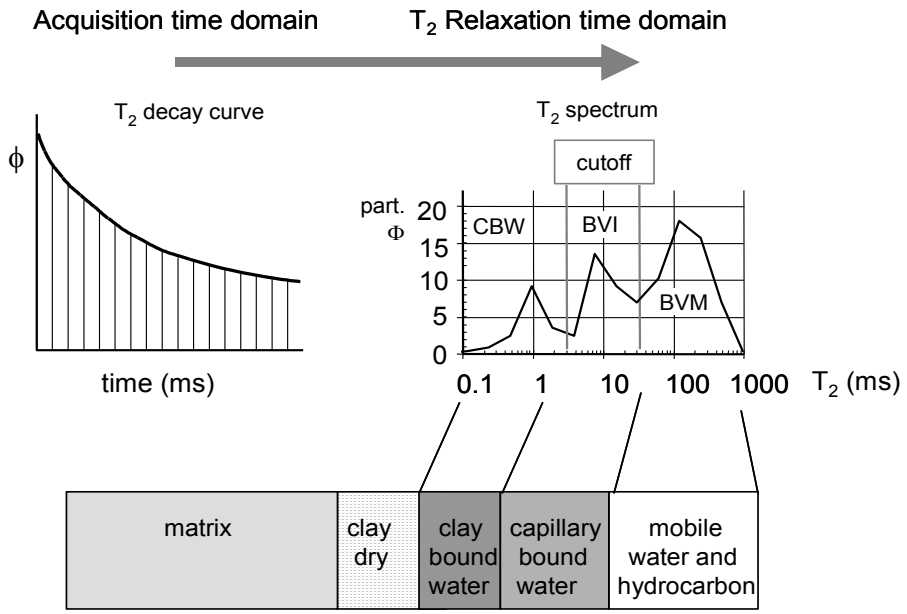

Figure 4-35: NMR data processing—principle. Measured data are in the time domain. The inversion process results in a partitioning of the individual relaxation contributions (bulk volumes) of the three regions clay bound water (*CBW*), capillary bound water (*BVI*), and free movable water (*BVW*). Regions are separated by cutoffs.

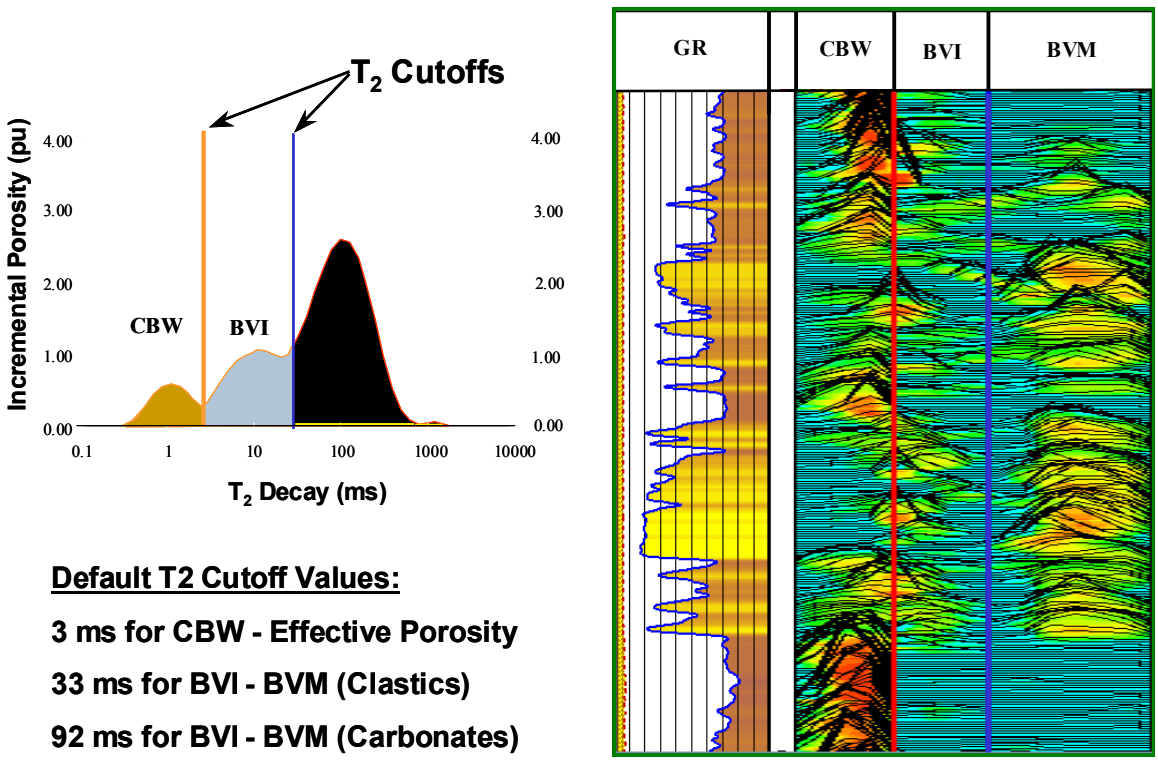

Figure 4-36: Example: Pore volumetric partitioning of T_2 (Spectra/Baker Atlas); see the dominant *CBW*-indications in the shaly parts on top and bottom (GR-log), and the dominant *BVW* in the reservoir zone (Baker Atlas, 2014).

Download free eBooks at bookboon.com

The analyse of each individual NMR-record is the basis for important applications:
The T_2 plot (Figure 4-36) provides

1) Information about the main components
   - Clay-bound water CBW (and shale content);
   - Irreducible water BVI; BVI represents the specific surface of pores; a low BVI is typical for large pores and high permeability;
   - Bulk volume moveable BVM represents the volume of free moveable fluids.
2) The numerical interpretation delivers
   a) The effective porosity by integration over BVI and BVM
   b) A permeability measure: The ratio BVI/BVM is a measure for the specific internal surface. "Coates equation" (Coates et al. 1999) gives a permeability estimate:

$$k = \left(\frac{\phi}{C}\right)^4 \cdot \left(\frac{BVM}{BVI}\right)^2$$

or generalized

$$k = \left(\frac{\phi}{C}\right)^m \cdot \left(\frac{BVM}{BVI}\right)^n$$

where C, m, n are calibration parameters determined by comparison of direct core measurements and NMR measurements (Figure 4-37). This parameter expresses the difference between a simple capillary and the complicated geometry of the real pore space.

Download free eBooks at bookboon.com

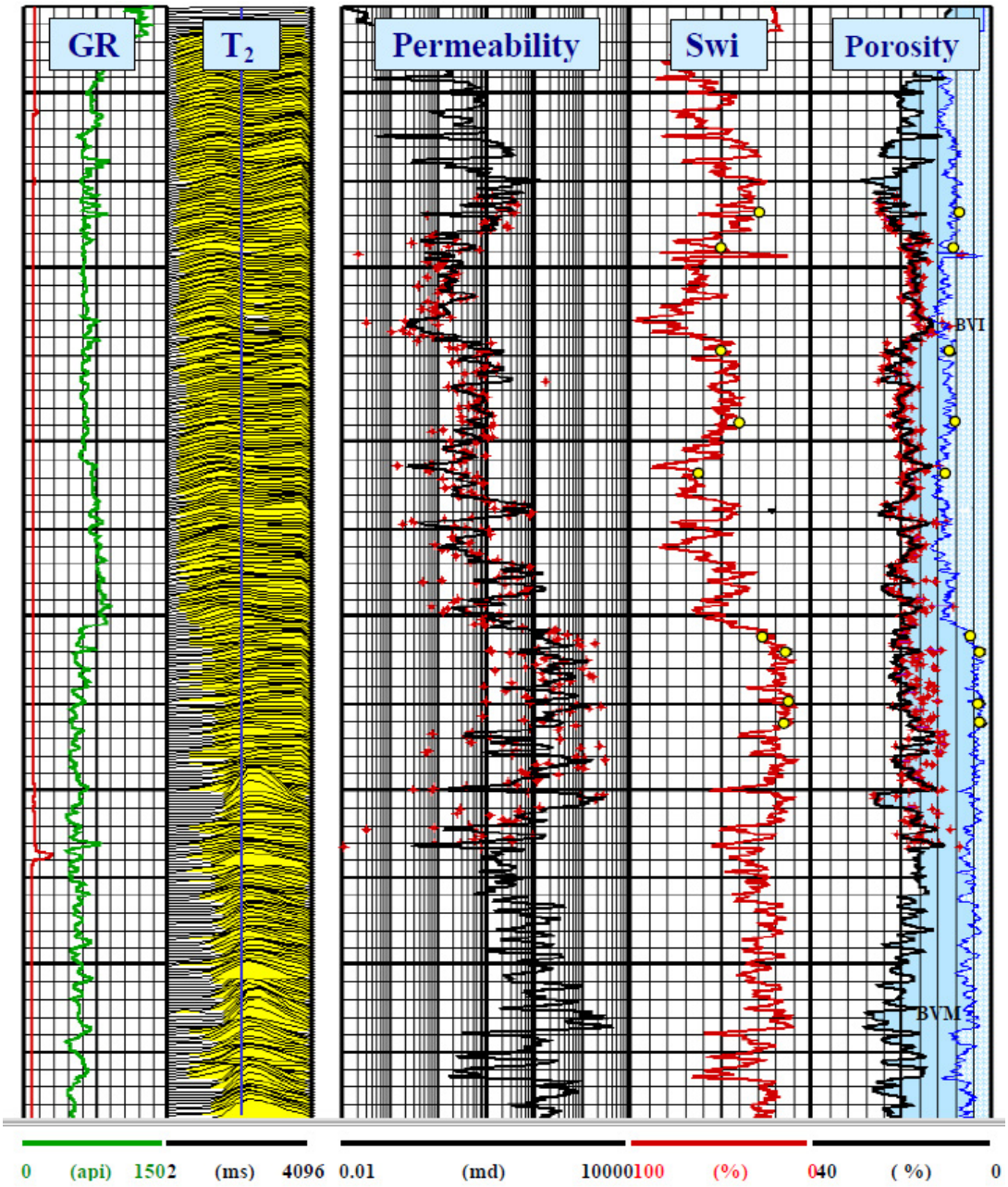

Figure 4-37: Core and log data comparison. The discrete points on the figure are the core data. The porosity and *BVI* data are displayed on the far right track, The *Swirr* data (irreducible water saturation) are presented on the 2nd track from the right, and the permeability data are displayed on the 3rd track from the right. The *BVI* data are estimated with T_2 cutoff = 80 ms, and the Coates permeability model employs the parameters m = 4, n = 1.73, and C = 10.91, along with the core-calibrated *BVI* as inputs (Chen et al., 2000).

NMR fluid typing techniques are based on differences of T_1 and T_2 relaxation time, diffusion coefficient (D), and derived properties for different fluids (Table 4-11); properties – particularly for gas – are dependent on temperature and pressure.

Download free eBooks at bookboon.com

Fluid	T_1 in ms	T_2 in ms	D in cm²/s
Brine	1 … 500	0.67… 200	$(3 \ldots 8) \cdot 10^{-5}$
Oil	5000	460	$(0.03 \ldots 2) \cdot 10^{-5}$
Gas	4400	40	$(80 \ldots 200) \cdot 10^{-5}$

Table 4-11: Averaged NMR properties of reservoir fluids; data compiled using more detailed tables from Akkurt et al. (1995, 1996)

The relevant NMR properties are acquired by modern techniques (Vinegar et al., 1996; Chen et al., 2000; Freedman and Heaton, 2004). As a result, data acquisition delivers a view into fluid properties using not only one but also two or three parameter-domain dimensions (2D and 3D NMR); Figure 4-38 shows an example.

Click on the ad to read more

Download free eBooks at bookboon.com

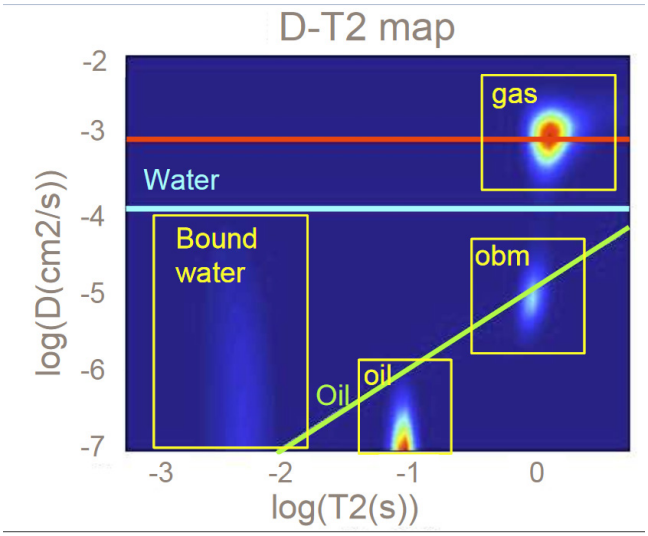

Figure 4-38: *D* – T_2 map – combining Diffusion (*D*) and Transverse Relaxation (T_2) after Spears and Saha (2005).

Some NMR tools are:

- Schlumberger: Combinable Magnetic Resonance Tool (CMR); Magnetic Resonance Fluid Characterization (MRF)
- Baker Hughes: Magnetic Resonance eXplorer (MReX)
- Halliburton: Magnetic Resonance Imaging Logging (MRIL).

4.6 Imaging Techniques

Acoustic or electrical resistivity scanning techniques can create electronic pictures ("images") of the borehole wall in optically non-transparent fluids (mud). Images have an azimuthal orientation and are characterized by extremely high resolution. Pictures carry valuable information about bedding dip, faults, vugs and pore types, fractures etc.

The acoustic borehole televiewer (Figure 4-39 left) scans the borehole wall with a rotating ultrasonic beam. The transducer emits a high frequency signal, which passes the mud and is reflected at the borehole wall. The reflected signal passes the mud in the opposite direction and is received by a transmitter. Thus, there are two parameters: The amplitude of the reflected signal and the two-way travel time for the distance transmitter – borehole wall.

This reflection process is realized during the rotation of the transducer system and delivers a full 360-degree scan in terms of amplitude and travel time. A gyro-based system additionally gives the azimuth and produces an oriented scan of the borehole wall.

Download free eBooks at bookboon.com

Acoustic borehole televiewers are very sensitive with respect to tool eccentricity and borehole ovality; centralization of the tool is therefore of critical importance.

With the simultaneously measured mud velocity, a detailed oriented caliper can be derived from the two-way traveltime.

The amplitude is color-coded in most cases and therefore looks like a real picture (Figure 4-40). Typical readings of electrical scanning systems are:

- High amplitudes in smooth dense formations and hard layers (dense limestone, anhydrite),
- Medium amplitudes in porous rocks, shale,
- Locally low amplitudes at fractures, vugs etc.

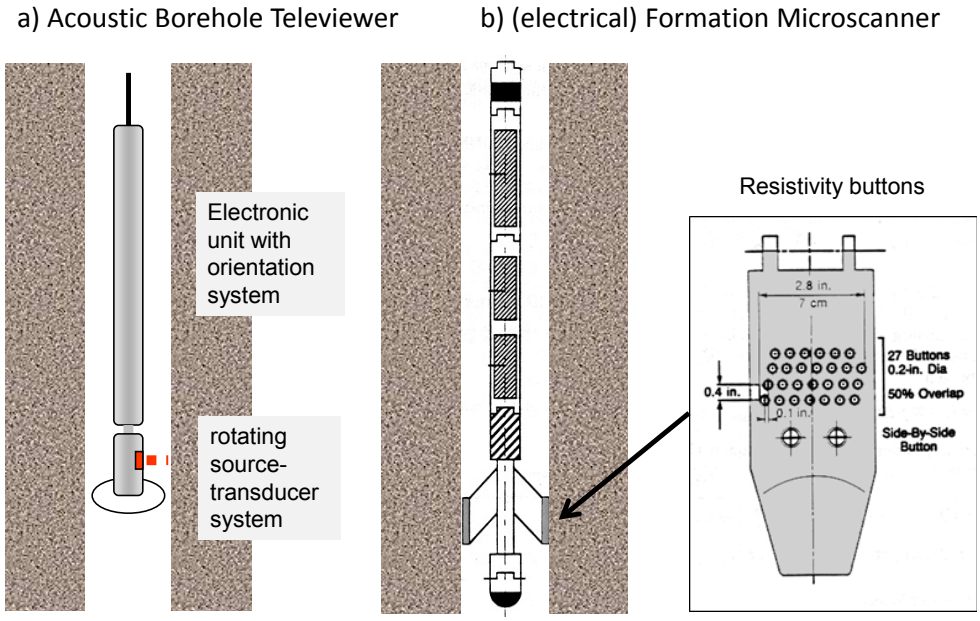

Figure 4-39: Principle of Acoustic Borehole Televiewer (a) and Formation Microscanner (b).

Electrical Resistivity Imaging is based on the registration of the electrical resistance at the vicinity of a number of electrode buttons fixed on a pad scratching along the borehole wall (conductive mud required). Each individual button measures the contact resistance. Depending on the electrode array and borehole diameter a system of four or more electrode pads scans in several sectors. Modern tools overlap these sectors and deliver the full circle. Resistance is plotted along with orientation mostly colour-coded which again looks like a picture.
Typical readings of electrical scanning systems are:

- High resistance in a smooth dense formation and hard layers (dense limestone, anhydrite).
- Medium to low resistance in water-bearing porous rocks, shale,
- Locally low resistivity at (open) fractures, vugs etc.

Download free eBooks at bookboon.com

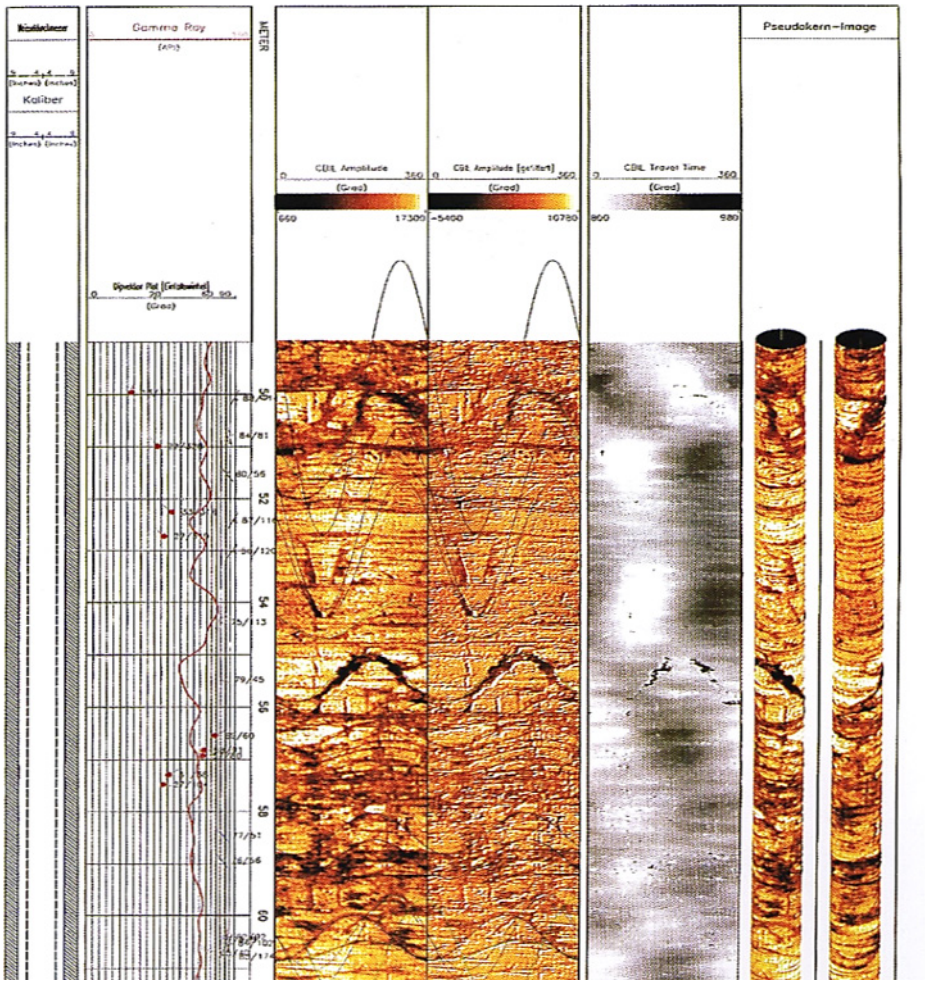

Figure 4-40: Acoustic Borehole Televiewer – Example; Fricke and Schön (1999).

Frequently both systems are combined as one tool (Figure 4-41). Experienced interpreters derive valuable information with respect to:

- Sedimentation (layering, lamination, dipping etc.),
- Pore types in carbonates (see Figure 2-4),
- Fractures, fracture direction and other tectonic elements,
- Stress field.

Some Imaging Tools are (selection):

Resistivity: FMS Formation Microscanner (Schlumberger): 4 pads, 64 electrodes.
FMS Formation MicroImager (Schlumberger): 8 pads, 192 electrodes

Acoustic/Sonic: UBI Ultrasonic Borehole Imager (Schlumberger).
CBIL Circumferential Borehole Imaging Log (Baker Atlas).

Download free eBooks at bookboon.com

Combination: FMI (Formation Micro Imager) – Schlumberger.
STAR SimulTaneous Acoustic and Resistivity Imager (Baker Atlas).
(compiled after Asquith and Krygowski, 2004)

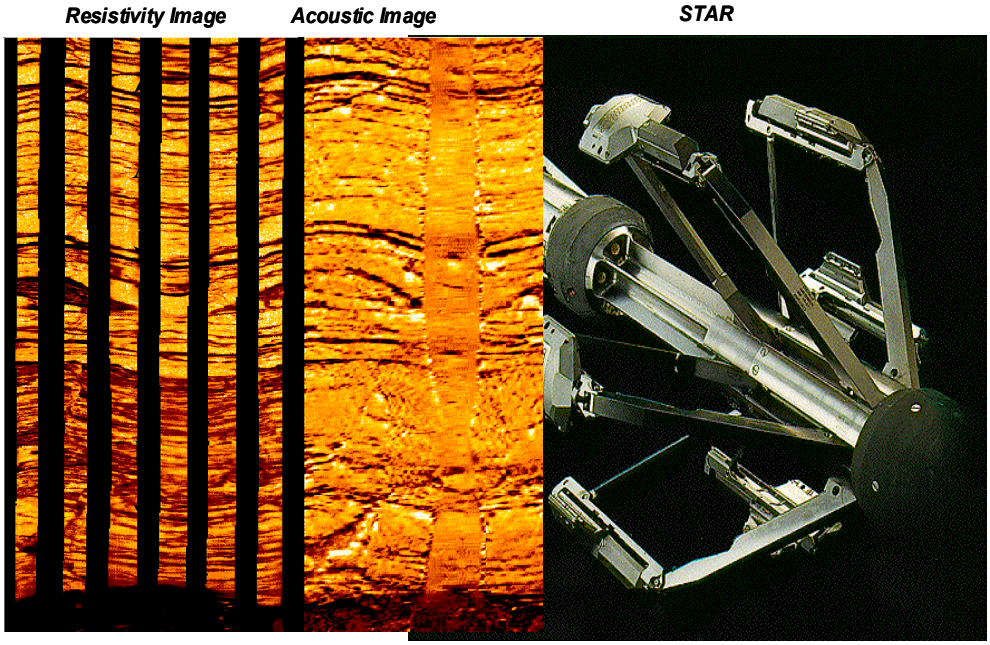

Figure 4-41: Resistivity and acoustic image; Baker Atlas STAR (SimulTaneous Acoustic and Resistivity Imager).

DON'T EAT YELLOW SNOW
What will your advice be?
Some advice just states the obvious. But to give the kind of advice that's going to make a real difference to your clients you've got to listen critically, dig beneath the surface, challenge assumptions and be credible and confident enough to make suggestions right from day one. At Grant Thornton you've got to be ready to kick start a career right at the heart of business.
Sound like you? Here's our advice: visit GrantThornton.ca/careers/students
Scan here to learn more about a career with Grant Thornton.
Grant Thornton
An instinct for growth™
© Grant Thornton LLP. A Canadian Member of Grant Thornton International Ltd
Click on the ad to read more

Download free eBooks at bookboon.com

5 Log Interpretation – Introduction

This section describes principles of log interpretation focused on the oil and gas exploration. Two connected practises are discussed:

1. Quick look interpretation for a first scanning of logs and information about zones of interest.
2. Methods of quantitative interpretation (determination of lithology/shale content, porosity and mineral composition, and fluid saturation.

Algorithms and inputs are the same for any computer supported interpretation.

5.1 Overview

Measured log data are given mostly as a data file in a special format (LAS-file). Data processing realizes important steps like corrections and extraction of true parameters from the measured data set (for example R_{xo} and R_t).

These data are the input of the petrophysical interpretation. As demonstrated in the following sections and the examples, an interpretation needs additional inputs from core data and/or cuttings analysis and information about fluids particularly mud and mud filtrate (at formation temperature).

The general goal of interpretation is the determination of:

- Lithological profile and the detection and characterization of the potential reservoir zones with exact depth,
- Shale content and shale type (e.g., laminated, or dispersed shale),
- Porosity (and mineral composition),
- Fluid saturation, water saturation, hydrocarbon saturation, movable hydrocarbons, type of hydrocarbon (oil, gas),
- Permeability.

Sophisticated interpretation concepts result in a combined methodology with corresponding computer programs in order to finally find a consistent rock model.

Download free eBooks at bookboon.com

Interpretation delivers a solution in two steps:

1. "Quick-look" interpretation for a qualitative description of lithology and zones of interest.
2. Detailed quantitative analysis in terms of porosity, saturation, shale content, mineral composition, and permeability.

Fundamentals and tools for log interpretation are:

a) Knowledge of characteristic log responses,
b) mpirically derived equations for quantitative interpretation,
c) Model-derived equations for quantitative interpretation,
d) Implementation of all information (geology, cuttings, cores, …)
…and the experience of the interpreter.

Logs have a particular sensitivity with respect to reservoir properties, based on their physical principle (Figure 5-1).

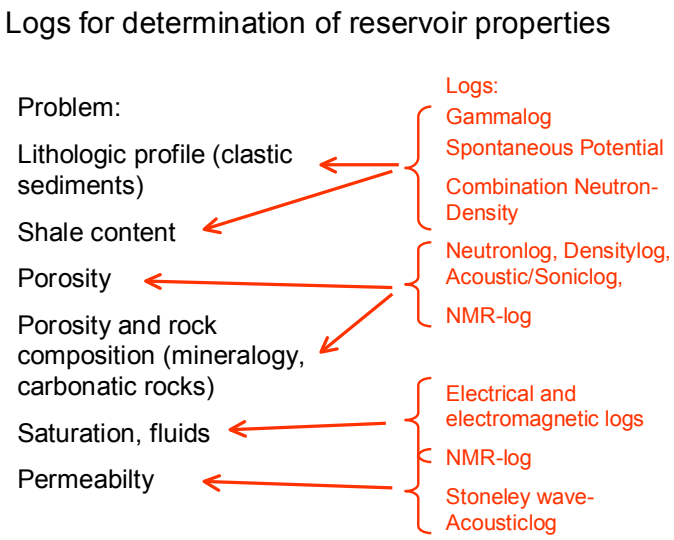

Figure 5-1: Fundamental log interpretation problems and the contribution from various logs.

The figure demonstrates

- There are typical logs which are generally preferred to contribute information for solving specific problems (for example Gamma log and SP-log for shale content, electrical and electromagnetic logs for water saturation determination),
- For porosity determination a combination of at least two methods (Gamma-Gamma-density and Neutron) is recommended,
- Besides that the "main application" methods deliver valuable information for solving other problems (the Gamma-Gamma-density and Neutronlog is a powerful shale indicator in addition to porosity).

Download free eBooks at bookboon.com

Figure 5-2 gives a more detailed compilation of logging methods used to determine reservoir properties.

Measurements	Resistivity	Porosity	Lithology	Mineralogy	Saturation	Pore geometry	Permeability	Fluid properties	Geomechanical properties	Geologic structure	Geologic bedding
Electrical resistivity											
Laterolog											
Induction											
Microlaterolog											
Spontaneous potential											
Electromagnetic propagation											
Nuclear											
Gamma ray density											
Neutron porosity											
Natural radioactivity											
Induced gamma ray spectrometry											
Nuclear magnetic resonance											
Acoustic											
Dipmeter and imaging											
Formation testing and sampling											
Rock sampling											
Fluids sampling											
Fluids pressure testing											
Seismic											

Measurement provides direct information about the reservoir property.
Measurement is influenced by or is sensitive to the reservoir property.
Measurement contributes to understanding the reservoir property.

Figure 5-2: Logging measurements used to determine reservoir properties. Blue – direct measurement of property; green – provide partial information that is combined with other measurements; brown – sensitive to property, but do not provide to property determination (Andersen, 2011).

Click on the ad to read more

Download free eBooks at bookboon.com

Two important steps are necessary before interpretation starts:

a) Compilation of all information about lithology, particularly expected rock type and mineral composition (clastic sediments, limestone, dolomite), presence and type of shale/clay, pore types etc.,
b) Check of quality and completeness regarding the measured logs: Quality Control/QC, calibration, complete header information, caliper log (breakouts, bad hole).

5.2 Quick-Look methods

Quick-look methods "…are helpful to the geologist because they provide flags, or indicators, that point to possible hydrocarbon zones requiring further investigation." (Asquith and Krygowski, 2004).

5.2.1 A General flowchart for scanning logs to identify zones of interest

Asquith and Krygowsky (2004) recommend the following flowchart (Figure 5-3) for "scanning logs" to identify zones of interest:

- Separate the shaly sections, select "clean sections", then
- If clastics are logged, look at (deep) resistivity first – if it is high, hydrocarbons may be present; then look at porosity (only in case of extremely low porosity the rock with the high resistivity is tight and no reservoir).
- If carbonates are logged, look at porosity first – if it is sufficient, look at resistivity – if it is high, hydrocarbons may be present.

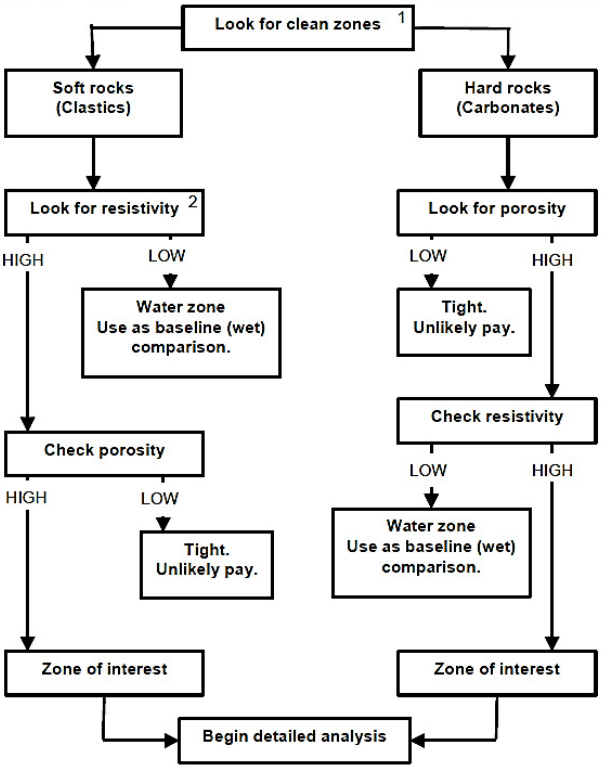

Figure 53: Flowchart for "Scanning Logs" to identify zones of interest (Asquith and Krygowsky, 2004).

Download free eBooks at bookboon.com

5.2.2 Permeable bed identification

Permeability of a formation is necessary for production; if a formation is permeable, it has also got a certain amount of porosity.
Permeable beds can be identified quickly using the following indicators:

- Spontaneous Potential (SP); the Diffusion Potential directly indicates a permeable formation,
- Mud filtrate invasion detected by multiple resistivity measurements,
- Presence of mudcake indicated by Caliperlog,

Note: The Gammalog gives an indication related to mineral composition, but not directly to permeable and non-permeable zones.

Figure 5-4 shows a section of a sand-shale profile with $R_{mf} > R_w$. The three resistivity curves fit well in the non-permeble shale beds (no invasion) and separate in the permeable sandstone. In the sandstone the Microlaterolog (MLL) – controlled by Rxo – shows a low resistivity compared with Laterolog deep (DLL) and Laterolog shallow (SLL) which are strongly influenced by the non-invaded zone (R_t). Because RMLL < RDLL and RSLL it can be concluded that the sandstone is hydrocarbon-bearing.

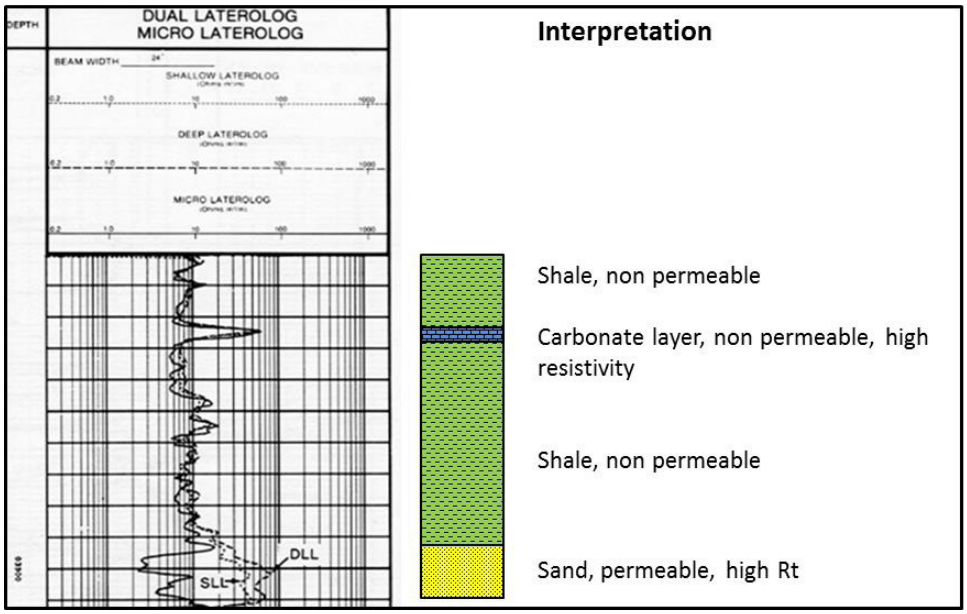

Figure 5-4: Permeable bed identification – Example (Baker Atlas, 2002).

5.3 Quantitative Interpretation: Shale Content

Standard methods for a shale content estimate are SP-log, Gammalog, and the Neutron-Density-Combination (see section 5.6.2).

Download free eBooks at bookboon.com

Calculation of the shale volume V_{sh} is the first step of quantitative interpretation. The calculated shale content is used for:

- General reservoir description,
- Volumetric rock model,
- Various "shale corrections" (see for example shaly sand equations).

5.4 Quantitative Interpretation: Porosity from a single log

Porosity as a fundamental reservoir property can be determined indirectly from Gamma-Gamma-Density log, Neutronlog, and Acoustic-/Sonic log.

Porosity calculation requires the matrix properties and the fluid properties as expressed in the equations (left side with Greek symbols, right side with Latin alphabet) as additional input:

$$\phi = \frac{\rho_{ma} - \rho_b}{\rho_{ma} - \rho_{fl}} \qquad PHI = \frac{RHO_{ma} - RHOB}{RHO_{ma} - RHO_{fl}}$$

$$\phi = \frac{\phi_N - \phi_{N,ma}}{\phi_{N,fl} - \phi_{N,ma}} \qquad PHI = \frac{NPHI - NPHI_{ma}}{NPHI_{fl} - NPHI_{ma}}$$

$$\phi = \frac{\Delta t_{ma} - \Delta t}{\Delta t_{ma} - \Delta t_{fl}} \qquad PHI = \frac{DT - DT_{ma}}{DT_{fl} - DT_{ma}}$$

ρ_b $(RHOB)$, ϕ_N $(NPHI)$, Δt (DT) are the measured (logged) data.

Matrix properties can be determined from:

- Known lithology/mineral composition; in this case representative values are recommended (Table 5-1); most critical is matrix slowness,
- Core laboratory measurements (for example grain density),
- Cross plot techniques (see following section).

Component	ρ_{ma}, ρ_{fl} in g/cm³	$\phi_{N,ma}$, $\phi_{N,fl}$	Δt_{ma}, Δt_{fl} in µs/m
Quartz	2.65	- 0.02 … – 0.04	180
Calcite	2.71	0	156
Dolomite	2.87	0.02 … 0.04	143
Water	1.00	1.00	620

Table 5-1: Recommended properties for matrix and fluid.

Download free eBooks at bookboon.com

In the presence of borehole fluid invasion into a **gas-bearing reservoir,** some specific conditions must be considered (Asquith and Krygowski, 2004):

Invasion tends to force the gas from the formation and replace it with borehole fluid. Porosity calculation from Neutron and Gamma-Gamma-Density measurement needs fluid properties. The influence upon the two porosity logs depends on their radial sensitivities and their depths of investigation (DOI).

If the invasion fluid front gets **deep** into the reservoir, the neutron and density porosity measurements approach the true porosity for the assumption of mud filtrate density and neutron response as fluid properties.

For **shallow** invasion (shallow with respect to the depth of investigation) the tools' responses are spatially weighted averages of the invaded and non-invaded regions of the formation. The problem in deriving porosity in the presence of shallow invasion comes from the fact that the neutron and density logging devices have different radial response:

- The 50% DOI of the thermal neutron porosity tool is 6 to 12 inches (15 to 30 cm).
- The 50% DOI of the density tool is about 2 to 3 inches (5 to 8 cm).

Click on the ad to read more

Download free eBooks at bookboon.com

Therefore the following rules are recommended:

- When the invasion front is greater than 12 inches (30 cm), both tools see only water-filled (mud filtrate) formations and the two porosity estimates agree and read true porosity.
- When the invasion front is less than 12 inches (30 cm) but greater than 6 inches (15 cm), the density tool sees only the invaded formation, while the neutron tool is sensitive to both the invaded and the non-invaded region. Under these conditions, the density porosity estimate is the true value, while the neutron porosity estimate is still low.
- Below 6 inches (15 cm) of invasion, both tools are sensitive to both the invaded and non-invaded regions. Thus, for a certain range of depths of invasion, accurate determination of formation porosity becomes very difficult. A root mean square (RMS) equation is recommended for gas reservoirs:

$$\phi_{ND,gas} = \sqrt{\frac{\phi_N^2 + \phi_D^2}{2}} \approx \frac{\phi_N}{3} + 2 \cdot \frac{\phi_D}{3}$$

5.5 Porosity and Mineral Composition – Multiple Porosity Methods

Motivated by the fundamental importance of an exact porosity value for reservoir characterization and for calculation of other properties (saturation), mostly two or more independent methods for porosity are applied. This gives the possibility of a combined interpretation (multiple porosity) directed on a derivation of porosity and rock composition. This situation is illustrated by the following cartoon (Figure 5-5).

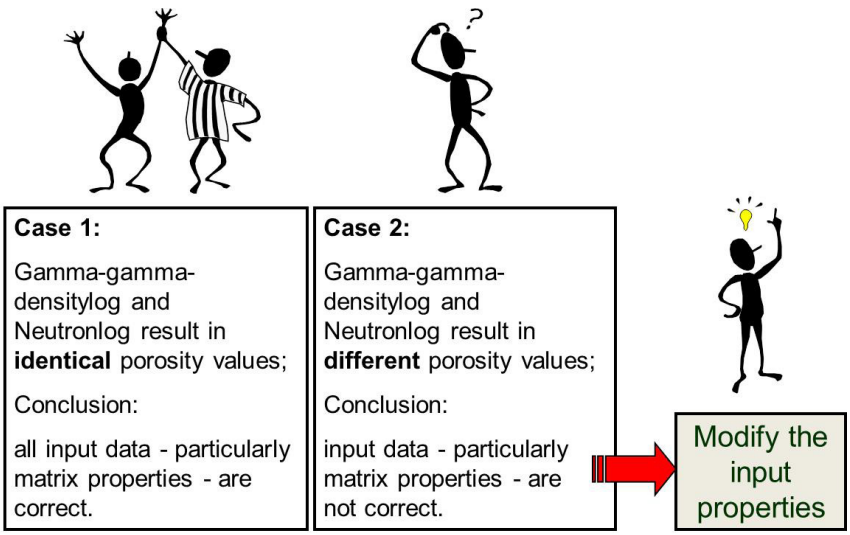

Figure 5-5: Multiple porosity determination – Cases and principle.

The combination of Gamma-Gamma-Density and Neutronlog is applied most frequently.

Download free eBooks at bookboon.com

If the lithology (mineralogy) and also water saturation can be assumed for a formation, then porosity can be calculated with both methods (for example for a limestone use neutron response matrix = 0, matrix density = 2.71 g cm^{-3}, neutron response fluid = 1.00, and fluid density = 1.00 g cm^{-3}). If both independent calculations deliver the same porosity (case 1) it can be concluded that:

1) The used interpretation model (limestone/calcite and water) is correct.
2) The calculated porosity is correct.

If the calculated porosities are different in case 2, the conclusion is that the used interpretation model (matrix mineralogy, fluid) is not correct. For combined interpretation the input must be modified or approximated. Thus, the conflict of two different answers can be solved by derivation of representative mineral composition and fluid type.

This idea is realized by different practical methods and techniques:

1) Overlay technique,
2) Cross plot technique,
3) Numerical solution of a system of response equations.

5.5.1 Overlays of two Logs

For the overlay technique two porosity curves are plotted in the same log trace and referenced to an identical porosity scale and a defined rock model (matrix and fluid). If, for example, Neutron porosity (limestone-calibrated tool) and Density-derived porosity (calculated also under assumption of calcite as matrix with density 2.71 g cm^{-3}) are plotted, then in a

- Water-saturated limestone both tools read same porosity,
- Sandstone or dolomite both tools read a somewhat different porosity,
- Shaly section neutron reads higher porosity than density resulting from the clay-bound water,
- Gas zone neutron reads lower porosity than density resulting from the lower H-concentration measured by the neutron log.

Important for overlay analysis is to understand the scales for both methods. There are two types:

Type 1:
Neutron Porosity (limestone-calibrated) and Density Porosity (using matrix density for limestone 2.71 g cm^{-3}) are plotted from left to right. In this case there is only one scale (or two identical scales). If there is dolomite or anhydrite in the formation, then density is higher than 2.71 g cm^{-3}. Calculation of limestone-referenced porosity therefore results in an apparently negative porosity value on the right-hand end of the scale.

Download free eBooks at bookboon.com

Type 2:
Again increasing Neutron Porosity (limestone-calibrated) and decreasing Density are plotted from right to left. The density scale is adapted for a limestone. Therefore:

- At Neutron porosity NPHI = 0.0, Density of RHOB = 2.7 g/cm³.
- At Neutron porosity NPHI = 0.3, Density of RHOB = 2.2 g/cm³.
- At Neutron porosity NPHI = 0.6, Density of RHOB = 1.7 g/cm³.

If the density of the formation is higher than 2.7 g/cm³ (anhydrite, dolomite), the scale must be expanded further to the right to accommodate, for example, at density 2.96 g cm⁻³ (anhydrite) a corresponding Neutron porosity of -0.15.Type 2 is illustrated in Figure 5-6.

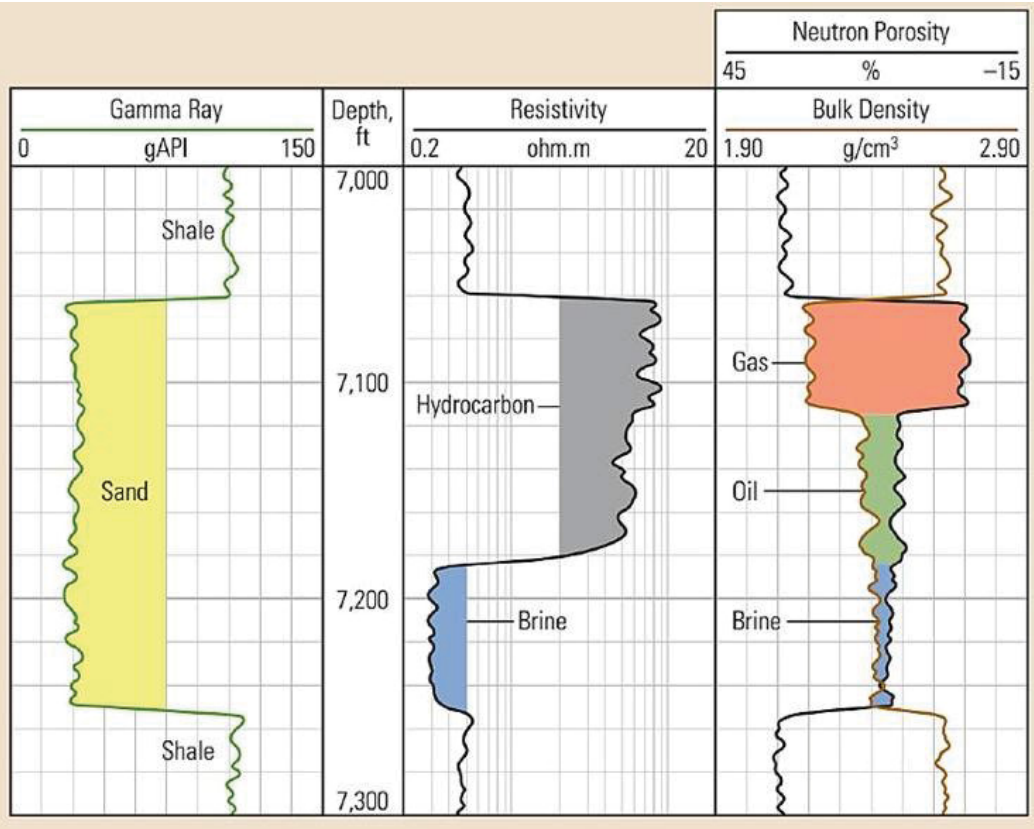

Figure 5-6: Gamma log GR, Resistivity, Density- and Neutronporositylog for some typical situations (Andersen, 2011).
The logs allow a first interpretration using following criteria:
Shale: High GR, crossover of Density (red curve) and very high apparent Neutronporosity,
Gas-bearing zone: Low GR, crossover of Density and very low Neutronporosity; high resistivity,
Oil-bearing zone: Low GR, low crossover of Density and Neutronporosity; high resistivity,
Water-bearing zone: Low GR, no crossover of Density and Neutronporosity; low resistivity.

If it is known that the formation is composed of different lithologies (for example a sandstone-shale formation) and this overlay technique is applied, the limestone-referenced scale delivers a deviation of the two curves. Therefore it is more comfortable to convert or transform both porosity logs to a sandstone matrix (see example 7.1 Oil-bearing Sandstone) and expect a fit for both logs in such cases.

Download free eBooks at bookboon.com

5.5.2 Cross plot – clean Matrix

While overlays present the logs of a section, the cross plot technique combines individual data sets of defined depth steps. For the combination of Neutron and Densitylog, the Neutron readings (limestone-calibrated porosity) from the LAS-file are plotted on the x-axis and the measured Gamma-Gamma-Density in reverse direction on the y-axis for each depth step (Figure 5-7).

Plots start in the lower left corner with the "matrix-points" and go up to the upper right corner to the "water-point" with linear scaled porosity. For practical use only the part for porosity < 0.45 (< 45%) is plotted:

- The coordinates x = *NPHI* = 0.0 and y = *RHOB* = 2.71 g cm^{-3} describe a dense (no porosity) calcite and is therefore called "matrix-point limestone".
- Increasing porosity (pore fluid water) moves the position linearly upward from this matrix point in the direction of a "fluid-point water" at x = *NPHI* = 1.0 and y = *RHOB* = RHO_{fl} = 1.0 gcm^{-3}. The connecting straight line represents a pure limestone with linear-scaled porosity.
- Different rocks (sandstone/quartz, dolomite) have a matrix point defined by matrix density and matrix neutron response.

Click on the ad to read more

Download free eBooks at bookboon.com

The result are three lines for limestone, dolomite, and sandstone. The deviation from a straight line of the dolomite and sandstone curve is contributed for a better approximation and depends on tool characteristics.[6]

Crossplots allow an estimate of mineralogy (lithology) and the determination of a consistent porosity. Measured data are plotted into the designed curve set. The position of the data point delivers the correct porosity and the mineral type or composition.

This is demonstrated in Figure 5-7 (example):

Log data:	Neutron porosity	*NPHI* = 15% (0.15)
	Gamma-Gamma-Density	*RHOB* = 2.56 g/cm³
Crossplot gives:	Porosity = 13% (0.13); the rock is a mixture of dolomite and limestone.	

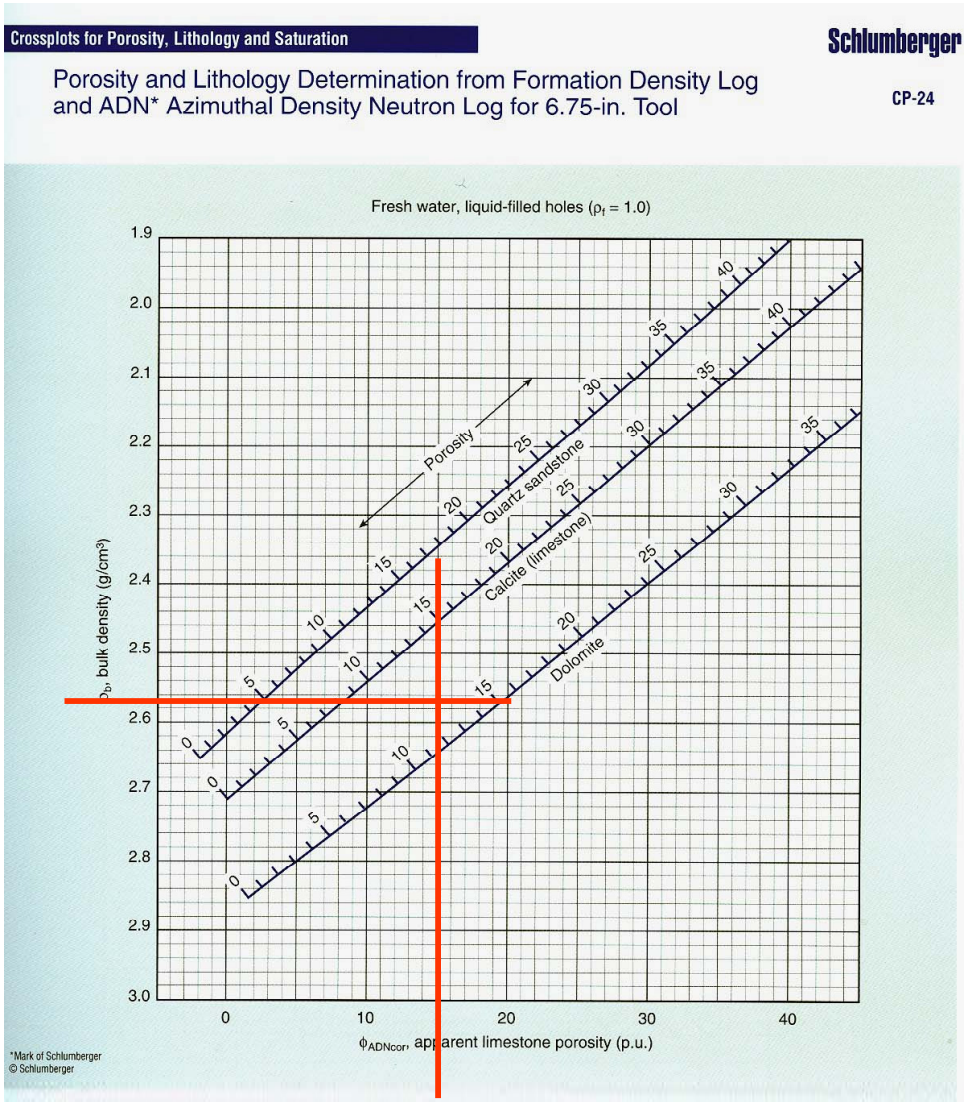

Figure 5-7: Example Neutron-Density Crossplot (Schlumberger Log Interpretation Charts, 2000 Edition).

Download free eBooks at bookboon.com

Deviations and problems occur for Neutron-Density-Crossplots if shale or gas is present:

- Gas in the formation shifts the points toward low neutron porosity, because gas has a lower H-concentration compared with water and in most cases the Neutronlog "reads" the non-invaded zone,
- Shale content shifts the points from the sand line towards dolomite, because apparent Neutron porosity increases (clay-bound water effect). For shaly sand a specific cross plot can be designed with a sand point, a wet-shale point, and a water point. This is a component of shaly sand analysis (see 7.2 Shaly sand profile).

A very helpful modification of the Neutron-Density-Cross plot is the implementation of a "third dimension": Individual data points are color-coded by their Gamma activity (Figure 5-8). If colour indicates low shale content (low Gamma), then the point represents a clean rock (in the sandstone, limestone or dolomite region). If color indicates high shale content and the point plots, for example, in the porous dolomite region then this is not really a highly porous dolomite but could be a shaly sandstone.

Crossplot – Shaly sand

A specific application is the interpretation of shaly sands. In a Neutron-Density crossplot data points of clean sandstone are arranged along the sandstone line. With increasing shale content the data points are shifted to higher Neutron porosity (clay-bound water effect). If data points are color-coded with Gamma intensity (GR) this effect is visible as demonstrated in Figure 5-8.

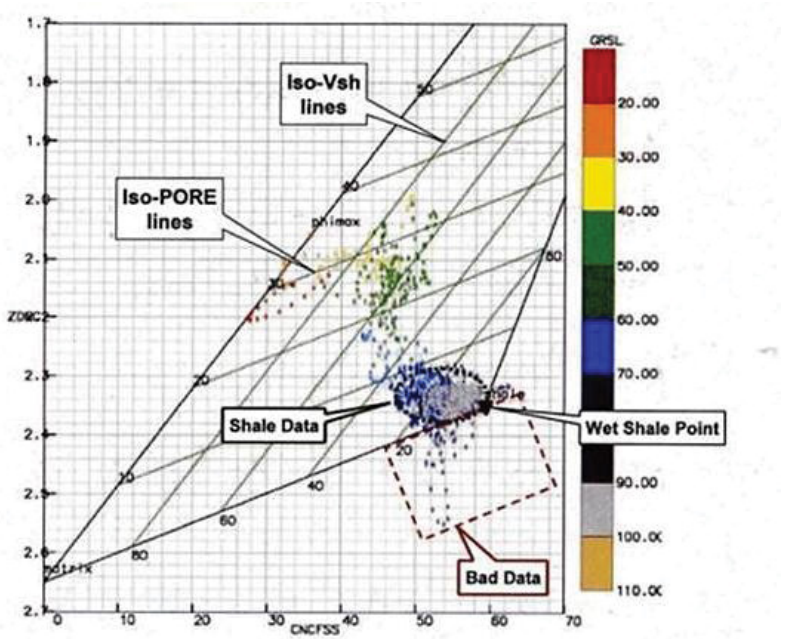

Figure 5-8: Determination of the "wet shale point" in a Neutron-Density-Plot (Baker Atlas document).

Download free eBooks at bookboon.com

The distribution of all data points allows picking the "wet shale point" at the highest GR (pure shale). It characterizes the shale including the clay bound water. The wet shale density can be extracted on the vertical axis and the wet shale Neutron porosity (neutron response wet shale) on the horizontal axis.

The volumetric rock model (Figure 5-9) describes density and porosity in terms of effective and shale porosity.

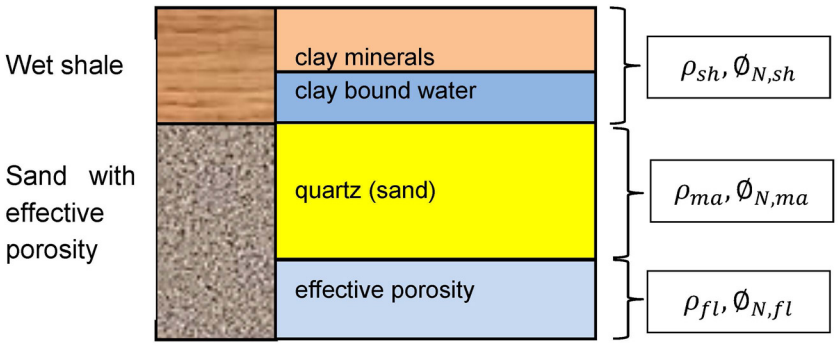

Figure 5-9: Shaly sand model.

Need help with your dissertation?

Get in-depth feedback & advice from experts in your topic area. Find out what you can do to improve the quality of your dissertation!

Get Help Now

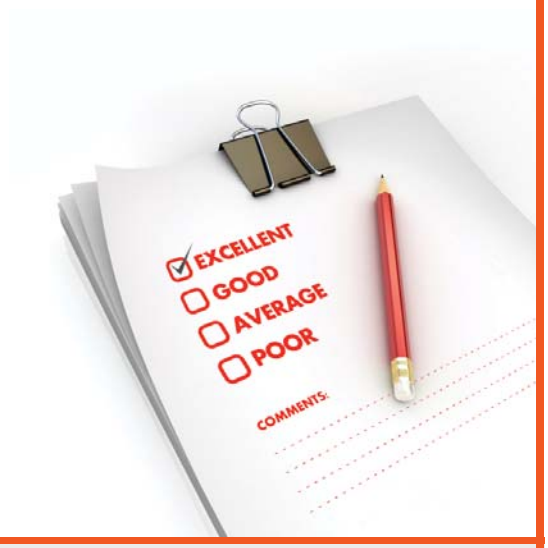

Go to www.helpmyassignment.co.uk for more info

Helpmyassignment

Click on the ad to read more

Download free eBooks at bookboon.com

The equations for (measured) Neutron porosity ϕ_N and bulk density ρ_b can be solved for shale content:

$$V_{sh} = \frac{(\phi_{N,fl} - \phi_{N,ma}) \cdot (\rho_{ma} - \rho_b) - (\phi_N - \phi_{N,ma}) \cdot (\rho_{ma} - \rho_{fl})}{(\phi_{N,fl} - \phi_{N,ma}) \cdot (\rho_{ma} - \rho_{sh}) - (\phi_{N,sh} - \phi_{N,ma}) \cdot (\rho_{ma} - \rho_{fl})}$$

effective porosity:

$$\phi_{eff} = \frac{(\phi_N - \phi_{N,ma}) \cdot (\rho_{ma} - \rho_{sh}) - (\phi_{N,sh} - \phi_{N,ma}) \cdot (\rho_{ma} - \rho_b)}{(\phi_{N,fl} - \phi_{N,ma}) \cdot (\rho_{ma} - \rho_{sh}) - (\phi_{N,sh} - \phi_{N,ma}) \cdot (\rho_{ma} - \rho_{fl})}$$

where

$\phi_{N,fl}$ is the neutron response (hydrogen index) of the fluid
$\phi_{N,ma}$ is the neutron response (hydrogen index) of the matrix
$\phi_{N,sh}$ is the neutron response (hydrogen index) of the wet shale
ρ_{fl} is the density of the fluid
ρ_{ma} is the density of the matrix
ρ_{sh} is the density of the wet shale.

5.5.3 Generalized solution for a composite matrix

Porosity and volume fractions of rock components (minerals) can be determined very elegantly mathematically by formulation of a system of linear equations. The response equations for a combination of Neutron porosity and Gamma-Gamma-density in case of a (clean) carbonate section consisting of limestone (calcite) and dolomite are:

$$\rho_b = RHOB = 2.71 \cdot V_{calcite} + 2.87 \cdot V_{dolomite} + 1.00 \cdot \phi$$
$$\phi_N = NPHI = 0 \cdot V_{calcite} + 0.02 \cdot V_{dolomite} + 1.00 \cdot \phi$$

The volume balance is $1 = V_{calcite} + V_{dolomite} + \phi$

This represents a system of 3 linear equations which can be solved for the 3 unknowns $V_{calcite}, V_{dolomite}, \phi$. The mathematical solution can be calculated comfortably by a "matrix (math) inversion". The response equations in matrix notation are:

$$\begin{bmatrix} \rho \\ \phi_N \\ 1 \end{bmatrix} = \begin{bmatrix} 2.71 & 2.87 & 1.00 \\ 0 & 0.02 & 1.00 \\ 1.00 & 1.00 & 1.00 \end{bmatrix} \cdot \begin{bmatrix} V_{calcite} \\ V_{dolomite} \\ \phi \end{bmatrix}$$

or $\mathbf{M} = \mathbf{RV}$
with
$\mathbf{M}$ matrix - measured properties, $\mathbf{R}$ matrix - response, $\mathbf{V}$ matrix - volume fractions

Download free eBooks at bookboon.com

The solution is $\mathbf{V} = \mathbf{R}^{-1}\mathbf{M}$ where $\mathbf{R}^{-1}$ is the inverse matrix[7].

$$\begin{bmatrix} V_{calcite} \\ V_{dolomite} \\ \phi \end{bmatrix} = \begin{bmatrix} -5.099 & -9.209 & 14.818 \\ 5.203 & 8.377 & -14.100 \\ -0.104 & 0.833 & 0.282 \end{bmatrix} \cdot \begin{bmatrix} \rho \\ \phi_N \\ 1 \end{bmatrix}$$

The set of linear equations can be generalized for a rock with *n* different material components (solids, fluids). For any property *g* with a linear response equation, the measured magnitude is:

$$g_m = \sum_{i=1}^{n} V_i \cdot g_{m,i}$$

where

g_m is the property, measured with a method *m*,
$g_{m,i}$ is the property (related to method *m*) of the component *i*,
V_i is the volume fraction of component *i*,
Additionally there is the volume balance equation $\sum_i V_i = 1$.

This is a system of $m + 1$ independent linear equations; it can be solved for $n = m + 1$ components (deterministic solution). The example has demonstrated this technique for two methods (Neutron and Gamma-Gamma). The system can be expanded by implementation of the PE-log (Photoelectric log), Acoustic log/Sonic log (if the linear principle of the time-average equation can be applied). In case of 4 independent measurements the system can be solved deterministically for 4 + 1 = 5 volume fractions (porosity + 4 minerals).

The calculation of rock composition and porosity based on this set of linear equations contains:

- The measured magnitude of the property,
- The properties of the expected components (rock model),
- The volume fractions of the components.

The definition of the expected rock composition (rock model) is a very important step[8]. Valuable input for this step comes from geological knowledge of the investigated formation, core data with respect to minerals, and cuttings data with respect to minerals.

Particularly in carbonates with mixture mineralogy some minerals with very strong effect on the measured properties (for example high density of anhydrite) can be present.

Download free eBooks at bookboon.com

5.6 Water Saturation from logs

The determination of water saturation S_w is – after shale content and porosity – the third key reservoir parameter. The difference (1 – S_w) gives the hydrocarbon saturation.

Calcualtion of water saturation applies electrical methods, because formation water is an electrolytic conductor and hydrocarbons are insulators. Electrical methods cannot distinguish between gas and oil (but the Neutronlog separates oil and gas).

Tools with different radial depth of investigation (deep-reading logs and micrologs) evaluate water saturation in the non-invaded (virgin) zone S_w and saturation with mud filtrate S_{xo} in the invaded zone. This technique results in a saturation profile and a determination of movable and non-movable hydrocarbons (see example 7.1 Oil-bearing Sandstone).

In clean rocks the formation water (and water-based mud filtrate) is the only conductive component – electrical properties are described by Archie's equations (Archie, 1942). If shale is present, a second electrical conductivity component occurs and Archie's equations must be replaced by a "shaly sand equation". The two dominant cases of shale presence in a rock are laminated and dispersed shale.

5.6.1 Clean rocks

In a clean reservoir the mud filtrate invasion creates a radial resistivity profile as simplified shown in Figure 4-6. Archie's equations can be applied on both regions:

Non-invaded zone with the conductive formation water (R_w):

$$S_w = \left(\frac{R_o}{R_t}\right)^{\frac{1}{n}} = \left(\frac{R_w}{R_t}\,\frac{1}{\phi^m}\right)^{\frac{1}{n}}$$

Invaded zone with the conductive mud-filtrate (R_{mf}):

$$S_{xo} = \left(\frac{R_{mf}}{R_{xo}}\,\frac{1}{\phi^m}\right)^{\frac{1}{n}}$$

For a calculation of S_w and S_{xo} the following inputs are necessary:

a) Porosity ϕ: From porosity logs,
b) rchie parameters m, n: Core laboratory measurements or recommended values from literature (frequently $m = n \approx 2$),
c) Formation water resistivity R_w: Derived from a water zone ($S_w = 1$), from SP-log (as demonstrated in example 7.1) or laboratory measurement at a formation water sample,
d) Mud filtrate resistivity R_{mf}: Measured at a fluid sample and temperature corrected for formation depth (see example 7.1).

Download free eBooks at bookboon.com

5.6.2 Shaly sands – shaly rocks

The presence of shale in a reservoir:

- Decreases reservoir quality (porosity, permeability),
- Originates an additional electrical conductivity; in most "shaly sand equations" the two conductivities are summarized (parallel conductor system),
- "Disturbs" traditional interpretation algorithms and techniques; application of Archie's equation results in an overestimate of water saturation.

For a correct S_w–calculation from resistivity logs this second conductivity effect therefore must be eliminated.

The conductivity contribution of shale/clay depends on:

1) Shale content (volume fraction), derived e.g., from Gamma log,
2) Shale type (clay mineralogy) controlling the "shale conductivity",
3) Distribution of shale in the formation (laminar shale or dispersed shale).

Click on the ad to read more

Download free eBooks at bookboon.com

Various "shaly sand equations" have been derived in order to model the different types of shale in a rock; only a few members are described in this section. Patchett and Herrick (1982) published a review of Saturation Models in a special Shaly Sand Reprint Review Volume of the SPWLA. A systematic overview and discussion is published by Worthington (1985).

Laminated Shaly Sand – The Poupon Equation

For the simple case of laminated shaly sand Poupon et al. (1954) derived an equation. The laminated shaly sand represents an alternating sand-shale layering with the thickness of the individual layers in the mm-range. Resistivity tools cannot resolve individual layers but measure the effect of a parallel conductor assuming current lines are parallel to the layering (Figure 5-10)).

Figure 5-10: The Laminated Shaly Sand Model.

The conductivity (the inverse of resistivity) of this parallel conductor model is:

$$\frac{1}{R_t} = \frac{1 - V_{sh-lam}}{R_{sd}} + \frac{V_{sh-lam}}{R_{sh}}$$

where:

V_{sh-lam}	is the (laminar) shale content,
R_{sh}	is the shale resistivity,
R_{sd}	is the sand resistivity.

Application of the equation has two steps:

1) Calculation of the resistivity of the sand fraction:

$$R_{sd} = (1 - V_{sh-lam}) \cdot \left(\frac{1}{R_t} - \frac{V_{sh-lam}}{R_{sh}}\right)^{-1}$$

2) Calculation of the water saturation for the sand fraction using Archie's equation:

$$S_w = \left[\frac{R_w}{R_{sd}} \cdot \frac{1}{\phi^m}\right]^{\frac{1}{n}}$$

Download free eBooks at bookboon.com

Thus, as input the following parameters are necessary:

R_t	from the log measurement	R_{sh}	resistivity of an adjacent shale bed,
V_{sh}	shale content e.g., from a Gamma log	ϕ	porosity (from porosity logs),
R_w	formation water resistivity	m, n	Archie exponents.

…and we must know that the shale is laminated (one possibility to discriminate between laminated and dispersed shale/clay is the so-called Thomas-Stieber plot (see end of this chapter).

Figure 5-11 shows the result of a forward calculation of formation resistivity R_t as a function of water saturation S_w for different laminar shale content V_{sh}. It demonstrates that the effect of shale is very strong at low water saturation and increases with increasing water resistivity.

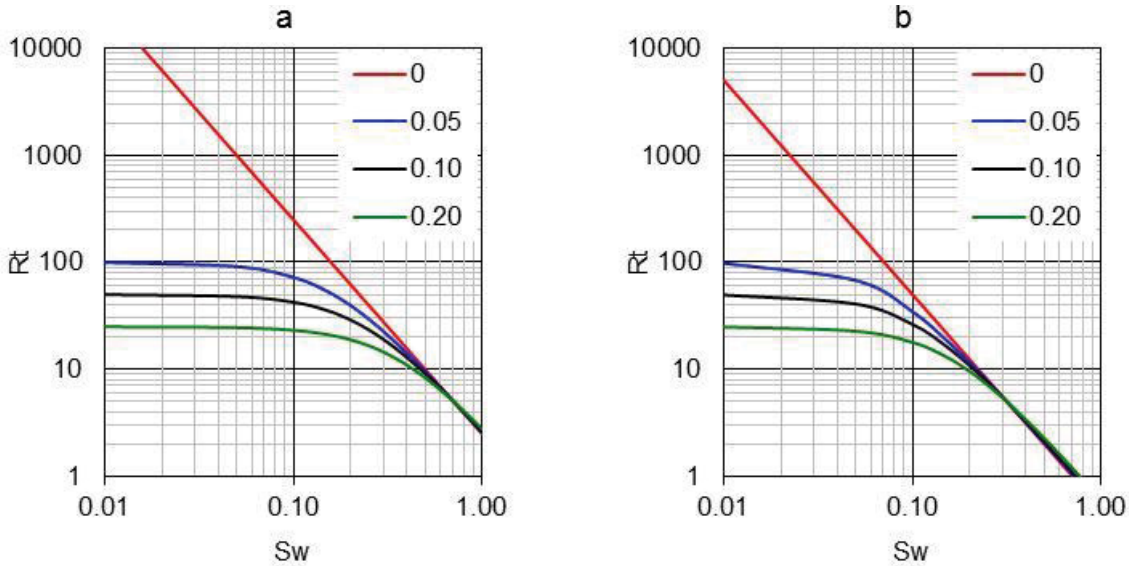

Figure 5-11: Formation resistivity R_t as function of water saturation S_w for four different laminar shale contents V_{sh}. Porosity = 0.2, m = n = 2, Rsh = 5 Ohmm. a) Water resistivity = 0.10 Ohmm; b) Water resistivity = 0.02 Ohmm.

An example may demonstrate the laminar shale effect on S_w:

Input data:	R_t = 4 Ohm m	R_{sh} = 1.5 Ohm m	V_{sh} = 0.20
	R_w = 0.02 Ohm m	$m = n = 2$	
	$\emptyset$ = 0.18	F = 31	

Wrong calculation: We neglect V_{sh} and apply Archie's equation directly:

$$S_w = \left(\frac{R_w}{R_t} \cdot \frac{1}{\phi^m}\right)^{\frac{1}{n}} = \sqrt{\frac{0.02}{4} \cdot 31} = 0.39$$

Download free eBooks at bookboon.com

Correct calculation: We consider V_{sh} and apply Poupon's equation:

$$S_w = \left[R_w \cdot \left(\frac{1}{R_t} - \frac{V_{sh}}{R_{sh}} \right) \cdot \frac{1}{\phi^m} \cdot \frac{1}{1 - V_{sh}} \right]^{\frac{1}{n}} = \left[0.02 \cdot \left(\frac{1}{4} - \frac{0.2}{1.5} \right) \cdot 31 \cdot \frac{1}{1 - 0.2} \right]^{\frac{1}{2}} = 0.30$$

Conclusion: The shale gives a contribution to the rock conductivity and decreases the resistivity. Shale has therefore an effect which acts in the same direction as water (in our example as 9% water). Neglecting the shale results in a non-realistically high water saturation (or low hydrocarbon saturation).

Dispersed Shaly Sand

If shale is distributed dispersed in the pore space then the "clay conductivity" must be placed in the pores at the same location as the pore water.

Waxman and Smits (1967) developed a model with the "architecture" of Archie's equation and replaced water conductivity $C_w = R_w^{-1}$ by the sum $C_w + BQ_v$, where the second term expresses the shale conductivity component.

For water saturated ($S_w = 1$) porous rocks results:

$$\frac{1}{R_o} = C_o = \frac{1}{F*} \cdot \left(C_w + B \cdot Q_v \right)$$

with the following terminology:

C_t conductivity of the shaly sand,
C_w conductivity of the formation water,
ϕ porosity,
S_w water saturation,
$F*$ formation factor of the shaly sand,
B equivalent conductivity of sodium clay-exchange cations,
Qv shalyness factor (cation exchange capacity per unit volume in meq cm^{-3}).

For an oil- or gas- bearing rock the Waxman-Smit equation is:

$$\frac{1}{R_t} = C_t = \frac{S_w^n}{F*} \cdot \left(C_w + \frac{B \cdot Q_v}{S_w} \right)$$

and water saturation S_w results (with $n = 2$) as

$$S_w = \left[\frac{F* \cdot R_w}{R_t} + \left(\frac{B \cdot Q_v \cdot R_w}{2} \right)^2 \right]^{-\frac{1}{2}} - \left(\frac{B \cdot Q_v \cdot R_w}{2} \right)$$

Download free eBooks at bookboon.com

BQ_v must be determined at the laboratory and depends on temperature.

The **Dual-Water Model** (Clavier et al., 1977, 1984) is based on the concept of two types of water:

- Free water in the pore space *wt,*
- Water near the clay surface (bound water) *bw.*

Both conductivities again form a parallel circuit:

$$C_t = \frac{1}{R_t} = \frac{\phi^m \cdot S_{wt}^n}{a} \cdot \left[C_w + \frac{S_{wb}}{S_{wt}} \cdot (C_{wb} - C_{wt}) \right]$$

C_t	rock conductivity		
C_{wt}	free water conductivity	C_{wb}	bound water conductivity
S_{wt}	free water saturation	S_{wb}	bound water saturation

The **Simandoux Equation** (Simandoux, 1963) is recommended for structural and dispersed type of shale distribution and was modified by Bardon and Pied (1969):

$$\frac{1}{R_t} = C_t = \frac{\phi^m}{R_w} \cdot S_W^n + V_{sh} \cdot C_{sh} \cdot S_W$$

TURN TO THE EXPERTS FOR
SUBSCRIPTION CONSULTANCY

Subscrybe is one of the leading companies in Europe when it comes to innovation and business development within subscription businesses.

We innovate new subscription business models or improve existing ones. We do business reviews of existing subscription businesses and we develope acquisition and retention strategies.

Learn more at linkedin.com/company/subscrybe or contact
Managing Director Morten Suhr Hansen at mha@subscrybe.dk

SUBSCRYBE - to the future

Click on the ad to read more

Download free eBooks at bookboon.com

for $n = 2$ results

$$S_W = \frac{1}{2} \cdot \frac{R_W}{\phi^m} \cdot \left[\sqrt{4 \cdot \frac{\phi^m}{R_W \cdot R_t} + \left(\frac{V_{sh}}{R_{sh}} \right)^2} - \frac{V_{sh}}{R_{sh}} \right]$$

The **Indonesia Equation** was published in 1971 by Poupon and Levaux and is recommended for shaly formations with fairly fresh water:

$$C_t = \frac{C_W}{F} \cdot S_W^2 + 2 \cdot \sqrt{\frac{C_W \cdot C_{sh}}{F} \cdot V_{sh}^{2-V_{sh}}} \cdot S_W^2 + V_{sh}^{2-V_{sh}} \cdot C_{sh} \cdot S_W^2$$

or in a simplified form for $V_{sh} \leq 0.5$

$$C_t = \frac{C_W}{F} \cdot S_W^2 + 2 \cdot \sqrt{\frac{C_W \cdot C_{sh}}{F} \cdot V_{sh}} \cdot S_W^2 + V_{sh} \cdot C_{sh} \cdot S_W^2$$

Figure 5-12 demonstrates the effect of the shale upon the result of a Sw-calculation for three shaly sand equations.

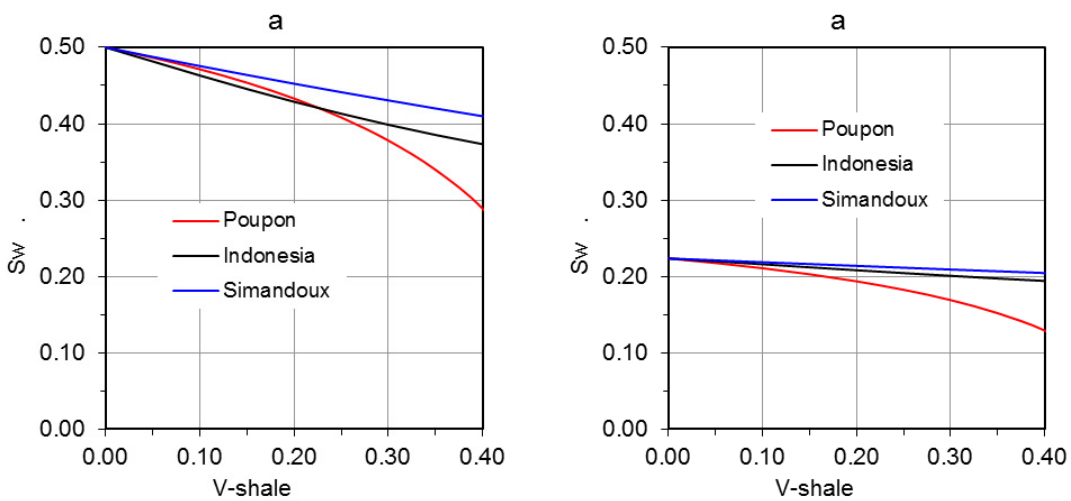

Figure 5-12: Water saturation versus shale content for three shaly sand equations; *Rt* = 10 Ohmm, *R – sh* = 5 Ohmm, porosity = 0.20, 2. *m* = *n* = 2 a) water resistivity *Rw* = 0.10 Ohmm; b) water resistivity *Rw* = 0.02 Ohmm. (http://www.elsevierdirect.com/companion.jsp?ISBN=9780444537966, Schön, 2011)

Thomas-Stieber Crossplot for Shale Type Investigation

Discussion of selected shaly sand equations demonstrates that three "pieces of information" on the shale are necessary:

1. Shale content (V_{sh}),
2. Shale and distribution type ($V_{sh\text{-}lam}$, $V_{sh\text{-}disp}$),
3. Shale properties (R-*shale*,*B* Q_v).

Download free eBooks at bookboon.com

Thomas and Stieber (1975) proposed a cross plot technique to determine the type of shale distribution using only log data. They plot a "porosity tool" (Density log) and a "shale volume tool" (Gamma log). Figure 5-13 demonstrates the principle:

- Laminated shaly sand plots along the connection of the two "corner values" for clean sand and pure shale
- Dispersed shaly sand plots starting at the clean sand point and by filling the pores with clay it reaches the end if $V_{shale} = \phi$ and all pores are filled.

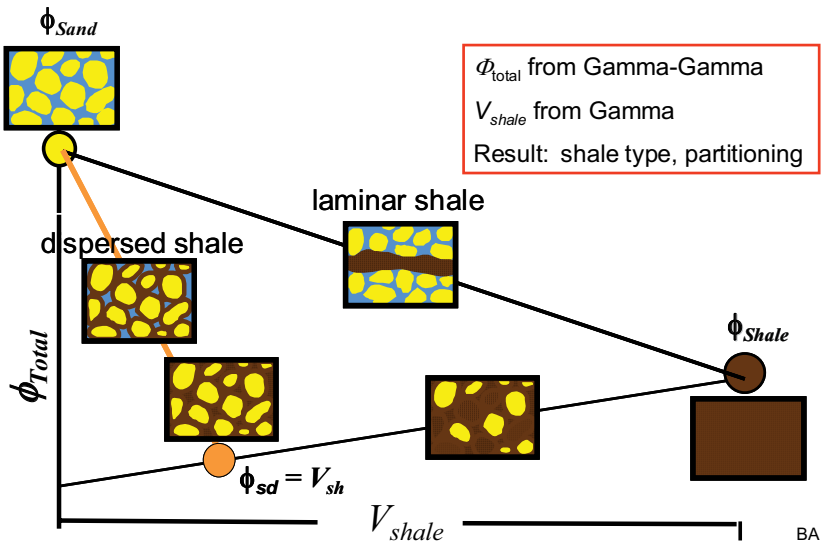

Figure 5-13: The Thomas-Stieber Plot for shale typing.

The example 7.2 Shaly sand profile demonstrates the application.

Download free eBooks at bookboon.com

6 Some Applications in Water Exploration

Borehole geophysical methods are also applied to various problems in water exploration, thermal- and mineral water exploration.

This section gives some specific characteristics of this type of application directed on two situations:

- Water wells in sediments, granular reservoirs,
- Water wells in hard rocks, fractured reservoirs.

In general, borehole measurements for water exploration apply a small number of logs and tools and depth of the wells is smaller compared with hydrocarbon exploration. The goal of a measurement in many practical applications is:

a) Investigation of the lithological profile,
b) The detection of aquifers (porous or/and fractured) with exact depth of bed boundaries,
c) The control of completion and production.

Click on the ad to read more

Download free eBooks at bookboon.com

Thus, the measuring program is significantly cheaper than any hydrocarbon log exploration. But the conditions in the investigated formations is also different:

- In many cases the profile consists of unconsolidated rocks (sand, shale), but also hard rocks with fractures are the target especially in thermal water and mineral water exploration.
- The pore or fracture-filling fluid is water with mostly low salinity (except mineral water). Therefore aquifers have relatively high resistivity compared with shale beds. This high water resistivity results in a high sensitivity of rock resistivity with respect to shale content – in a fresh water-saturated reservoir a small amount of shale decreases rock resistivity much more strongly than in a (deep) reservoir with saline formation water.

Two examples may illustrate typical applications.

6.1 Water well in an unconsolidated formation

The left part of Figure 6-1 shows a selection of standard logs measured (open hole) in an unconsolidated lithology. Gamma log combined with conventional 4-electrode resistivity logs (short and long normal) delivers a detailed lithological profile following the rules:

- Sand (aquifer): Low gamma and high resistivity,
- Shale: High gamma and low resistivity (clay conductivity).

Sand (aquifer) layers are marked and the completion design (screened sections) is derived.

After completion a second series of logs was measured (right part of Figure 6-1): Temperature log and different modes of flowmeter.

Flowmeters measure the (vertical) flow speed of the water in the well. Frequently an impeller flowmeter is used in water exploration. The rotations of an impeller per second are a measure of the velocity of the fluid (water) relative to the tool. In case of a continuous measurement (tool is moving with constant speed) the measured flowmeter rate (rot/sec) gives the sum of the two velocities (water flow and tool speed). Therefore registration of tool speed for correction is part of a flowmeter measurement.

Download free eBooks at bookboon.com

Figure 6-2 shows the measuring principle and the two modes for water wells.

- Flow profile (left figure): The tool (with a packer disk) moves downward. There is a high rate as result of an inflow from aquifer A and aquifer B and from the speed of the tool in the upper section. Below aquifer A the measured signal results only from aquifer B and from the speed of the tool. And below aquifer B there is no inflow – the measured signal represents the tool speed effect. This curve allows a quantitative description of the inflow (inflow profile). If aquifers are not artesian a pump above the uppermost aquifer can activate the inflow.
- Hydraulic function of screens (right figure): This mode controls the hydraulic function of the completion. The well is completed. The down going flowmeter gives the highest flowrate within the tube because all displaced water must pass the sensitive impeller section. If the tool passes a permeable screened section, a part of the displaced water flows behind the screen crossing the permeable gravel pack. Thus, a step to a low flowrate indicates a screened section with good permeability. If the gravel pack is not permeable then the step is less steep and indicates the well completion is of low hydraulic quality.

Click on the ad to read more

Download free eBooks at bookboon.com

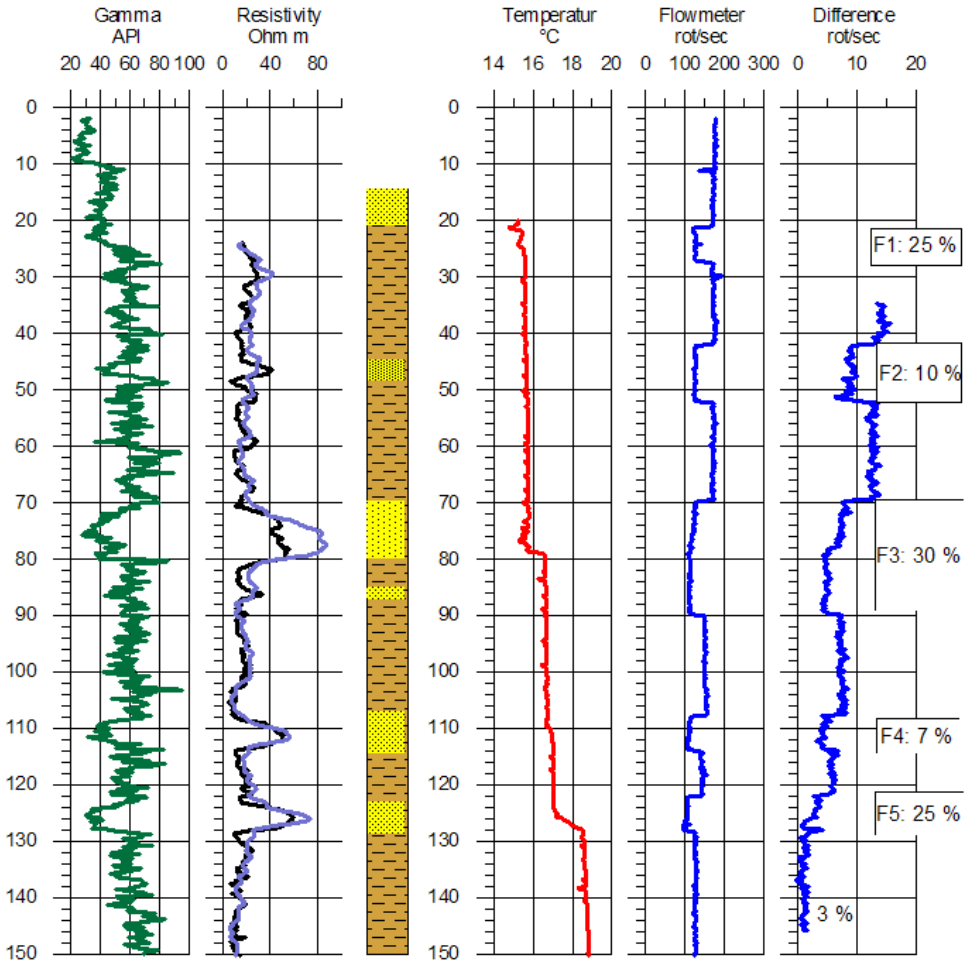

Figure 6-1 Borehole measurements in a water well (unconsolidated formation).

The second track in the right-hand part of Figure 6-1 shows the result of hydraulic completion control. All screens are at the correct depth position and have a full hydraulic function indicated by high permeability. The temperature curve (first track) gives sharp changes at 78 m and 127 m which indicate that 3 different water types are flowing from the individual aquifers.

Download free eBooks at bookboon.com

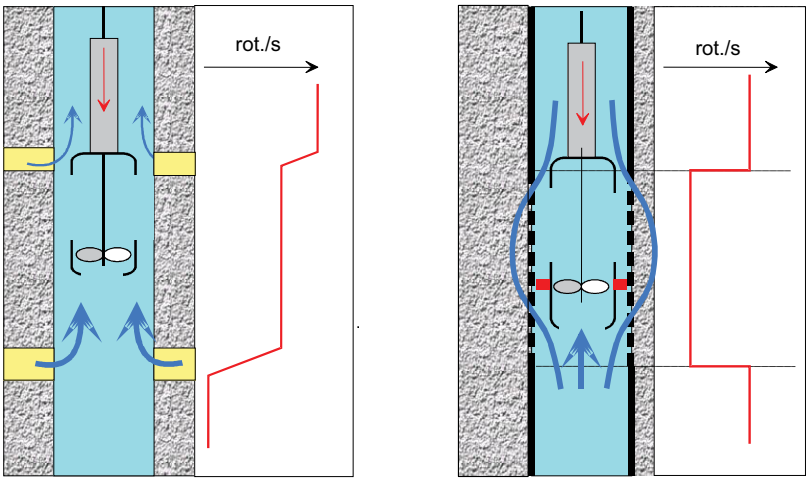

Figure 6-2: The two modes of a Flowmeter for water wells.

6.2 Mineral water well in a fractured carbonate formation

A well for mineral water exploration was drilled in a carbonate formation. Figure 6-3 shows selected logs: Gammalog (API), Deep Resistivity log (Ohmm), Acousticlog (compressional velocity in m/s) and the Flowmeter measurement during pumping (in cps). Cuttings show marl/breccia, dolomite and limestone.

Interpretation:

- The Gammalog separates marl/breccia 600 … 619 m, carbonate 619 … 680 m,
- Resistivity indicates a porous/fractured carbonate section from 621 … 645 m followed by a dense section,
- The Acousticlog confirms a fractured section 621 … 445 m with vp ≈ 4000 m/s followed by a dense section with vp ≈ 7000 m/s.

Thus the hydraulically active zone is the dolomite from 621 m to 645 m. A Flowmeter measurement (pump was located at a depth of 600 m) confirms the inflow in this section; spikes on the log result from caliper irregularities in the open well.

Download free eBooks at bookboon.com

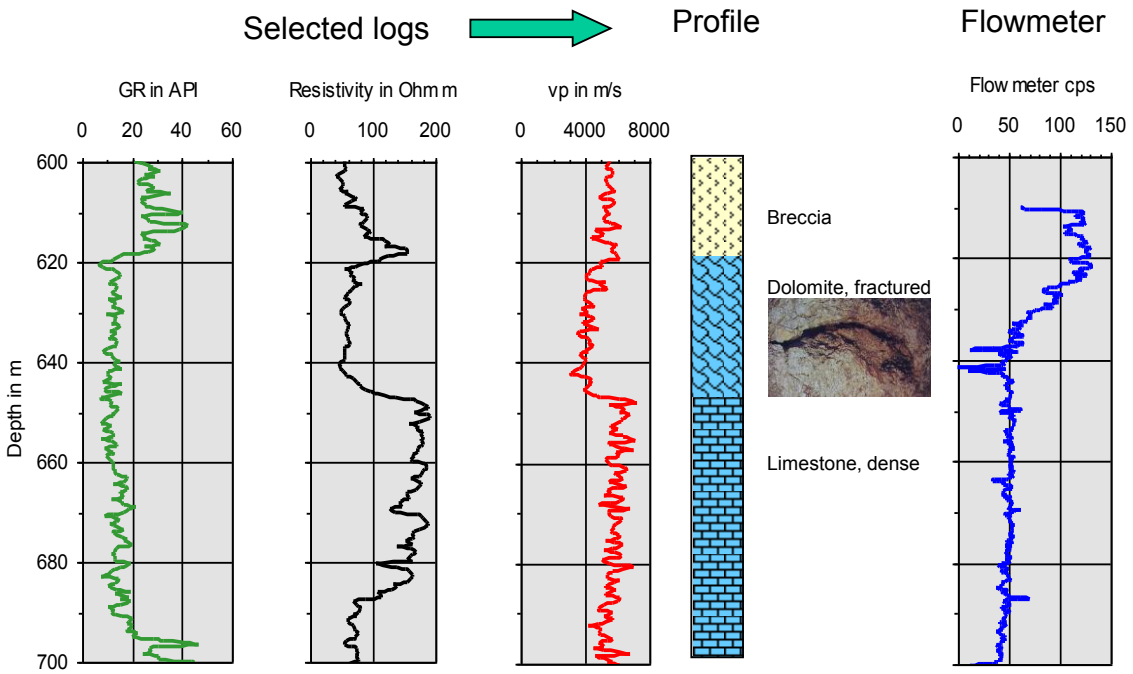

Figure 6-3: Detection of hydraulically active sections in a mineral water well in a carbonate formation. Track 1: Gammalog; track 2: Resistivity log; track 3: Acousticlog (vp); track 4: derived lithology; track 5: Flowmeter log with a pump at 600 m depth. The photo of the borehole wall in the dolomite is an optical borehole-televiewer picture (an optical scan was possible because of clear water in well).

This e-book
is made with
SetaPDF
SETASIGN
PDF components for PHP developers
www.setasign.com
Click on the ad to read more

Download free eBooks at bookboon.com

7 Examples and Exercises

In this section three log example are discussed. Numerical calculations are implemented in order to apply equations and rules.

Please note that the same algorithms are applied in software packages. Therefore, the same parameters (for example, rock components/minerals, mineral and fluid parameter) are also necessary as input in these sophisticated programs.

The first example is an oil-bearing (clean) sandstone. Goal of the exercise is the derivation of a lithologic profile and the calculation of porosity and fluid saturations including derivation of *Rw* from log data.

The second example is a shaly sandstone. Goal of the exercise is the characterization of the shale component in the reservoirs and its effect on water saturation determination.

The third example is the analyse of a mixture carbonate profile. Goal of the exercise is the simultaneous calculation of mineral composition and porosity.

7.1 Oil-bearing Sandstone

The example is a North African Well. The profile consists of sand (reservoir) with some authigenic clay and parts with silty material. Non-reservoir zones are shale and anhydrite layers.

Goal of this exercise:

- Lithologic profile with description of reservoirs,
- Compilation of input parameters for quantitative interpretation,
- Determination of porosity,
- Determination of water saturation; derivation of hydrocarbon saturation,
- Determination of moveable and non-moveable oil saturation.

7.1.1 Data base

Table 7-1 shows the selected logs for the interpretation and Table 7-2 the mud filtrate resistivity and formation temperature.

Download free eBooks at bookboon.com

Log	Name	Unit
CALI	Caliper	inch
GR	Natural gamma	API
SP	Spontaneous Potential	mV
RHOB DRHO	Bulk density Density correction	g/cm^3
PEF	Photoelectric cross section	b/e
NPHISS	Neutron-porosity-sandstone	decimal
DT	Sonic	µs/ft
RT, RXO; MFSL	Specific resistivities calculated from original measurements Spherical focusing log, microspherical focusing log	Ohm m Ohm m

Table 7-1: Logs.

Parameter	magnitude
Rmf – measured at 90 °F (32 °C) Formation temperature	0.336 Ohm m 178 °F (81 °C)

Table 7-2: Temperature and R_{mf}.

7.1.2 Logplot and Quick-look Interpretation

Figure 7-1 shows the plotted logs. The original limestone-calibrated Neutron porosity was transformed into sandstone-referenced Neutron porosity (NPHISS) because the reservoir is sandstone.

First track:	CAL (IN)	Caliper inch
	DRHO (PU)	Correction for Density (in porosity units)
Second track:	PEF (BARN)	Photoelectric cross section in barn
	GR (GAPI)	Gamma log in GR
	SP (MV)	Spontaneous Potential in mV
Third track:	RT (OHMM)	Formation Resistivity in Ohm m
	RXO (OHMM)	Resistivity of invaded zone in Ohm m
	MSFL (OHMM)	Resistivity Micro Spherical Focusing Log in Ohm m
Fourth track:	RHOB (GC	Bulk Density in g cm-3
	NPISS (DE	Neutron Porosity (Sandstone converted) as fraction
Fifth track:	DT (µS/FT)	Slowness in µs/ft

Download free eBooks at bookboon.com

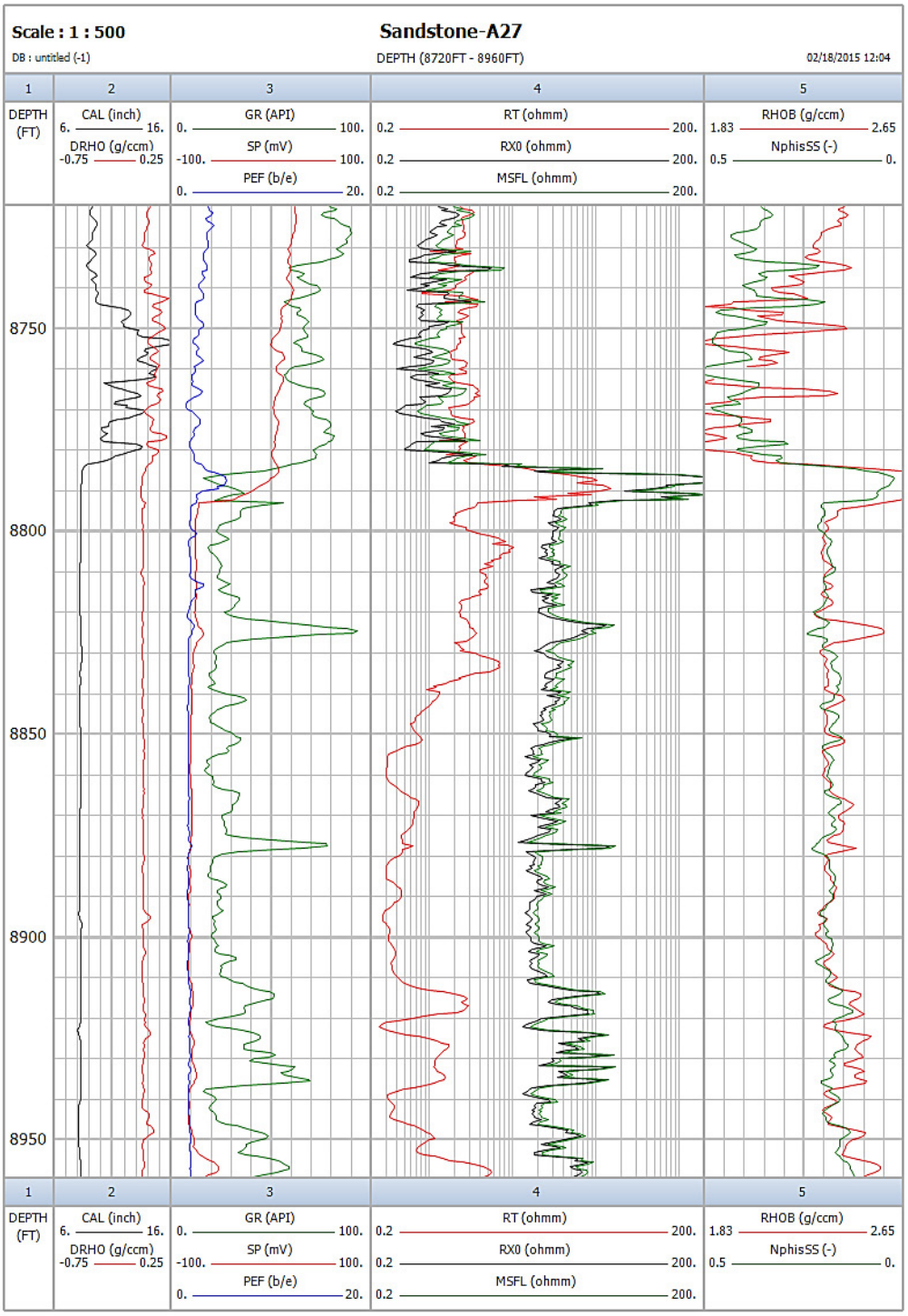

Figure 7-1: Logplots.

The caliper log (first track) shows in the uppermost part – particularly from 8745 to 8785 ft – a caliper enlargement ("bad hole").

Download free eBooks at bookboon.com

A look on the Gammalog and SP-log indicates this section as shale with some stability problems. The correction term for density-derived porosity DRHO is very high (up to – 0.23) and does not allow any further quantitative density interpretation.

The "Lithology logs" GR and SP clearly separate sand and shaly zones of the section. The following profile can be derived:

- Shale zone from top to 8784 ft; bad hole.
- The zone from 8784 to 8795 ft is characterized by correct Caliper, low GR, PEF of about 5 b/e, extremely high resistivity, very low NPHI and extremely high RHOB (data in LAS-file show > 2.9 g cm^{-3}), and low DT. All these indications – particularly the density – are typical of anhydrite. It forms a cap rock covering the reservoir.
- Sand zone (reservoir) from 8795 to 8910 ft. with shaly/silty interlayers at 8822 to 8826 ft, 8876 to 8879 ft[9]. – PEF confirms a (quartz) sand with 1.8 p/e. The log plot shows Neutron porosity in the porosity column. NPHISS is plotted from 0 to 0.5 and Density RHOB from 2.65 gcm^{-3} to 1.83 gcm^{-3}. Thus, the fit of Neutron- and Density-Porosity is indicative for a sandstone.
- The following zone is a shaly sand (increase of GR).

The Neutron-Density crossplot (Figure 7-2) confirms the lithological units.

Click on the ad to read more

Download free eBooks at bookboon.com

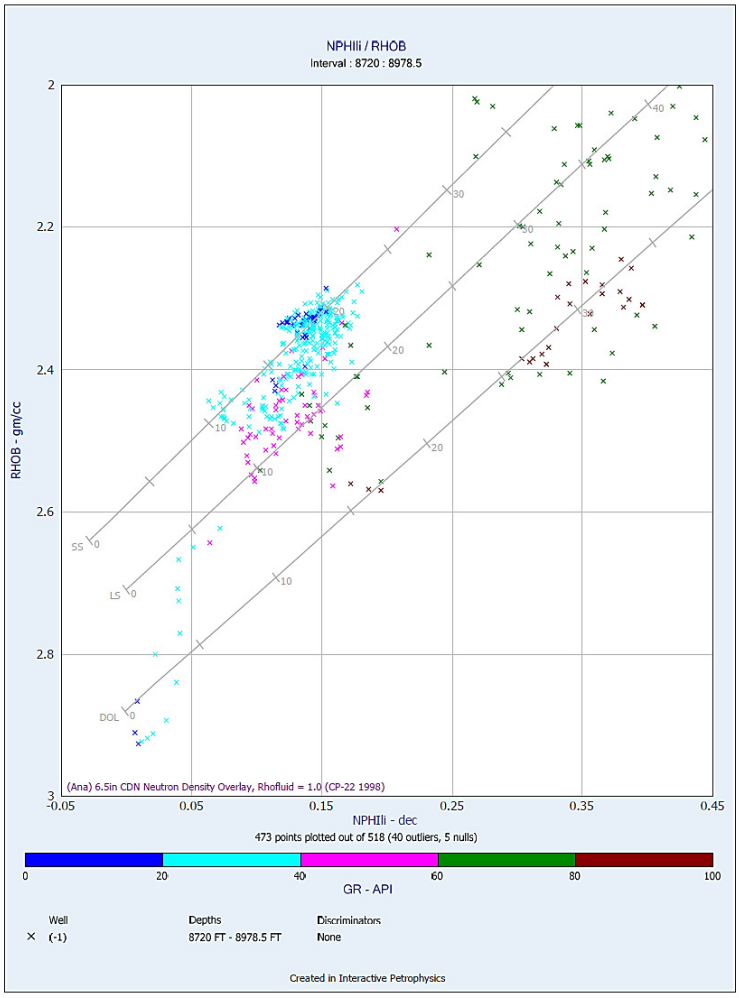

Figure 7-2: Neutron-Density crossplot: Most data points are close to the sandstone line (porosity 15 … 20%); data points in the upper right part are influenced by the shale section and caliper. Note that there are also some data points in the lower left corner indicating anhydrite.

For the following quick-look interpretation of resistivity, it is important to note that the reservoir is characterized by a nearly constant porosity of about 20% – it is a homogeneous reservoir.

The resistivity R_t below 8855 ft is very low (0.02 … 0.04 Ohmm); this indicates a very high salinity and a strong contrast to the mud filtrate resistivity (therefore SSP is very high – about 200 mV).
From a depth of 8800 ft upwards, the resistivity R_t increases by a factor of about 10. R_t is still below R_{xo} (R_{xo} is controlled by low saline mud filtrate). This increase of R_t must be originated by a decrease of water saturation (because porosity is constant). This part is probably the transition zone. From 8834 ft to 8795 ft, the reservoir is above transition zone.
The nearly constant level of R_{xo} (and MSFL) confirms reservoir homogeneity and clearly indicates invasion as a result of permeability.

Download free eBooks at bookboon.com

7.1.3 Compilation of input parameter for quantitative interpretation

Shale content from Gammalog:
Minimum and maximum magnitude (average for the reservoir): GR_{min} = 16 API; GR_{max} = 110 API. Note: Particularly GR_{max} cannot be taken from the shale zone of this plot because of bad hole conditions!

Matrix and fluid parameter for porosity calculation (matrix data from core measurements):

ρ_{matrix} = 2.65 g cm^{-3} $\qquad$ $_{fluid}$ = 1.00 g cm^{-3},

Δt_{matrix} = 52 µs/ft $\qquad$ Δt_{fluid} = 190 µs/ft.

Archie parameter (from core measurements): $m = n = 2$

Fluid parameter for resistivity analysis:

a) Calculation of R_{mf} at formation temperature 178 °F:
R_{mf} at 90 °F is 0.336 Ohmm; conversion with Arps equation 4.2.1results in

$$R_{mf,178} = 0.336 \cdot \frac{90+6.77}{178+6.77} = 0.176 \text{ Ohmm.}$$

b) Determination of R_w at formation temperature:

This fundamental property for calculation of water saturation will be derived from resistivity in the water zone and from SP-analysis:

Calculation of R_w from water zone:
Within the water zone, the resistivity equals R_o. For a selected part (8890 … 8900 ft) it is (on average) 0.3 Ohmm. For this part porosity is 0.2 and

Formation factor is $\qquad F = \frac{1}{0.20^2} = 25$

Formation water resistivity results as $\qquad R_w = \frac{R_o}{F} = \frac{0.30}{25} = 0.012$ Ohmm.

This principle is implemented in software-systems as the “Rwa-technique”.

Calculation of R_w from SP:

Download free eBooks at bookboon.com

In section 4.2.7 the connection between SSP (static spontaneous potential) and the ratio of the resistivity of the mud filtrate to the resistivity of the formation water R_{mf}/R_w was described as:

$$SSP = k_{SP} \cdot \log\left(\frac{R_{mf}}{R_w}\right)$$

where the factor k_{SP} is mainly controlled by temperature; this dependence is presented in the nomogram in Figure 7-3.

Log shows a maximum SSP difference of SSP = -100 mV. At the formation temperature of T = 178 °F the circle in Figure 7-3 results in a ratio:

$$\frac{R_{mf}}{R_w} = 15 \qquad R_w = \frac{0.176}{15} = 0.012 \text{ Ohmm}$$

This is in confidence with the value from the water zone and confirms the very high salinity of formation water.

Click on the ad to read more

Download free eBooks at bookboon.com

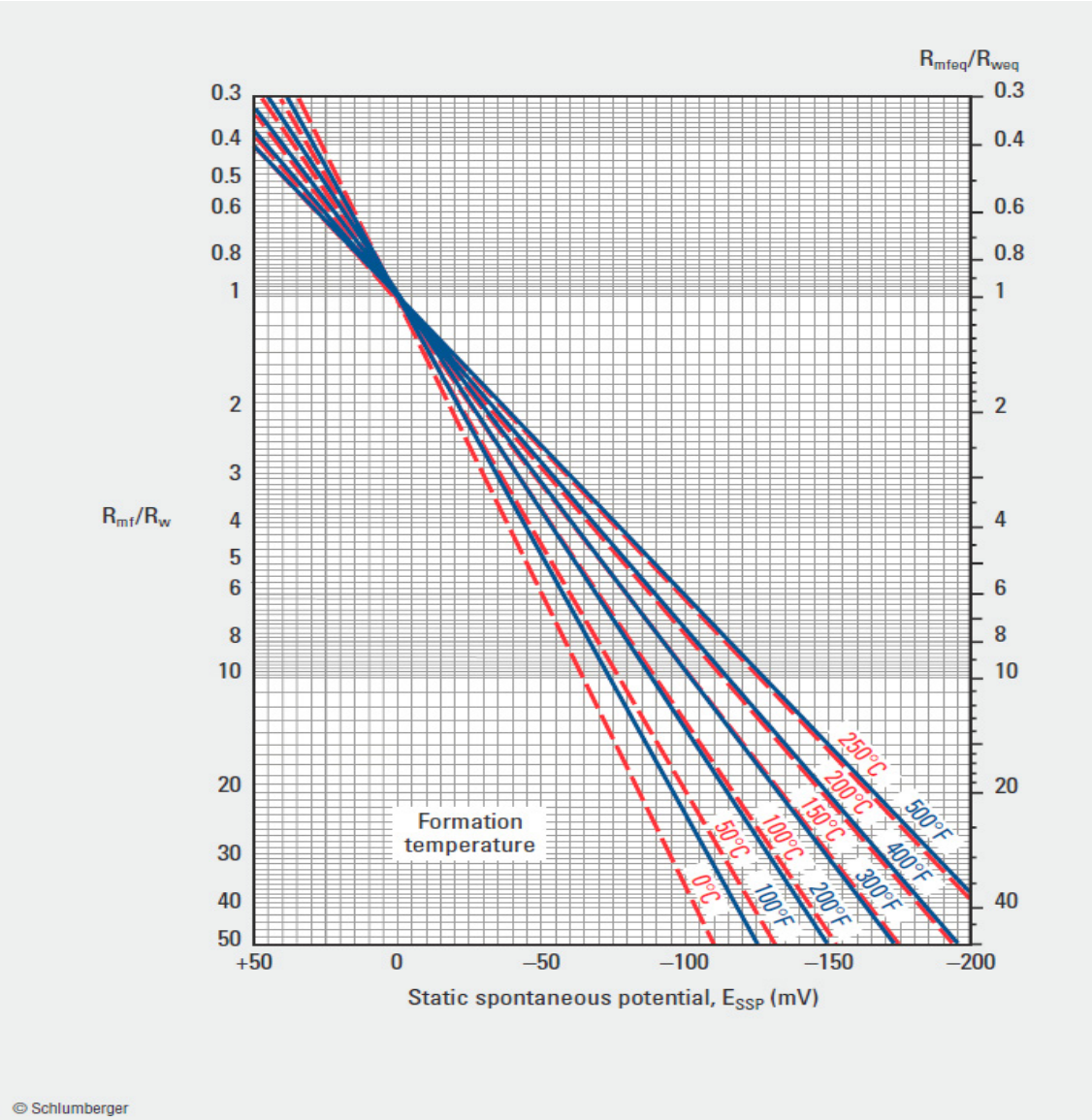

Figure 7-3: Determination of Rw from SSP, Schlumberger Chart Book, 2000.

7.4.1 Quantitative interpretation for 4 reservoir zones

Table 7-3 shows the measured data (from the LAS-file) for 4 depths. In the following part the calculation is demonstrated step by step for the depth of 8804 ft (Table 7-4: Calculation for depth 8804 ft). For the other 3 depths results are given in Table 7-5. In Figure 7-4 the volumetric composition of the 4 selected reservoir zones is presented and the final result produced by Interactive Petrophysics software is summarized in Figure 7-5.

Download free eBooks at bookboon.com

Depth	GR	DT	RHOB	NPHI_SS	RT	RX0
8804	18.5	79.6	2.321	0.188	3.818	6.837
8820	26.7	84.9	2.291	0.226	1.242	6.025
8839	20.7	74.7	2.328	0.163	0.635	6.735
8859	16.7	76.9	2.325	0.189	0.272	5.327

Table 7-3: Log data from selected depths (from LAS-file).

Numerical interpretation for depth 8804 ft:	
Property	Calculation
Shale content	$V_{sh} = \frac{18.5-16}{110-16} = 0.026$ (shale content 2.6 %) This low shale content (note that linear equation delivers the maximum shale content) is not implemented in the following calculations. Particularly for resistivity interpretation the very low shale content and the high water conductivity allow application of Archie's equation.
Porosity	Porosity from Densitylog $DPHI = \frac{2.65-2.321}{2.65-1.00} = 0.199$ Porosity from Neutronlog $NPHI = 0.188$ Averaged porosity $PHI = 0.194$ or 19.4 % For comparison Acousticlog-porosity is calculated as $DTPHI = \frac{79.6-52}{190-52} = 0.20$ and confirms the value.
Formation factor	$F = \frac{1}{PHI^2} = 26.67$
Sw	$R_o = F \cdot R_w = 0.320$ Ohmm the formation would have this resistivity, if it were totally water-saturated[10] – but the measured resistivity is distinctly higher because non-conducting oil is present. $S_w = \sqrt{\frac{R_o}{R_t}} = 0.29$ water saturation 29%, oil saturation 71%
non-movable oil in the invaded zone	Saturation with respect to mud-filtrate is $S_{xo} = \sqrt{\frac{F \cdot R_{mf}}{R_{xo}}} = 0.83$ The invaded zone is 83% saturated with mud filtrate (it has displaced the original fluid). But there are still 17% non-displaced (non-moveable) oil in the pore space.

Table 7-4: Calculation for depth 8804 ft.

Summary:[10]

- The reservoir point has 19.4% porosity and a water saturation of 29%.
- The oil saturation in the non-invaded zone is 71%; 17% oil are non-movable, 54% are movable.

Download free eBooks at bookboon.com

Properties	8804 ft	8820 ft	8839 ft	8859 ft
Shale content	0.026	0.113	0.050	0.007
PHI_DEN NPHI_SS Average PHI-DT	0.199 0.188 0.194 0.200	0.218 0.226 0.222 0.238	0.195 0.163 0.179 0.164	0.197 0.189 0.193 0.180
F	26.67	20.30	31.16	26.90
Sw	0.290	0.443	0.767	1.08
Sxo	0.829	0.747	0.902	
S-oil movable non-movable	0.71 0.54 0.17	0.56 0.30 0.26	0.23 0.13 0.10	0

Table 7-5: Results for 4 depth points of the reservoir.

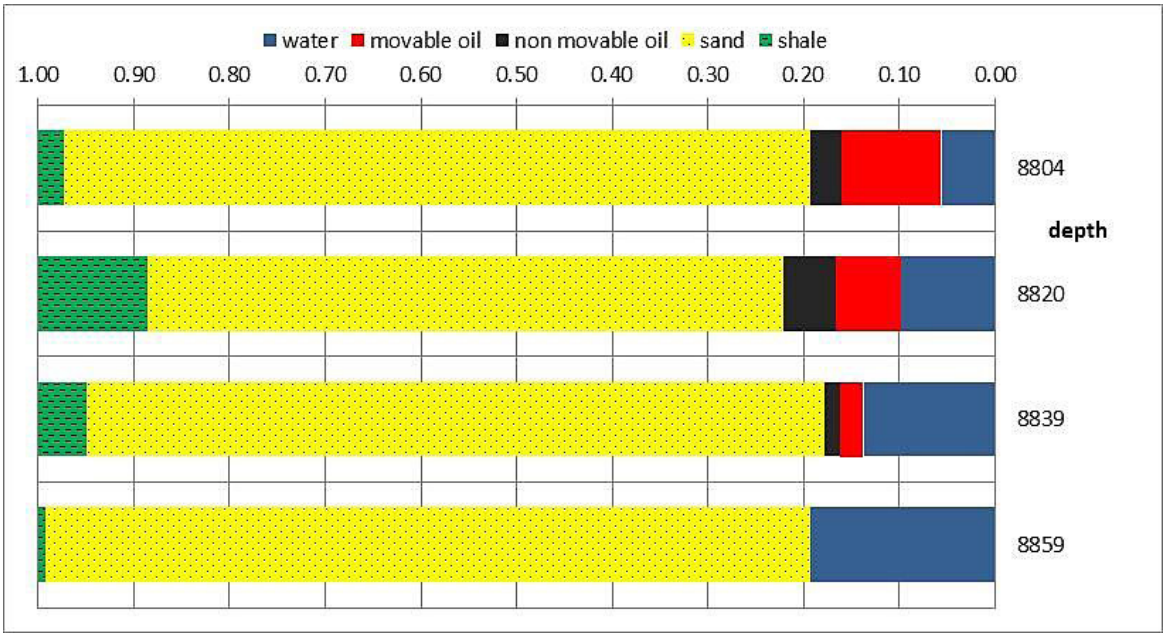

Figure 7-4: Volumetric composition of the 4 selected reservoir zones.

Download free eBooks at bookboon.com

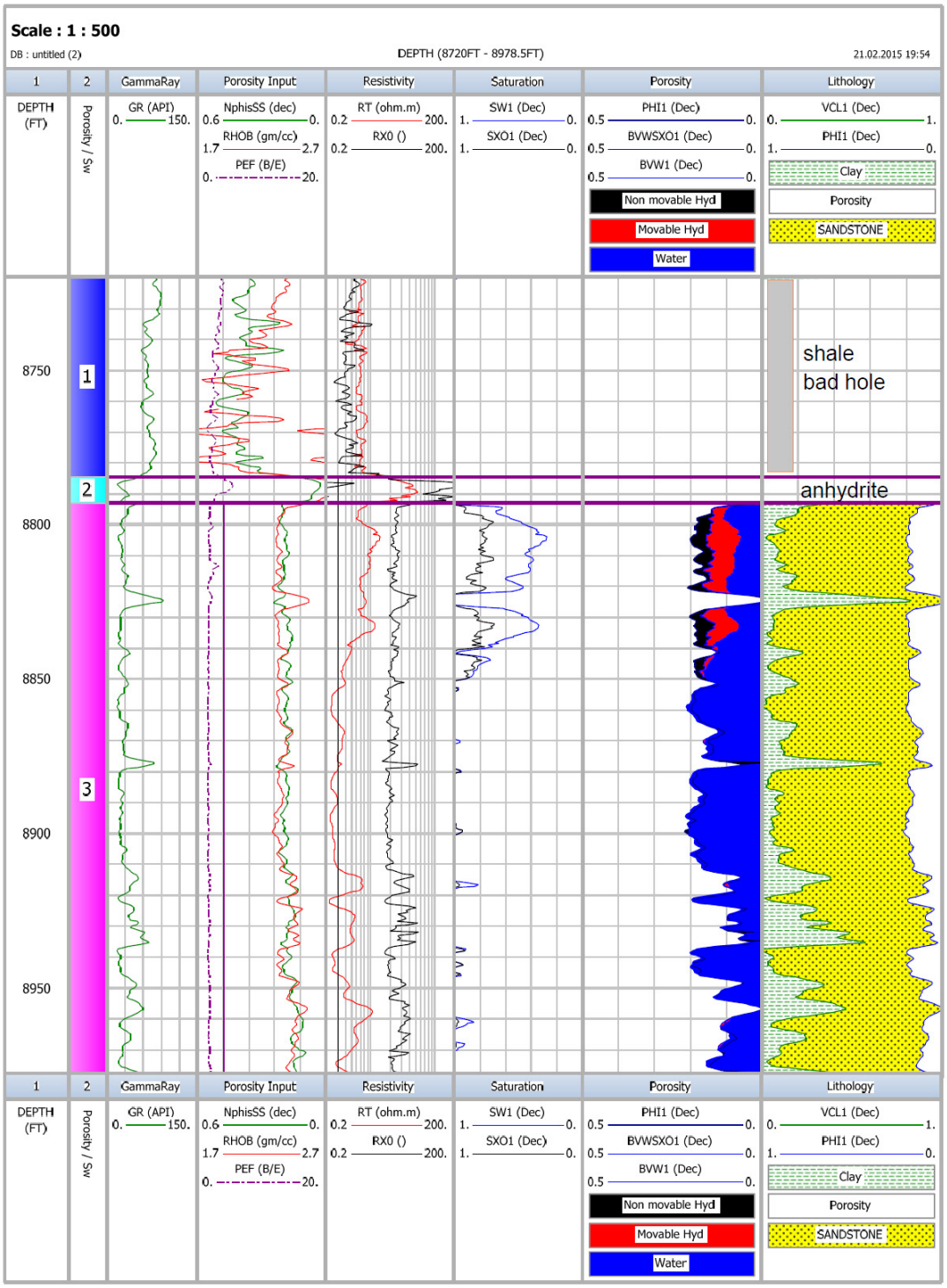

Figure 7-5: Result of interpretation (Interactive Petrophysics).

7.2 Shaly sand profile

The example is a North Sea Well. The reservoir units are sandstones of early and middle Jurassic age. Reservoir zones of the example show water and oil.

Download free eBooks at bookboon.com

Goal of the exercise:

- Evaluation of the shale type and determine the "wet shale parameters".
- Application of a shaly sand equation and comparison with formal application of Archie's equation (neglecting shalyness). Demonstration of the influence of shalyness on a precise determination of water saturation.

7.2.1 Data base

Table 7-6 shows the selected logs for the interpretation and Table 7-7 the fluid properties at formation temperature.

Log	name	unit
CALI	Caliper	inches
GR	Natural Gamma	API
RHOB	Bulk Density	g/cm^3
NPHI-SS	Neutron-Porosity (sandstone referenced)	decimal
DT	Acoustic-/Sonic log	µs/ft
Rxo, Rt	Processed resistivity from LLD, LLS, ILD, MSFL	Ohm m

Table 7-6: Selected Logs.

Discover the truth at www.deloitte.ca/careers

Deloitte.

© Deloitte & Touche LLP and affiliated entities.

Click on the ad to read more

Download free eBooks at bookboon.com

Parameter	magnitude
Rmf – at formation temperature	0.110 Ohm m
Rw – at formation temperature	0.065 Ohm m

Table 7-7: Fluid parameters.

The Archie parameters for reservoir zones are: $m = 1.95,\ n = 2.00$. Figure 7-6 shows the logplot.

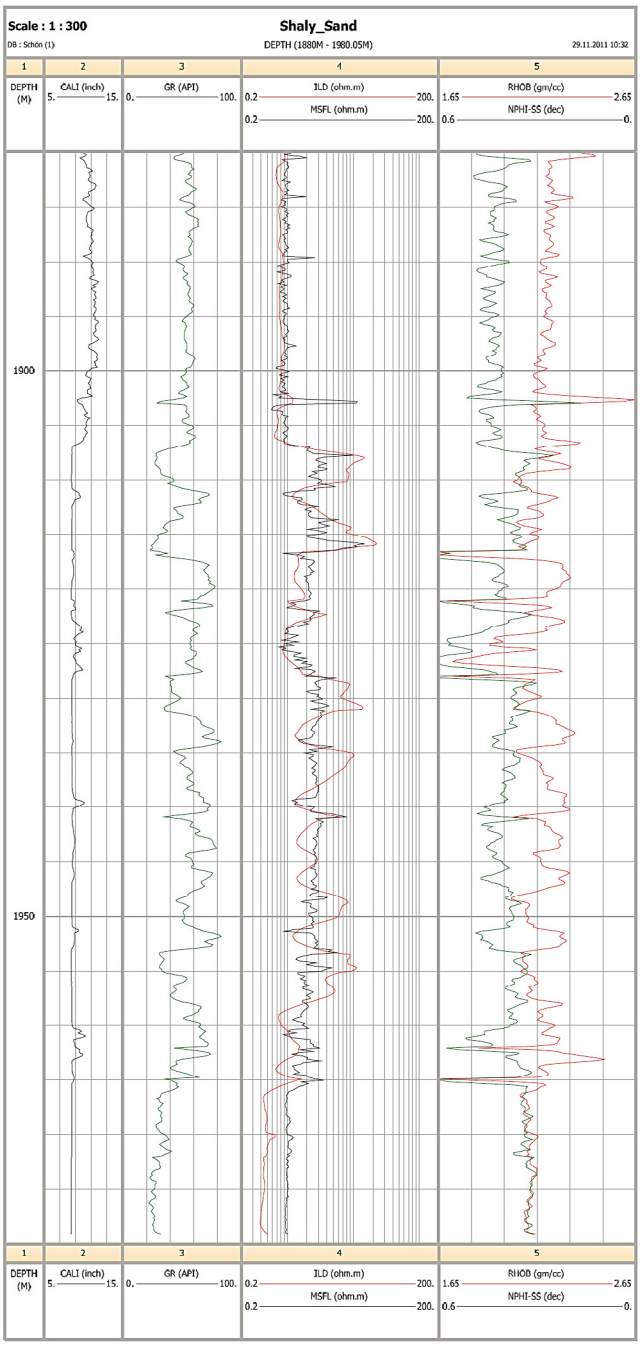

Figure 7-6: Left: Logplots for the example (plot created with Interactive Petrophysics). Note the right scale for Neutron porosity (sandstone-referenced) NPI-SS = 0 corresponds to RHOB = 2.65 g/cm³, which indicates the same porosity scale assuming a sandstone.

Download free eBooks at bookboon.com

7.2.2 Step 1 Selection of zones of Interest

A first visual interpretation of Figure 7-6 shows:

- Upper part (1860 … 1907 m): Shale with GR ≈ 60 API, caliper enlarged. The fit of the two resistivities (no invasion) and the separation/crossover of Neutron and Densitylog confirm shale.
- Middle part (1907 … 1966 m): More sandy and more shaly layers alternate. Shaly layers are indicated by high GR and separation/crossover of Neutron and Density log. The sandy layers with low GR, fit of Neutron and Density log and high *Rt* are probably oil-bearing layers. In the figure only four layers are selected. Note: High *Rt* indicates hydrocarbon (or less water) and the fit of Neutron and Density indicates oil (gas would show a crossover Neutron < Density).
- Lower part (below 1966 m): Sand (low shale content), water-bearing. The low Resistivity ILD indicates water saturation. Note also the fit of Neutronlog (sandstone referenced) and Densitylog.

7.2.3 Step 2: Determination of shale properties

Because reservoir zones are shaly, a determination of shale properties as input for shaly sand interpretation is necessary. Relevant shale parameters are:

a) Shale content,
b) Type of shale (laminar or dispersed),
c) Shale properties: Shale resistivity, wet shale neutron porosity, wet shale density.

Shale content is calculated from GR in two steps:

1. Calculation of "Gamma ray-Index" with GR, min = 20 API GR, max = 80 API.
2. Application of the Larionov equation.

A Thomas-Stieber plot (Figure 7-7) indicates laminated shaly sand.

Download free eBooks at bookboon.com

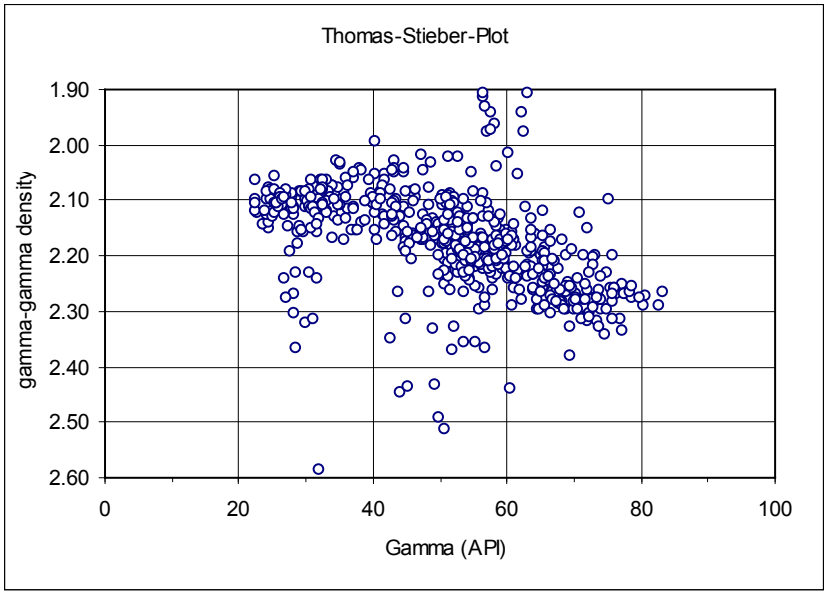

Figure 7-7: Thomas-Stieber crossplot.

Properties of the wet shale are taken from a Neutron-Density crossplot (Figure 7-8). Data points at the lower right corner of the cloud represent pure shale with the properties of the "wet shale point": $NPHI - shale$ = 0.47 and $RHO - shale$ = 2.30 g cm^{-3}.

SIMPLY CLEVER
ŠKODA
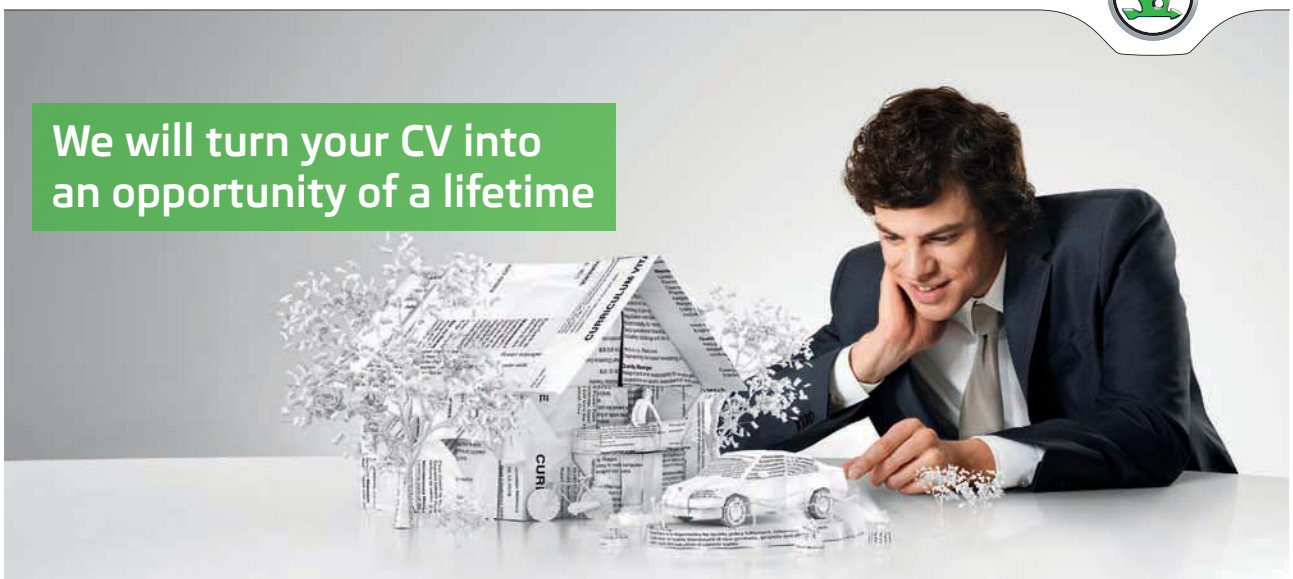
We will turn your CV into an opportunity of a lifetime
Do you like cars? Would you like to be a part of a successful brand?
We will appreciate and reward both your enthusiasm and talent.
Send us your CV. You will be surprised where it can take you.
Send us your CV on
www.employerforlife.com
Click on the ad to read more

Download free eBooks at bookboon.com

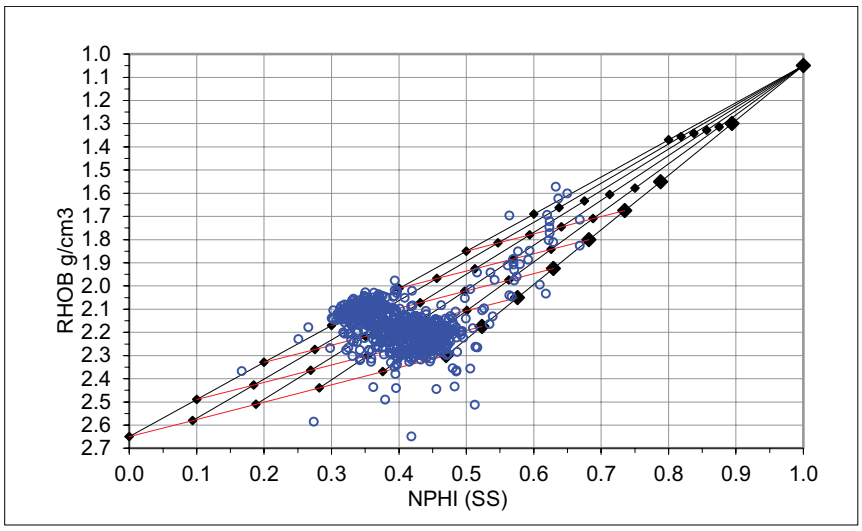

Figure 78: Crossplot RHOB versus NPHI-SS; a grid is inserted in the plot with the endpoints sand-matrix, wet shale, water and the lines for porosity and shale content.

R_{sh} = 1.8 Ohm m is used for shale resistivity (taken from a thick shale bed outside of this section; because the measured shale resistivity in the upper part is reduced by the caliper effect).

7.2.4 Step 3: Effective porosity

The Neutron-Density combination solved for effective porosity gives (see section 5.5):

$$\phi_{eff} = \frac{(\phi_N - \phi_{N,ma})\cdot(\rho_{ma} - \rho_{sh}) - (\phi_{N,sh} - \phi_{N,ma})\cdot(\rho_{ma} - \rho_b)}{(\phi_{N,fl} - \phi_{N,ma})\cdot(\rho_{ma} - \rho_{sh}) - (\phi_{N,sh} - \phi_{N,ma})\cdot(\rho_{ma} - \rho_{fl})}$$

7.2.5 Step 4: Saturation calculation

For a saturation estimate we apply the Poupon-equation for laminated shaly sand. The first step is the calculation of sand resistivity:

$$R_{sd} = \frac{1 - Vsh}{\frac{1}{R_t} - \frac{Vsh}{R_{sh}}}$$

The second step is the application of Archie's equation for determination of water saturation:

$$S_w = \left(\frac{Ro}{R_{sd}}\right)^{\frac{1}{n}} = \left(\frac{Rw \cdot F}{R_{sd}}\right)^{\frac{1}{n}} = \left(\frac{Rw \cdot \phi^{-m}}{R_{sd}}\right)^{\frac{1}{n}}$$

As example, the numerical calculation is demonstrated for one point (1914.8 m) in the second reservoir frame (Table 7-8: Calculation for depth 1914.8 m).

Download free eBooks at bookboon.com

Data set from LAS-file				
depth	GR API	Rt Ohmm	RHOB g/cm^{-3}	NPHI-SS
1914.8	35.6	7.68	2.123	0.382
Property	Calculation			
Shale content from GR	GR_{min} = 20 API GR_{max} = 83 API GR shale index $IGR = \frac{35.6-20}{83-20} = 0.247$ Larionov V_{sh} = 0.135			
Porosity	non-corrected from Neutronlog *NPHI* = 0.382 non-corrected from Density log *DPHI* = (2.65 – 2.123)/(2.65 – 1.00) = 0.319 effective porosity from Neutron-Density combination PHI_{eff} = 0.287			
Water saturation	Calculation of sand resistivity with shale resistivity R_{sh} = 1.8 Ohmm $R_{sd} = \frac{1-V_{sh}}{\frac{1}{R_t}-\frac{V_{sh}}{R_{sh}}} = \frac{1-0.135}{\frac{1}{7.68}-\frac{0.135}{1.8}} = 15.69$ $S_w = \sqrt{\frac{F \cdot R_w}{R_{sd}}} = \sqrt{\frac{(0.287^{-1.95})\cdot 0.065}{15.69}} = 0.218 \approx 0.22$ Oil saturation $S_{oil} = 1 - 0.22 = 0.78$			

Table 7-8: Calculation for depth 1914.8 m.

Note:

- The sand resistivity (15.69 Ohmm) is much higher than the measured shaly sand resistivity (7.68 Ohmm). This difference is originated by 13.5% laminated shale.
- A formalistic application of Archie's equation (neglecting the shale) would result in an overestimate of water saturation (and underestimate of oil saturation):

$$S_{w,Archie} = \sqrt{\frac{F \cdot R_w}{R_t}} = \sqrt{\frac{(0.287^{-1.95}) \cdot 0.065}{7.68}} = 0.31$$

Figure 7-9 shows the whole interpreted section.

Download free eBooks at bookboon.com

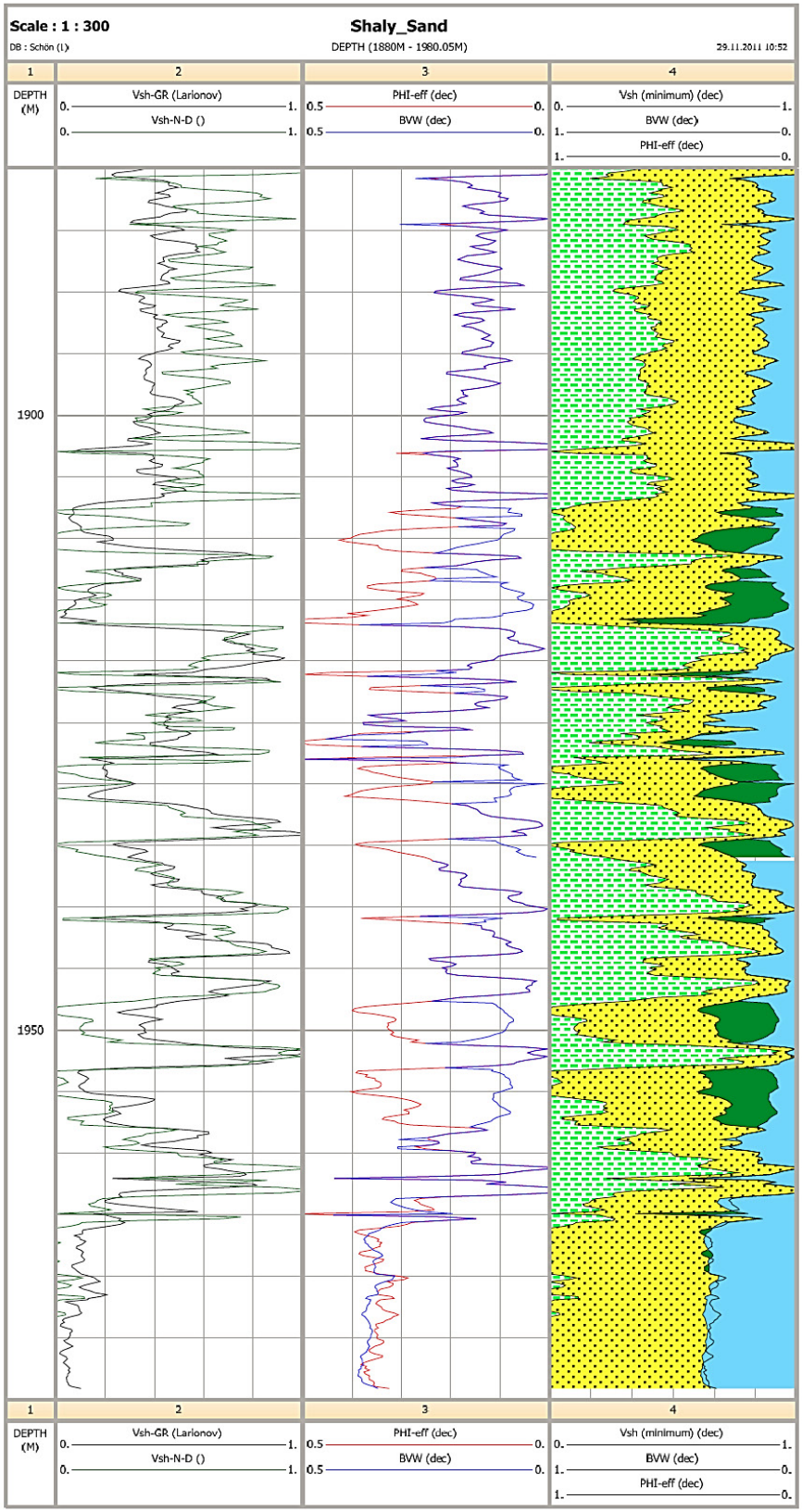

Figure 7-9: Result of interpretation plotted with Interactive Petrophysics. The third trace shows the volumetric composition of shale (light green), sand (yellow), water (blue) and oil (dark green). In shaly zones with Vsh > 0.3, water saturation is set Sw = 1.

Download free eBooks at bookboon.com

7.3 Mixed lithology Carbonate rock

This example demonstrates the determination of porosity and rock composition (minerals) from a combination of Density log and Neutronlog for a carbonate reservoir.
Example uses data from the textbook "Basic Well Log Analysis" (Asquith and Krygovski, 2004); see also: http://www.elsevierdirect.com/companion.jsp?ISBN=9780444537966

Data base

The section 9200 to 9252 ft consists of mixed-lithology carbonate rocks. Cored sections (9302 … 9358 ft) show dolomite, microcrystalline limestone and anhydrite. Table 7-9 lists the used logs and Table 7-10 gives the fluid properties.

Log	name	unit
CALI	Caliper	inches
GR	Natural gamma	API
RHOB	Bulk density	g/cm^3
NPHI	Neutron-porosity	decimal
Rt, Rxo	Calculated resistivity from Laterolog-deep, Laterolog-shallow, Microspherical Focused Log	Ohm m

Table 7-9: Logs.

Parameter	magnitude
Rmf – measured at 74 °F (23°C) Rmf – at formation temp. 207 °F (97°C)	0.046 Ohm m 0.017 Ohm m
Rw – at formation temp. 207 °F (97°C)	0.023 Ohm m

Table 7-10: Rmf and Rw data.

Both fluid resistivities are very low at formation temperature and in the same order of magnitude. The well was drilled with high saline mud (because of salt in the profile).

7.3.1 Log plot and Quick-look Interpretation

Figure 7-10 shows selected logs for the following discussion and numerical interpretation.

Quick look interpretation:

- Caliperlog shows a correct caliper, no breakouts or other critical parts.
- Gammalog with low magnitude (15 API in the upper part and 30 API in the lower part) characterizes the section as nearly clean carbonate.

Download free eBooks at bookboon.com

- The porosity logs Neutron porosity *NPHI* (limestone-calibrated) and Density *RHOB* (also limestone referenced) show no fit in the whole section. The following conclusions result:
  - The section is not a pure limestone,
  - The upper part (down to 9202 ft) is anhydrite (*RHOB* = 2.95 g cm^{-3}, *NPHI* ≈ 0),
  - Below 9202 ft a variation of porosity can be expected: Porous zones are presebt at, for example, 9204 … 9208 ft, dense zones, for example, at 9210 … 9214 ft. The porosity variation is also indicated by the resistivity curve (especially in RMFSL ≈ Rxo).
  - The two resistivity curves show (below 9236 ft) the same shape and nearly the same level in the lower section. This section is probably water-saturated (remember Rw and Rmf are of the same magnitude). Above 9236 ft the two curves separate with $Rt > Rxo$ and indicate the presence of hydrocarbon. The behaviour of Neutronlog and Densitylog characterize the hydrocarbon as oil.

Click on the ad to read more

Download free eBooks at bookboon.com

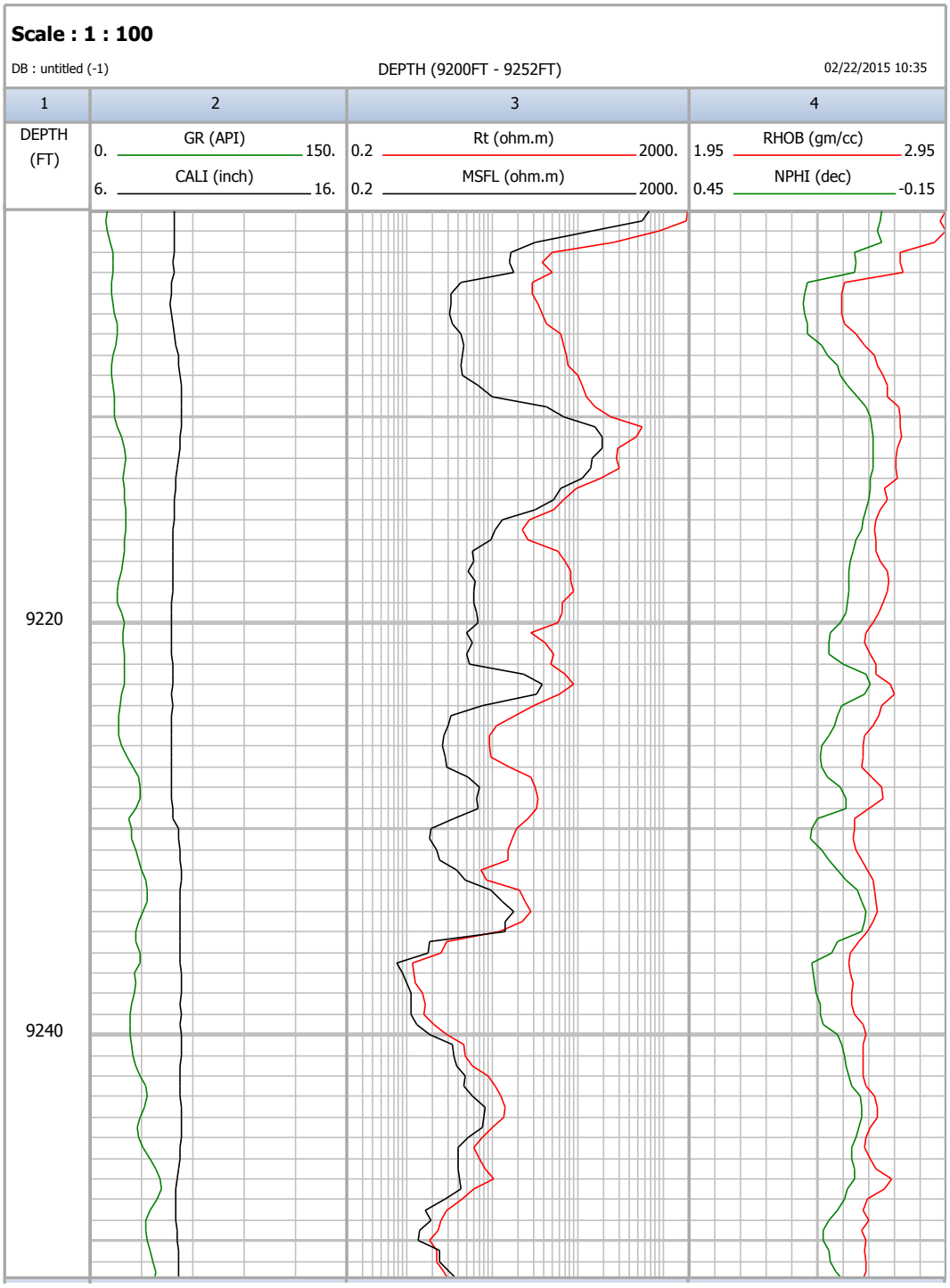

Figure 7-10: Log plots carbonate profile.

7.3.2 Quantitative interpretation – Application of crossplot

Figure 7-11 shows the Density-Neutron crossplot with three selected points (data values from LAS-file) for demonstration (results see Table 7-11).

Download free eBooks at bookboon.com

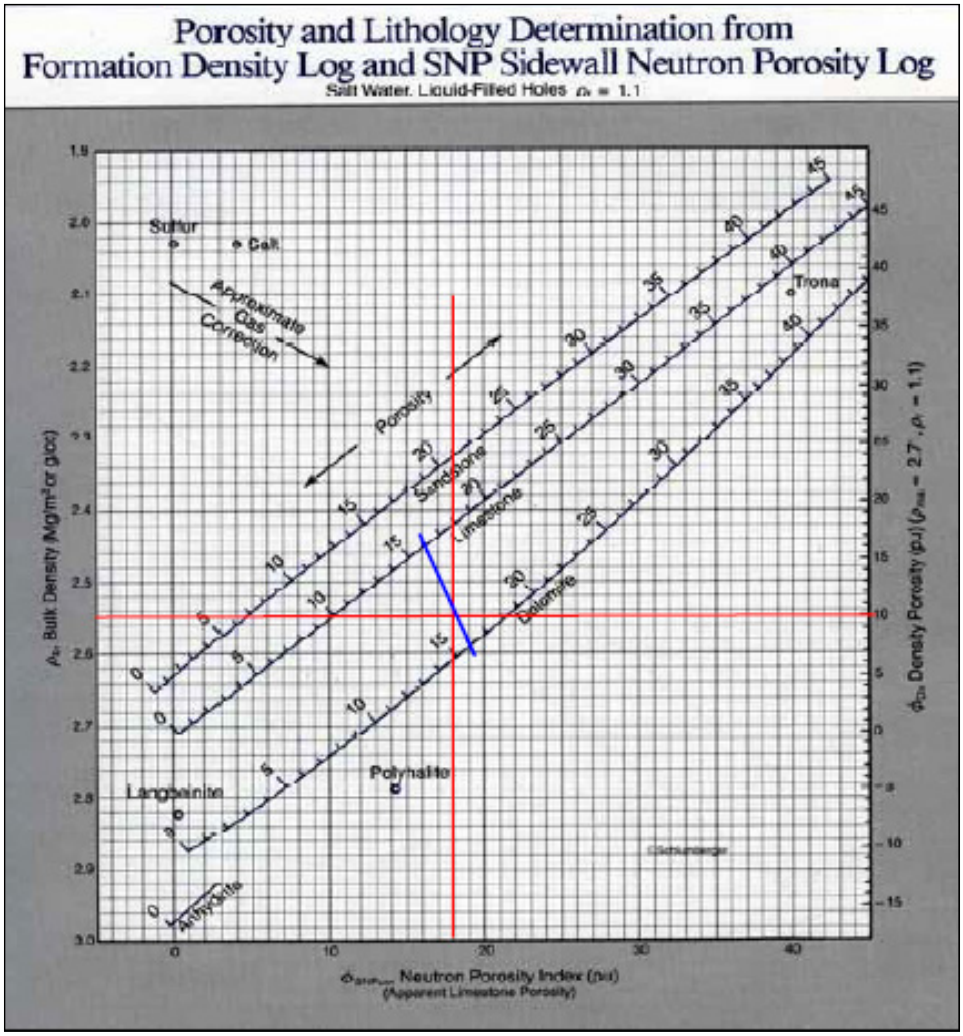

Figure 7-11: Density-Neutron crossplot; circles indicate the position of three data points (see text), Schlumberger Chart Book.

Depth	Log data	Interpretation; Position of cross (circle) represents the solution
9205 ft	*NPHI* = 0.179 *RHOB* = 2.545 gcm^{-3}	Red circle gives as solution: porosity = 0.16 mineral composition: about 70% dolomite, 30% limestone.
9217 ft	*NPHI* = 0.072 *RHOB* = 2.692 gcm^{-3}	Blue circle gives as solution: porosity = 0.06 mineral composition: about 50% dolomite, 50% limestone.
9230 ft	*NPHI* = 0.179 *RHOB* = 2.545 gcm^{-3}	Black circle gives as solution: porosity = 0.14 mineral composition: about 80% dolomite, 20% limestone.

Table 7-11: Rock mineralogy and porosity for the three selected points after crossplot interpretation (Figure 7-11).

Figure 7-12 presents all data points. It confirms the mixed mineralogy (calcite and dolomite). Also note the position of the anhydrite layer in the left lower corner.

Download free eBooks at bookboon.com

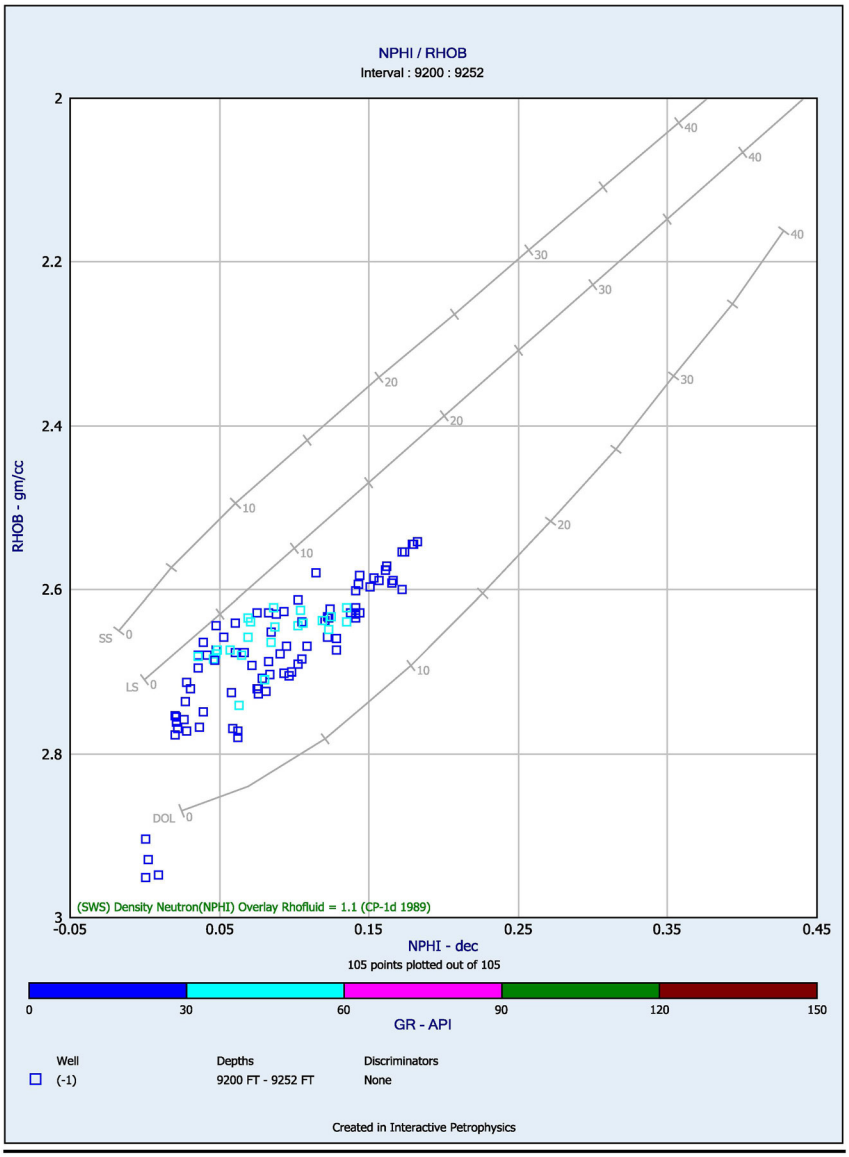

Figure 7-12: Density-Neutron crossplot with all measured data.

7.3.3 Quantitative interpretation – Combined interpretation (porosity and mineral composition)

For a detailed numerical analysis of mineral composition and porosity, the technique described in 5.3.3 is applied.

The response equations for the Density- and Neutronlog are:

$$\rho_b = RHOB = 2.71 \cdot V_{calcite} + 2.87 \cdot V_{dolomite} + 1.10 \cdot \phi$$
$$\phi_N = NPHI = 0 \cdot V_{calcite} + 0.02 \cdot V_{dolomite} + 1.00 \cdot \phi$$
$$1 = V_{calcite} + V_{dolomite} + \phi$$

Download free eBooks at bookboon.com

In matrix notation:

$$\begin{bmatrix} RHOB \\ NPHI \\ 1 \end{bmatrix} = \begin{bmatrix} 2.71 & 2.87 & 1.10 \\ 0 & 0.02 & 1.00 \\ 1.00 & 1.00 & 1.00 \end{bmatrix} \cdot \begin{bmatrix} V_{calcite} \\ V_{dolomite} \\ \phi \end{bmatrix}$$

Matrix inversion (excel tool) results in:

$$\begin{bmatrix} V_{calcite} \\ V_{dolomite} \\ \phi \end{bmatrix} = \begin{bmatrix} -5.099 & -9.209 & 14.818 \\ 5.203 & 8.377 & -14.100 \\ -0.104 & 0.833 & 0.282 \end{bmatrix} \cdot \begin{bmatrix} RHOB \\ NPHI \\ 1 \end{bmatrix}$$

Therefore, the final equations for the volumetric components are:

$$V_{calcite} = -5.099 \cdot RHOB - 9.209 \cdot NPHI + 14.818$$
$$V_{dolomite} = 5.203 \cdot RHOB + 8.377 \cdot NPHI - 14.100$$
$$\phi = -0.104 \cdot RHOB + 0.833 \cdot NPHI + 0.282$$

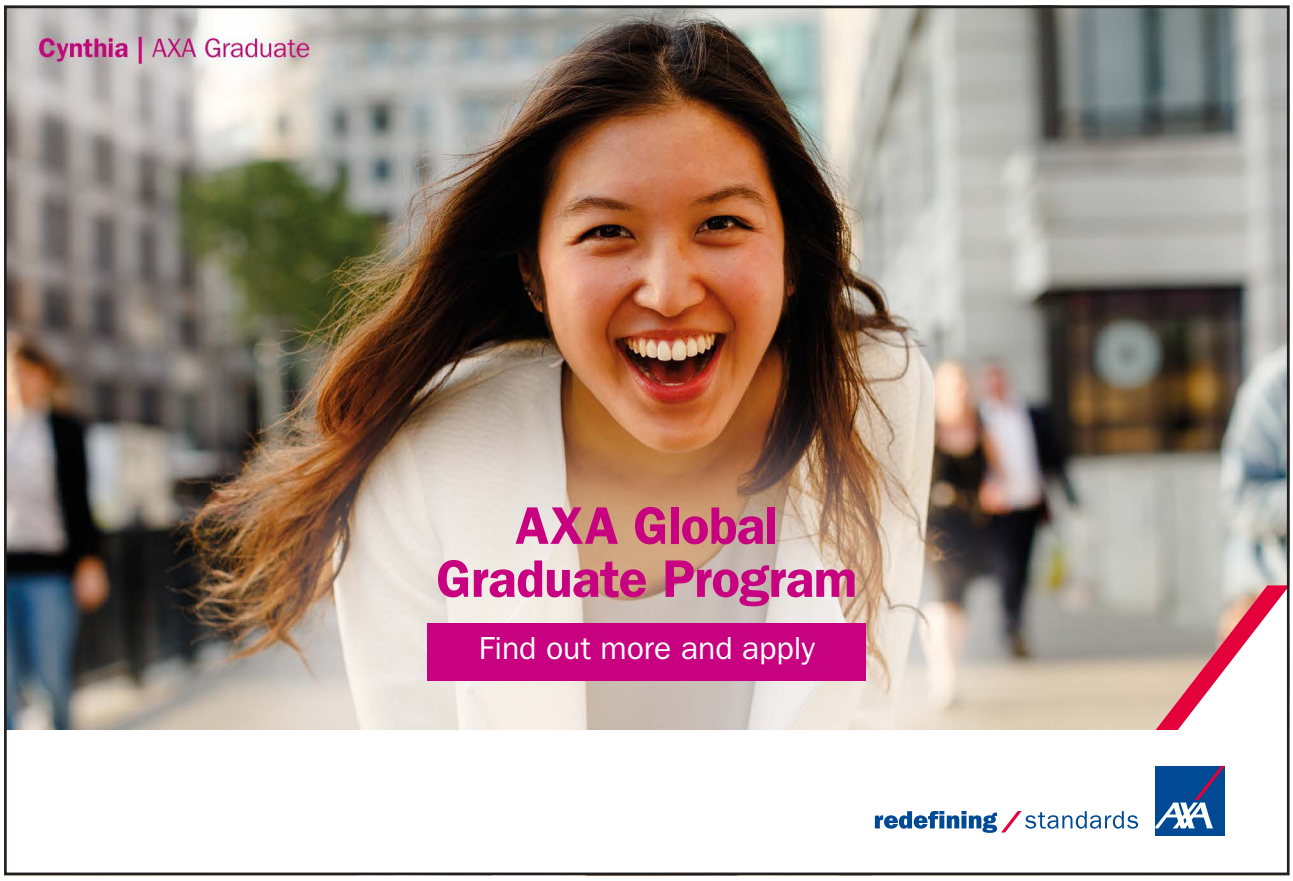

Click on the ad to read more

Download free eBooks at bookboon.com

Application to the three selected points gives the following numerical result (Table 7-12). Note that the mineral fraction is referenced to total rock volume in Table 7-12 whereas in the crossplot technique (Table 7-11) to total solid volume.

Depth	Measured data		Result		
	NPHI	RHOB	Porosity	Calcite	Dolomite
9205	0.179	2.545	0.166	0.193	0.641
9217	0.072	2.692	0.062	0.509	0.429
9230	0.165	2.592	0.150	0.082	0.078

Table 7-12: Rock mineralogy and porosity for the three selected points (matrix inversion).

With the same principle the volumetric composition is calculated for the whole section (Figure 7-13) by the computer program. Sections with higher dolomite content show a tendency towards higher porosity PHI, probably as result of a dolomitization process. Higher limestone content tends to lower porosity PHI.

7.3.4 Saturation calculation

For the water saturation calculation Archie's equation can be applied because of extremely low or no shale content and high water salinity or low R_w.
With Archie parameters $m = n = 2$ and R_w = 0.023 Ohmm the water saturation results as:

$$S_w = \sqrt{\frac{R_o}{R_t}} = \sqrt{\frac{R_w \cdot \mathrm{F}}{R_t}} = \sqrt{\frac{R_w \cdot \phi^{-2}}{R_t}} = \sqrt{\frac{0.023 \cdot \phi^{-2}}{R_t}}$$

Bulk Volume Water ($BVW = PHI \cdot S_w$)and Bulk Volume Oil ($= PHI \cdot (1 - S_w)$) are plotted in Figure 7-13. The Oil-Water contact at 9235 ft is exactly at the depth where the R_t and R_{xo} separate.

Download free eBooks at bookboon.com

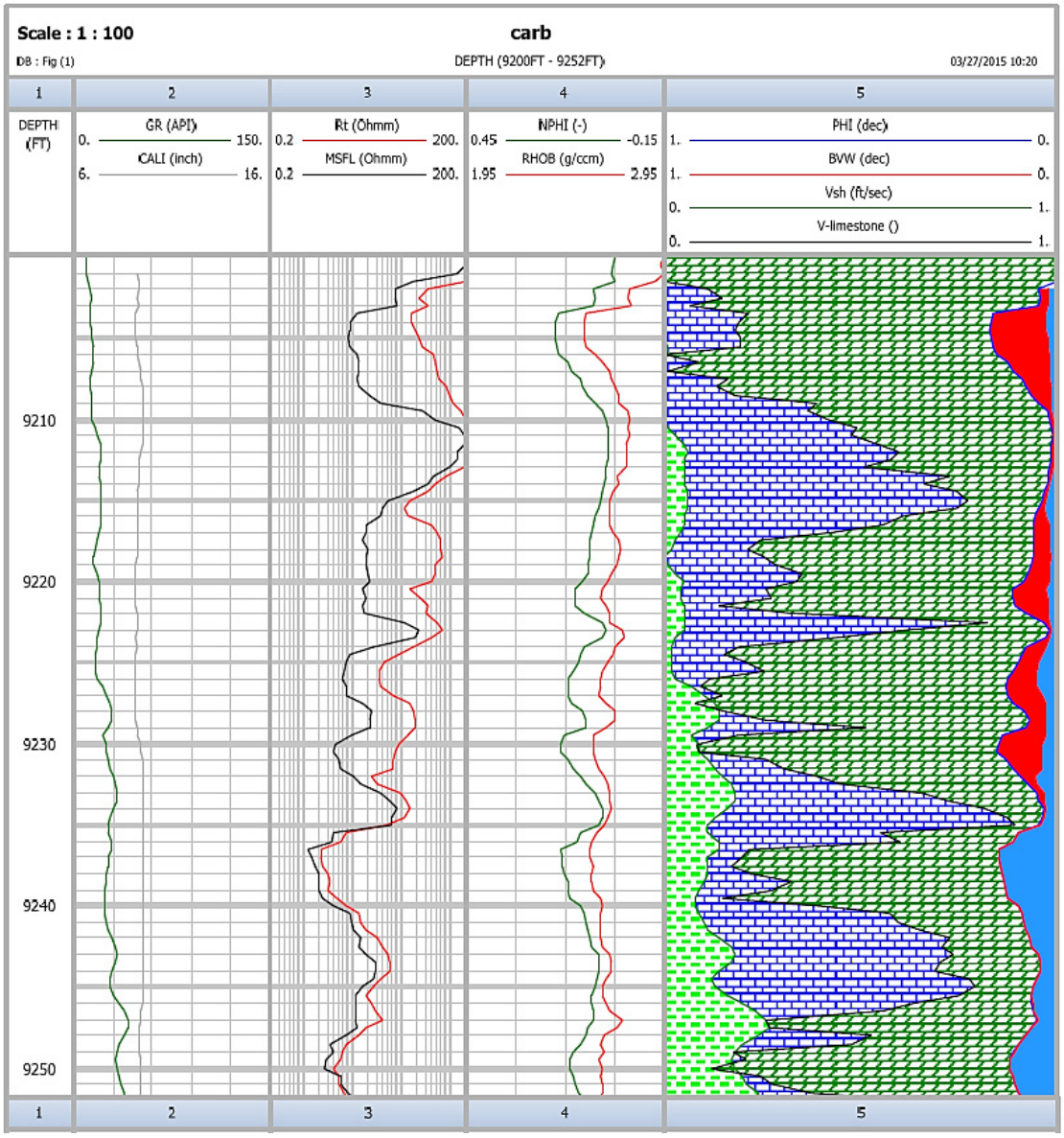

Figure 7-13: Carbonate profile with result of interpretation.

Track 1: Gammalog and Caliper, Track 2: Resistivity logs, Track 3: Porosity logs.

Track 4: Volume fractions of dolomite, calcite/limestone and porosity; water and oil volume.

Download free eBooks at bookboon.com

8 Appendix

8.1 Physical properties of rock-forming minerals

The following table is compiled from Logging Parameters summarized in Logging Chart books from Baker Atlas and Schlumberger.

ρ_b bulk density in g cm^{-3}

$\rho_{\log}$ log density (gamma-gamma-density) in g cm^{-3}

Z / A ratio atomic number/atomic mass number

PE photoelectric cross section in barns/electron

$\Delta t_b, \Delta t_s$ slowness for compressional and shear wave in μs m^{-1}

Σ macroscopic cross section in capture units

ϕ_N neutron porosity in porosity units (%). In the first line, the first raw datum gives the value for epithermal measurement; the second raw, the value for thermal measurement (Baker Atlas). In the second line, the first raw datum gives the value for SNP (Sidewall) measurement; the second raw, the value for CNL (Compensated Neutron) measurement (Schlumberger).

ε relative dielectric permittivity (Schlumberger, 2000)

Click on the ad to read more

Download free eBooks at bookboon.com

Minerals	References: First line Baker Atlas – Log Interpretation Charts, 1985 Second line Schlumberger – Log Interpretation Charts, 2000									
	ρ_b	ρ_{log}	Z/A	PE	Δt_b	Δt_s	Σ	ϕ_N	ϕ_N	ε
Silicates										
Quartz SiO_2	2.65	2.64 2.64	0.499	1.81	51	74	4.26 4.3	-1.1 -1	-2.1 -2	4.65
Feldspars – Alkali										
Orthoclase $KAlSi_3O_8$	2.56	2.53 2.52	0.496	2.86 2.9	69		15 16	-1.5 -2	-1.1 -3	4.4 … 6.0
Anorthoclase (Na,K) $AlSi_3O_8$	2.59	2.56 2.59	0.496	2.86 2.9			9.4 16	-2	-2	4.4 … 6.0
Microcline $KAlSi_3O_8$	2.59	2.57 2.53	0.496	2.86 2.9			13.1 16	-2	-3	
Feldspars – Plagioclase										
Albite $NaAlSi_3O_8$	2.62	2.59 2.59	0.496	1.68 1.7	47 49	98 85	7.49 7.5	-1.0 -1	-1.3 -2	4.4 … 6.0
Anorthite $CaAl_2Si_2O$	2.76	2.74 2.74	0.496	3.13 3.1	45 45		7.28 7.2	-1.3 -1	-1.6 -2	4.4 … 6.0
Micas										
Biotite $K(Mg,Fe)_3$ $(AlSi_3O_{10})(OH)_2$	3.01	2.99 2.99	0.493	6.27 6.3	51 50.8	224 224	30.0 30	15.8 11	22.5 21	4.8 … 6.0
Muscovite $KAl_2(Si_3AlO_{10})(OH)_2$	2.83	2.82 2.82	0.497	2.40 2.4	47 49	79 149	16.9 17	13.4 12	16.5 20	6.2 … 7.9
Glauconite (K,Na) $(Al,Fe,Mg)_2$ $(Al,Si)_4O_{10}(OH)_2$	2.58	2.54 2.86	0.494	6.37 4.8			23.4 21			
Clay minerals										
Kaolinite $Al_2O_3 \cdot 2SiO_2 \cdot 2H_2O$	2.59	2.62 2.41	0.504	1.49 1.8	212	328	12.8 14	47.8 34	45.1 37	5.8
Chlorite $Mg_5(Al,Fe)$ $(OH)_8(Al,Si)_4O_{10}$	2.88	2.88 2.76	0.497	6.30 6.3			25.3 25	37	52	5.8
Illite $K_{1-1.5}\ Al_4(Si,Al)_8$ $O_{20}(OH)_4(O,OH)_{10}$	2.64	2.63 2.52	0.499	3.45 3.5			15.5 18	12.7 20	15.8 30	
Montmorrillonite $(Na,Ca)_{0.33}(Al,Mg)_2$ $Si_4O_{10}(OH)_2 \cdot nH_2O$	2.06	2.02 2.12	0.502	2.04 2.0			14.5 14	12.6 60	11.5 60	
Carbonate										
Calcite $CaCO_3$	2.71	2.71 2.71	0.508	5.08 5.1	46 49.0	89 88.4	7.08 7.1	0.0 0.0	0.0 0.0	7.5
Aragonite $CaCO_3$	2.93	2.95	0.508	5.08	53	84	7.65	0.7	1.0	
Dolomite $CaMg(CO_3)_2$	2.87	2.87 2.85	0.499	3.14 3.1	42 44	77 72	4.7 4.7	1.7 1	0.5 1	6.8

Download free eBooks at bookboon.com

Siderite $FeCO_3$	3.94	3.89 3.89	0.483	14.69 15	44 47	85	52.3 52	6.3 5	12.9 12	6.8 … 7.5
Ankerite $Ca(Fe,Mg)(CO_3)_2$	2.97	2.96 2.86	0.496	9.32 9.3			14.9 22	2.1 0	5.7 1	
Magnesite $MgCO_3$	2.87	2.87	0.499		44	75				
Evaporites, salt										
Halite NaCl	2.16	2.03 2.04	0.479	4.65 4.7	67 67	116 120	748 754	-2.2 -2	-1.8 -3	5.6 … 6.3
Sylvite KCl	1.99	1.87 1.86	0.483	8.51 8.5	74	140	546 565	-2.7 -2	-4.1 -3	4.6 … 4.8
Carnallite $KMgCl_3{\cdot}6H_2O$	1.60	1.56 1.57	0.511	4.09 4.1	81		365 369	49.1 41	58.4 60+	
Sulfides, Sulfates										
Pyrite FeS_2	5.01	5.00 4.99	0.483	16.97 17	38 39.2	59 62.1	89.8 90	-2.2 -2	-1.9 -3	
Anhydrite $CaSO_4$	2.96	2.98 2.98	0.499	5.06 5.1	54 50	98	12.3	-1.2 -1	-0.7 -2	6.3
Gypsum $CaSO_4{\cdot}2H_2O$	2.31	2.33 2.35	0.511	3.99 4.0	53 52		18.8	58.5 50+	57.6 60+	4.1
Barite $BaSO_4$	4.48	4.09 4.09	0.466	266.8 267	69	133	21.0	-1.0 -1	0.2 -2	6.8
Polyhalite K_2Mg $Ca_2(SO_4)_4{\cdot}2H_2O$	2.78	2.79 2.79	0.501	4.32 4.3	58		23.6 24	16.5 14	21.6 25	
Coals										
Anthracite $C_{720}H_{258}N_6O_{16}$	1.60	1.57 1.47	0.513	0.16 0.16	105 105		10.49 8.7	46.1 37	41.4 38	
Bituminous $C_{532}H_{418}N_8O_{41}$	1.35	1.33 1.24	0.527	0.17 0.17	120 120		16.36 14	>60 50+	>60 60+	
Lignite $C_{480}H_{412}N_7O_{101}$	1.10	1.05 1.19	0.525	0.20 0.20	160 160		12.79 13	55.6 47	54.2 52	
Graphite C	2.27	2.24	0.500		100	164	0.41			

8.2 Some conversions

Length:

1 m = 3.281 ft = 39.37 inch 1 ft = 0.3048 m = 12.00 inch

1 inch = 0.0833 ft = 0.0254 m

Velocity:

1000 m/s = 3280.8 ft/s 1000 ft/s = 304.8 m/s

Download free eBooks at bookboon.com

Slowness:

100 μs/m = 30.48 μs/ft 100 μs/ft = 328.08 μs/m

Density:

1000 kg/m^3 = 1.000 g/cm^3 = 0.0361 lb/in^3 0.100 lb/in^3 = 2767.8 kg/m^3 = 2.768 g/cm^3

Pressure:

1000 Pa = 0.010 bar = 0.00987 atm = 0.145 psi
0.010 atm = 1013 Pa = 0.10 bar = 0.147 psi
1.00 bar = 10,000 Pa = 0.98693 atm = 14,504 psi
1.00 psi = 6895 Pa = 0.06895 bar = 0.06805 atm

Temperature:

Temperature in K = (Temperature in °C) + 273.16
Temperature in °C = 5/9 * (Temperature in °F – 32)
Temperature in °F = 32 + 1.8* (Temperature in °C)

Click on the ad to read more

Download free eBooks at bookboon.com

9 Recommended books and sources

The Schlumberger Oilfield Glossary http://glossary.oilfield.slb.com gives you in many situations a concentrated explanation of subjects an terms in the oil industry.

For a detailed study textbooks and manuals are recommended, for example:

Asquith, G., Krygowski, D., 2004, Basic Well Log Analysis (second edition), AAPG Methods in Exploration Series, No. 16, Tulsa.

Ellis, D.V. and J.M. Singer, 2007, Well logging for earth scientists, Springer, Dordrecht.

Hearst, J.R. and Nelson, P.H., 1985, Well logging for physical properties, McGraw-Hill.- New York

Fricke, S., Schön, J., 1999, Praktische Bohrlochgeophysik, Ferd. Enke Verlag Stuttgart.

Hyne, N.J., 2001, Nontechnical Guide to Petroleum Geology, Exploration, Drilling, and Production, PennWell Corp., Tulsa.

Lucia, F.J. 2007, Carbonate reservoir characterization (2nd edition). Berlin, Heidelberg, Springer.

Schön, J.H., 1996, Physical properties of rocks, Fundamentals and Principles of Petrophysics (Handbook of Geophysical Exploration Series, 583 p.) – Pergamon Press, last reprint 2004.

Schön, J.H., 2011, Physical Properties of Rocks – a Workbook (Elsevier Publ.) http://www.elsevierdirect.com/companion.jsp?ISBN=9780444537966

Serra, O., 1984, Fundamentals of Well-log Interpretation. – Elsevier Amsterdam Oxford New York Tokyo 1984.

Darling, T., 2005, Well logging and Formation Evaluation, Gulf Profess. Publish./Elsevier Inc.

Theys, P., 1991, Log data acquisition and quality control. – Editions Technip, Paris.

Tiab, D., Donaldson, E.C., 2014, Petrophysics; Gulf Publishing Company, Houston

Download free eBooks at bookboon.com

10 References

The text uses figures, tables and text from various material from Schlumberger and Baker Atlas. A part of the figures was taken from our course material "Introduction to Petrophysics and Formation Evaluation" (Baker Atlas); I thank my colleagues particularly Dan Georgi and Allen Gilchrist (formerly with Baker Atlas).

Akbar, M., B. Vissapraganda, A.I. Alghamdi. 2000/2001. A snapshot of carbonate reservoir evaluation, Schlumberger Oilfield Review, Winter, 20–41.

Akbar, M., M. Petricola, M. Watfa, M. Badri, A. Boyd, M. Charara, B. Cassell, N. Roy, J.P. Delhomme, M. Graze, B. Kenyon, J. Rostenburg, 1995, Classic interpretation problems: evaluating carbonates, Schlumberger Oilfield Review, Jan., 38–57.

Akkurt R., H.J. Vinegar, P.N. Tutunjian, and A.J. Guillory. 1996. NMR logging in natural gas reservoirs, The Log Analyst, November-December: 33–42.

Andersen, M.A., 2011, Core Truth in Formation Evaluation, Schlumberger Oilfield Review, Spring 2011: 23, no. 1, 60–62.

Click on the ad to read more

Download free eBooks at bookboon.com

Andersen, M.A., Duncan, B., McLin, R., 2013, Core Truth in Formation Evaluation, Schlumberger Oilfield Review Summer 2013, 25, no. 2, 16–25.

API American Petroleum Institute API, 1998, Recommended Practices for Core Analysis, 2-nd Edition.

Appel, M. 2004. Tutorial nuclear magnetic resonance and formation porosity, Petrophysics, 45(3): 296–307.

Archie, G.E., 1942: The electrical resistivity log as an aid in determining some reservoir characteristics.- Trans. AIME, 146, S. 54 –62 (also in: Trans. SPE, 1941, 146).

Arps, J.J., 1953: The effect of temperature on the density and electrical resistivity of sodium chloride solutions.- Journ. Petrol. Technol. Techn. Note 175, 17–20.

Asquith, G., Krygowski, D., 2004, Basic Well Log Analysis (second edition), AAPG Methods in Exploration Series, No. 16, Tulsa.

Baker Atlas, unpublished course material, 2014.

Baker Atlas. 1992, 2000, 2002: Introduction to wireline log analysis. Houston TX.

Baker Atlas/Baker Hughes. 1985, 2003. Log interpretation charts. Baker Hughes Inc., Houston TX.

Bardon, C. and B. Pied, 1969, Formation water saturation in shaly sands, in SPWLA 10th Annual Logging Symposium Transactions, Houston, Texas, 25–28 May, paper Z.

Bigelow, E. (ed.), 2002, Introduction to Wireline Log Analysis, Baker Atlas

Chen, S., Ostroff, G., Georgi, D.T., 2000, Improving Estimation of NMR Log T2cutoff Value with Core NMR and Capillary Pressure Measurements, SCA-9822

Clavier, C., Coates, G., Dumanoir, J., 1984, The theoretical and experimental bases for the dual-water model for interpretation of shaly-sands, Soc. Pet. Engrs. J., 24, 153–167.

Clavier, C., G. Coates and J. Dumanoir. 1984. The theoretical and experimental bases for the "dual water" model for the interpretation of shaly sands, Soc. Pet. Engrs. J., 24(2):153–168.

Coates, G., Dumanoir, J.L., 1974, A new approach to improved log derived permeability; Log Analyst, 15, 1.

Download free eBooks at bookboon.com

Coates, G.R, Xiao, L., Prammer, M., 1999, NMR Principles and Applications, Halliburton Energy Services Publ. H02308.

Darling, T., 2005, Well logging and Formation Evaluation, Gulf Profess. Publish./Elsevier Inc.

Desbrandes, R., 1985, Encyclopedia of Well Logging.- Editions Technip, Paris.

Ellis, D.V. and J.M. Singer. 2007, Well logging for earth scientists, Springer, Dordrecht.

Fertl, W., 1979, Gamma ray spectral data assists in complex formation evaluation, The Log Analyst, September–October 1979, 3–37.

Freedman, R. and N. Heaton, 2004, Fluid characterization using nuclear magnetic resonance logging, Petrophysics, 45(3): 241–250.

Fricke, S., Schön, J, 1999, Praktische Bohrlochgeophysik, Ferd. Enke Verlag Stuttgart.

Gilchrist, W.A., E. Prati, R. Pemper, M.W. Mickael, and D. Trcka, D., 1999, Introduction of a New Through-Tubing Multifunction Pulsed Neutron Instrument, Paper SPE 56803, Trans., SPE 74th Annual Technical Conference and Exhibition, Houston, 1999.

Click on the ad to read more

Download free eBooks at bookboon.com

Gilchrist, W.A., R.R. Pemper, D. Trcka, E. Frost, and W. Wilson, 2000, Initial Field Applications of a New 1.7-Inch Pulsed Neutron Instrument, Paper FF, Trans., SPWLA 41st Annual Logging ymposium, Dallas, 2000.

Han, X., R. Pemper, T. Tutt, T., F. Li., 2009, Environmental Corrections and System Calibration for a new Pulsed-Neutron Mineralogy Instrument, SPWLA 50th Annual Logging Symposium, paper S.

Hearst, J.R. and Nelson, P.H., 1985, Well logging for physical properties, McGraw-Hill.- New York.

Hertzog, R., L. Colson, B. Seeman, M. O'Brien, H. Scott, D. McKeon, P. Wraight, J. Grau, D. Ellis, J. Schweitzer, J., and M. Herron. 1987, Geochemical Logging with Spectrometry Tools, Paper SPE 16792, Trans., SPE 62nd Annual Technical Conference and Exhibition, Dallas, 1987.

Hyne, N.J., 2001, Nontechnical Guide to Petroleum Geology, Exploration, Drilling, and Production, PennWell Corp., Tulsa

Kleinberg, R.L. and H.J. Vinegar, 1996, NMR properties of reservoir fluids, The Log Analyst, November-December: 20–32.

Kleinberg, R.L., W.E. Kenyon, P.P. Mitra, 1994, Mechanism of NMR relaxation of fluids in rocks, Journal of Magnetic Resonance, Series A, 108: 206–214.

Larionov, W.W., 1969, Borehole radiometry, Izdatelstvo Nedra, Moscow.

Lehnert, K., Rothe, K., 1962, Geophysikalische Bohrlochmessungen, Akademie Verlag, Berlin

Lucia, F.J. 2007. Carbonate reservoir characterization (2nd edition). Berlin, Heidelberg: Springer.

Lucia, F.J., 1983, Petrophysical parameters estimated from visual descriptions of carbonate rocks: a field classification of carbonate pore space, SPE: 88–96, paper presented at the 1981 SPE Ann. Conf. and Exhib. San Antonio (SPE 10073); and Journ. Petr. Technol, March 1983, 626–637.

Mohhammadlou, M., M.B.E. Mork and H. Langeland., 2010, Quantification of shale volume from borehole logs calibrated by SEM analysis: a case study, First Break, 28, 2010, 47–55.

Mollison, R.A., Schön, J., Fanini, O., Gupta, P., Kriegshäuser, B., Meyer, W.H., 1999, A model for hydrocarbon saturation determination from an orthogonal tensor relationship in thinly laminated anisotropic reservoirs, Transactions 40th Annual Logging Symposium SPWLA paper OO, Oslo,

Patchett, J.G., Herrick, D.C., 1982, A Review of Saturation Models, Shaly Sand Reprint Review Volume, SPWLA, 3, 1–7.

Download free eBooks at bookboon.com

Poupon, A., Levaux, J. (1971) Evaluation of water saturation in shaly formations, Trans SPWLA 12th Logging Ann. Symp., paper O1–2, also in: Shaly Sand Reprint Volume, SPWLA, pp IV 81–95.

Poupon, A., Loy, M.E., Tixier, M.P., 1954, Contribution to electrical log interpretation in shaly sands, Trans. AIME, Philadelphia, 201, 138.

Schlumberger, 1982, Natural Gamma Ray Spectrometry, Essentials of N.G.S. Interpretation.

Schlumberger, 1982, Well evaluation developments – Continental Europe, Schlumberger.

Schlumberger, 1989, 2000: Log interpretation charts. Schlumberger Ed. Serv.

Schlumberger, 1989, Log interpretation principles/applications. Schlumberger Ed. Serv.

Schlumberger, 2008, "Carbonate Advisor" Brochure (www.slb.com/carbonates).

Schoen, J.H., Fanini O.N., Liming Yu, and Georgi, D.T., 2000, Aspects of Multicomponent Resistivity Data and Macroscopic Resistivity Anisotropy SPE Ann. Techn. Conf., SPE Paper 62909.

Schoen, J.H., Mollison, R.A., Georgi, D.T., 1999, Macroscopic Electrical Anisotropy of Laminated Reservoirs: A Tensor Resistivity Saturation Model, SPE Ann. Techn. Conf., SPE Paper 56509.

Schön, J.H., 1996, Physical properties of rocks: Fundamentals and Principles of Petrophysics (Handbook of Geophysical Exploration Series,) – Pergamon Press.

Schön, J.H., 2013, Physical Properties of Rocks – a Workbook, Elsevier Publ., http://www.elsevierdirect.com/companion.jsp?ISBN=9780444537966.

Simandoux, P., 1963, Dielectric measurements on porous media: application to the measurement of water saturation, In: Shaly Sand Reprint Volume, SPWLA, pp. IV 97–124.

Spears, R., Saha, S., 2005, Improved Fluid Typing with NMR: Better Field Development Planning in Deepwater Nigeria, SPWLA 46-th Ann. Logging Symp., June 26–29, paper FFF.

Tang, X.M., Patterson, D., 2004, Estimating formation permeability and anisotropy from borehole Stoneley waves, SPWLA 45th Annual Logging Symposium, 2004,

Thomas, E.C. and S.J. Stieber, 1975, The distribution of shale in sandstones and its effect upon porosity, in SPWLA 16th Annual Logging Symposium Transactions, 4–7 June, paper T.

Download free eBooks at bookboon.com

Tiab, D., Donaldson, E.C., 2014, Petrophysics; Gulf Publishing Company, Houston.

Timur, A., 1968, An investigation of permeability, porosity, and residual water saturation relationships for sandstone reservoirs: The Log Analyst, v. 9, n. 4, p. 8–17.

Torres-Verdin, C., 2004, Lecture Presentation PGE368, Fall 2004, Fundamentals of Well Logging, Univ. of Texas at Austin.

Vinegar, H.J., 1995, SPWLA Short course notes on NMR, SPWLA Houston 1995.

Waxman, M.H. and Smits, L.J., 1967, Electrical conductivities in oil-bearing shaly sands, SPE-1863-A, 42nd Annual Fall Meeting: Society of Petroleum Engineers, 1967, 8, 107–122.

Worthington, P.F., 1985, The evolution of shaly-sand concepts in reservoir evaluation. The Log Analyst, 26, no. 1, 23–40.

Wyllie, M.R.J., A.R. Gregory, L.W. Gardner, 1956, Elastic wave velocities in heterogeneous and porous media, Geophysics, 21,41–70.

American online
LIGS University
is currently enrolling in the
Interactive Online BBA, MBA, MSc,
DBA and PhD programs:

- enroll by September 30th, 2014 and
- save up to 16% on the tuition!
- pay in 10 installments / 2 years
- Interactive Online education
- visit www.ligsuniversity.com to find out more!

Note: LIGS University is not accredited by any nationally recognized accrediting agency listed by the US Secretary of Education.
More info here.

Click on the ad to read more

Download free eBooks at bookboon.com

11 Index

Symbols

\„Quick-look\“ interpretation 110

A

Acoustic log 90
anhydrite 142
API-unit 72
Archie's (1942) equations 46
Arps' equation 45

B

bad hole 141
bulk volume
  fluid 20

C

Calibration 31
Caliper log 41
capillary bound water 20, 101
cap rock 15
Capturing interactions 83
Carbonate Advisor (Schlumberger) 90
Carbonate rocks 14
cation exchange capacity (CEC) 51
cementation exponent 47
Cement bond log 97
characteristic energy, neutron interaction 84
classification
  clastic sediments 16
Clastic rocks 14
Clay 16
clay bound water 101
claystone 15
clean porous rock 44
clean rocks 125
Coates equation 102
compaction correction 94
composite matrix 123
Compressional wave 90
Compton effect 78
core laboratories 14
CPMG (Carr, Purcell, Meiboom and Gill) sequence 97
cross plot technique 119
Cuttings 28

D

Density-Neutron crossplot 159
Determination of shale properties 152
diffusion
  coefficient 103
Dispersed clay 16
Dispersed Shaly Sand 129
Dolomite 17

E

Elastic scattering 83
elemental analyses, spectral nuclear measurement 89

F

Fluid type 14
fluid typing 103
focusing electrode-systems 53
formation resistivity factor 46
free movable water 20, 101
from SP 144
from water zone 144

G

Galvanic resistivity measurements 44
Gamma-Gamma-log 78
Gammalog 68
gyromagnetic ratio 97

H

Header 31
hydrogen index 86

I

Indonesia Equation 131

Download free eBooks at bookboon.com

Inductionlog 58
Inductive conductivity measurements 44
Inelastic scattering 83
Integral measurement 70
invaded zone 36

L

Laminar clay 16
laminated shaly sand 127
Larmor frequency 97
laterolog 53
Limestone 17
limestone-calibrated 85
logging equipment 28
Logging methods – Classification 33
Logging While Drilling (LWD) 35
log interpretation 110
Long Normal 53

M

Measurement While Drilling (MWD) 35
Microlog 58
Mixed lithology Carbonate rock 157
Multiple Porosity Methods 116

N

neutron capture spectroscopy 90
Neutron-Density-Cross plot 121
Neutronlog for porosity determination 85
Neutron methods 82
neutron porosity 87
Nuclear logs 66
Nuclear Magnetic Resonance (NMR) 97
nuclear measurements, mineral analysis 89

O

Oil-bearing Sandstone 139
overlay technique 117

P

permeability 21
Permeability 14, 21
Permeable beds 113
Photoelectric effect 78
Poisson distribution 67
Poisson's ratio 91
porosity
  effective 19
  total 19
Porosity 14, 19, 114
Porosity and Mineral Composition 116
Porosity determination from density 81
potassium K-40 68

Q

Quantitative Interpretation 113
Quick-look methods 112

R

radius of investigation 38
relaxation time 99
Reservoir rock type 14
resistivity index 47

S

sandstone 15
saturation 20
Saturation 14, 19
saturation exponent 47
sealing formation 15
shale 15
Shale conductivity 51
shale content 73
Shaly sand 121, 132, 149
shaly sand equations 127
Shaly sands 126
Shear modulus 91
Shear wave 90
Short Normal 53
shoulder bed effect 53
siltstone 15
Simandoux Eq 130
slow formations 96
slowness 91
Sonic log 90
spacing 53
Specific electrical resistivity of rocks 44
spectral gamma measurement 76

Download free eBooks at bookboon.com

Spectral measurement 70
spin-lattice relaxation time 98
spin-spin relaxation time 98
Spontaneous potential SP 64
Stoneley wave 96
Structural clay 16

T

Thomas-Stieber Plot 132
thorium series 68
time-average equation 93
tool characteristic 36
tornado charts 58
Total Organic Content 77

U

uninvaded or virgin zone 36
uranium-radium series 68

V

vertical resolution 38
viscosity 21

W

water saturation 125
Waxman and Smits 129
Wyllie's equation 93

Y

Young's modulus 91

Click on the ad to read more

Download free eBooks at bookboon.com

12 Endnotes

1. Please note: Saturation and bulk volume fluid give only an information about the volume fraction, but not about the position or distribution ofthe fluids in the pore space. This is controlled mainly by the wettability (see Tiab and Donaldson 2014, Schön 2011).
2. Horizontal means parallel to layering or lamination, vertical means orthogonal to the plane of layering or lamination.
3. The "macroscopic" pressure gradient refers to the sample dimension, whereas a "microscopic" pressure gradient refers to the true pore channels length.
4. Note: Highly resistive zones within a reservoir are of special interest because of hydrocarbons.
5. this technique eliminates the travel time crossing the mud parts of the way.
6. Note: The individual plots are designed for specific tools and different fluid properties (water) on top of the crossplot.
7. The matrix inversion algorithm is a tool in Microsoft-Excel.
8. note: The algorithm delivers a mathematically exact solution also in case of a non-realistic composition!
9. Note the crossover of Neutron and Density. The low SP-indication could result from lower vertical resolution compared with GR and from some permeability (silty), because resistivity curves do not indicate a non-permeable layer.
10. Compare with the picked value of 0.3 for the water zone.

Download free eBooks at bookboon.com